



2000

Air-ground temperature exchange

William L. Schmidt
University of North Dakota

[How does access to this work benefit you? Let us know!](#)

Follow this and additional works at: <https://commons.und.edu/theses>



Part of the [Geology Commons](#)

Recommended Citation

Schmidt, William L., "Air-ground temperature exchange" (2000). *Theses and Dissertations*. 264.
<https://commons.und.edu/theses/264>

This Dissertation is brought to you for free and open access by the Theses, Dissertations, and Senior Projects at UND Scholarly Commons. It has been accepted for inclusion in Theses and Dissertations by an authorized administrator of UND Scholarly Commons. For more information, please contact und.common@library.und.edu.

AIR-GROUND TEMPERATURE EXCHANGE

by

William L. Schmidt
Master of Science, University of North Dakota, 1994
Bachelor of Science, University of Wisconsin, 1991

A Dissertation

Submitted to the Graduate Faculty

of the

University of North Dakota

in partial fulfillment of the requirements

for the degree of

Doctor of Philosophy

Grand Forks, North Dakota
December
2000

UMI Number: 9996602

UMI[®]

UMI Microform 9996602

Copyright 2001 by Bell & Howell Information and Learning Company.

All rights reserved. This microform edition is protected against
unauthorized copying under Title 17, United States Code.

Bell & Howell Information and Learning Company
300 North Zeeb Road
P.O. Box 1346
Ann Arbor, MI 48106-1346

This dissertation, submitted by William L. Schmidt in partial fulfillment of the requirements for the Degree of Doctor of Philosophy from the University of North Dakota, has been read by the Faculty Advisory Committee under whom the work has been done and is hereby approved.

W.D. Doedd
(Chairperson)
Richard D. Lester
Ahmad Elhaneem
Scott A. Korman
B. H. Lybbin

This dissertation meets the standards for appearance, conforms to the style and format requirements of the Graduate School of the University of North Dakota, and is hereby approved.

Carl Fox
Dean of the Graduate School

12-11-00
Date

PERMISSION

Title Air-ground Temperature Exchange

Department Geology

Degree Doctor of Philosophy

In presenting this dissertation in partial fulfillment of the requirements for a graduate degree from the University of North Dakota, I agree that the library of this University shall make it freely available for inspection. I further agree that permission for extensive copying for scholarly purposes may be granted by the professor who supervised my dissertation work or, in his absence, by the chairperson of the department or the dean of the Graduate School. It is understood that any copying or publication or other use of this dissertation or part thereof for financial gain shall not be allowed without my written permission. It is also understood that due recognition shall be given to me and to the University of North Dakota in any scholarly use which may be made of any material in my dissertation.

Signature Walter L Smith

Date Dec 5, 2000

TABLE OF CONTENTS

LIST OF FIGURES	v
LIST OF TABLES	x
ACKNOWLEDGEMENTS	xi
ABSTRACT	xii
CHAPTER 1. INTRODUCTION	1
CHAPTER 2. GROUND SURFACE TEMPERATURE EXCHANGE	4
CHAPTER 3. SEPARATION OF AIR AND GROUND TEMPERATURES	12
CHAPTER 4. ANALYSIS OF AIR AND GROUND TEMPERATURES	36
CHAPTER 5. SNOW COVER EFFECTS	60
CHAPTER 6. THE CONDUCTION MODEL	71
CHAPTER 7. LATENT ENERGY AND PRECIPITATION	88
CHAPTER 8. A FORWARD MODELING ANALYSIS	96
CHAPTER 9. CONCLUSIONS	110
APPENDIX. MODEL DESCRIPTION	113
REFERENCES CITED	119

LIST OF FIGURES

Figure	Page
1. Map of North Dakota showing the location of data recording sites, including Fargo, Bottineau, Langdon, Minot, and Streeter.	7
2. Daily mean air and 50cm depth temperatures recorded at Fargo from March 15, 1982 to March 10, 1983.	13
3. Daily mean air and 50cm depth temperatures recorded at Bottineau from March 15, 1994 to March 10, 1995.	14
4. Daily mean air and 50cm depth temperatures recorded at Langdon from March 15, 1994 to March 10, 1995.	15
5. Daily mean air and 50cm depth temperatures recorded at Minot from March 15, 1994 to March 10, 1995.	16
6. Daily mean air and 50cm depth temperatures recorded at Streeter from March 15, 1994 to March 10, 1995.	17
7. Daily mean air and 50cm depth temperatures recorded at Fargo from October 10, 1980 to April 16, 1990.	18
8. Daily mean air and 50cm depth temperatures recorded at Bottineau from November 25, 1993 to January 1, 2000.	19
9. Daily mean air and 50cm depth temperatures recorded at Langdon from November 1, 1993 to January 1, 2000.	20
10. Daily mean air and 50cm depth temperatures recorded at Minot from November 1, 1993 to January 1, 2000.	21
11. Daily mean air and 50cm depth temperatures recorded at Streeter from November 1, 1993 to January 1, 2000.	22
12. Daily mean air and 50cm depth temperatures from Fargo recorded from January 1, 1981 to December 26, 1981. Monthly averaged residual temperatures (resid temps) are also shown.	23
13. Monthly averaged air and 50cm-depth temperature differences from Fargo.	24

14. Monthly averaged air and 50cm-depth temperature differences from Bottineau. . .	25
15. Monthly averaged air and 50cm-depth temperature differences from Langdon. . .	26
16. Monthly averaged air and 50cm-depth temperature differences from Minot.	27
17. Monthly averaged air and 50cm-depth temperature differences from Streeter. . . .	28
18. Monthly averaged incident solar radiation recorded from 1953 to 1975 in Bismarck, ND (Enz, 1985).	31
19. Mean annual air temperatures recorded at Fargo from 1884 to 1999. A least-squares linear regression line is shown.	37
20. Daily mean 80cm, 250cm, 470cm, and 1170cm depth temperatures recorded at Fargo from October 10, 1980 to April 16, 1990. Phase lag and attenuation of the annual temperature signal with depth are observable.	38
21. Air and ground temperatures from all measurement depths averaged over the period January 1, 1981 to December 31, 1989, and plotted as a function of depth.	41
22. Ground temperatures in the upper 50cm of the ground at Fargo averaged over the period 1981 to 1989. An exponential smoothing curve is plotted for ground temperatures. The steady-state background heat flow from a 60m-deep borehole is shown.	42
23. Warming magnitudes per decade of Fargo mean annual ground temperatures from 125-1170cm depths plotted as a function of depth.	44
24. Mean annual air and ground temperatures averaged from all depths from Fargo. A least-squares linear regression line is shown on ground temperatures. . .	46
25. Mean annual modeled and recorded ground temperatures averaged from 10-1170cm depths at Fargo. Mean annual air temperatures are also shown.	48
26. Mean annual air temperatures from Bottineau.	50
27. Mean annual air temperatures from Langdon.	51
28. Mean annual air temperatures from Minot.	52
29. Mean annual air and ground temperatures averaged from all depths at Bottineau. A least-squares linear regression line is shown on ground temperatures.	54

30. Mean annual air and ground temperatures averaged from all depths at Langdon. . .	55
31. Mean annual air and ground temperatures averaged from all depths at Minot. . . .	56
32. Mean annual air and ground temperatures averaged from all depths at Streeter. . .	57
33. Mean annual recorded air and ground and modeled ground temperatures averaged from all depths at Bottineau. The least-squares linear regression line shows the $1.17 \pm 0.15^\circ\text{C}$ warming trend in recorded ground temperatures during the 6-year period.	58
34. Total days with snow cover (days) and ground – air temperature differences ($T_{5\text{cm}} - T_{\text{air}}$) from Fargo averaged annually from November 15 to April 1.	62
35. Seasonal air temperature trends, including summer (June-Aug), fall (Sep-Nov), winter (Dec-Feb), and spring (Mar-May). Changes per decade in mean seasonal temperatures are: $+2.43 \pm 0.78$ (summer), -0.75 ± 0.24 (fall), -0.51 ± 0.16 (winter), and $+1.26 \pm 0.41^\circ\text{C}$ (spring). Least-squares linear regression lines are shown for winter and summer temperatures.	63
36. Monthly averaged values of total percent daily sunlight recorded in Fargo from January 1, 1981 to December 31, 1989.	65
37. Total days of measurable snow cover per winter plotted with $T_{5\text{cm}} - T_{\text{air}}$ values averaged from November 15 to April 1 at Bottineau.	67
38. Total days of measurable snow cover per winter plotted with $T_{5\text{cm}} - T_{\text{air}}$ values averaged from November 15 to April 1 at Langdon.	68
39. Total days of measurable snow cover per winter plotted with $T_{5\text{cm}} - T_{\text{air}}$ values averaged from November 15 to April 1 at Minot.	69
40. Total days of measurable snow cover per winter plotted with $T_{5\text{cm}} - T_{\text{air}}$ values averaged from November 15 to April 1 at Streeter.	70
41. Daily mean 1cm-depth temperatures recorded from November 25, 1984 to March 22, 1985 at Fargo. The black line indicates the division between freezing and thawing periods.	73
42. Observed 125cm-depth temperatures (observed temp.) for the 1982-freezing season at Fargo. Model temperatures shown are calculated with and without a term for latent energy.	79

43. Daily residual temperatures calculated with three trial thermal conductivity values from the winter 1982 modeling period. Residual temperatures averaged during this modeling period are $T_{av\ res} = 0.187^{\circ}\text{C}$ ($k_{un} = 0.50$, $k_{fr} = 1.13\ \text{Wm}^{-1}\text{K}^{-1}$), $T_{av\ res} = 0.005^{\circ}\text{C}$ ($k_{un} = 0.60$, $k_{fr} = 1.23\ \text{Wm}^{-1}\text{K}^{-1}$), and $T_{av\ res} = -0.163^{\circ}\text{C}$ ($k_{un} = 0.70$, $k_{fr} = 1.33\ \text{Wm}^{-1}\text{K}^{-1}$).	81
44. Average residual temperatures from all depths plotted as a function of trial thermal conductivity values with latent energy held constant at $LE = 195\ \text{Wm}^{-3}$. Thermal conductivity is varied around best-fit values of $k_{un} = 0.60$, $k_{fr} = 1.23\ \text{Wm}^{-1}\text{K}^{-1}$, with a constant difference of $0.63\ \text{Wm}^{-1}\text{K}^{-1}$ maintained between k_{un} and k_{fr} . A linear regression line is shown.	82
45. Average residual temperatures from all depths plotted as a function of trial latent energy. Thermal conductivity is held constant at $k_{un} = 0.60$, $k_{fr} = 1.23\ \text{Wm}^{-1}\text{K}^{-1}$. A linear regression line is shown.	83
46. Subsurface warming due to a three-day precipitation event at Fargo, beginning May 27, 1984. Daily residual temperatures ($T_{calc} - T_{obs}$) are shown for 150, 250 and 370cm depths.	86
47. Modeled annual latent energy of fusion (energy) versus precipitation (precip) totaled 60 days prior to the onset of ground freezing from Fargo.	89
48. Modeled annual latent energy of fusion (energy) versus total fall precipitation (precip) from Bottineau.	91
49. Modeled annual latent energy of fusion (energy) versus total fall precipitation (precip) from Langdon.	92
50. Modeled annual latent energy of fusion (energy) versus total fall precipitation (precip) from Minot.	93
51. Modeled annual latent energy of fusion (energy) versus total fall precipitation (precip) from Streeter.	94
52. Total fall (Sep, Oct, Nov) precipitation averaged from climate stations in northwestern North Dakota. A 10-point moving average is shown.	97
53. Mean annual surface air temperatures averaged from climate stations in northwestern North Dakota. A least-squares linear regression line indicates a slope of $1.57 \pm 0.23^{\circ}\text{C}$	99
54. Individual ground surface temperature histories from Minot N, Landa, Glenburn, and Wawanesa boreholes.	100

55. Average ground surface temperature history from the four boreholes showing a warming magnitude per century of 1.8°C. The error bars are the standard deviation of mean warming.	101
56. Ground surface temperature history of the transient generated with direct air-ground coupling.	105
57. Total fall precipitation and modeled latent energy of ground freezing from the 1994 to 1999 modeling analysis of Minot data. A least-squares linear regression line is shown.	106
58. Ground surface temperature history of the transient resulting solely from the effects of latent energy of ground freezing.	108

LIST OF TABLES

Table	Page
1. Thermocouple depths and vertical spacing between thermocouples from Fargo and Bottineau, Langdon, Minot, and Streeter sites.	9
2. Elevation and soil properties of temperature recording sites.	11
3. Air and ground temperatures averaged from January 1, 1981 to December 31, 1989. Differences between air and ground temperatures and warming magnitudes per decade determined by least-squares linear regression lines are also shown.	40
4. Average best-fit thermal conductivity (k) and latent energy of freezing (LE) values from Fargo, including unfrozen (unfr), frozen (fr), upper (up) and lower (low) thermal conductivity and evapotranspiration (evapotrans).	77
5. Average best-fit thermal conductivity (k) and latent energy of freezing (LE) values from four sites, including unfrozen (unfr) and frozen (fr) thermal conductivity. These values are averaged over all modeling periods.	77
6. Nodal depth and spacing.	102

ACKNOWLEDGEMENTS

I gratefully acknowledge the assistance and friendship of Dr. Rao, Frank Beaver, Richard LeFever, John Reid, Scott Korom, Henn Soonpaa, and Gloria Pederson. I acknowledge the financial assistance of EPSCoR Dissertation Grant #EPS-9874802.

I wish to thank my parents, Wayne and Phyllis, for their love and support over the years, as well as Steve, Kate, Roger, Dick, and Mary. I especially wish to thank Georgia, for her love and support during this dissertation work.

To Georgia

ABSTRACT

Most borehole paleoclimate studies have been based on the assumption that the exchange of temperature between the air and ground surface remains constant. However, secular changes in boundary-layer factors can generate anomalous ground temperatures. This dissertation is an investigation of factors that cause separation of air and ground temperatures on a seasonal to inter-annual time scale, including snow cover duration, latent energy of ground freezing, daily sunlight, precipitation, and vegetation.

Continual records of surface air and near-surface ground temperatures from five sites in North Dakota show similar trends in seasonal air-ground temperature separation. Statistical regressions of mean annual ground temperatures from Fargo and Bottineau sites indicate respective warming trends of $0.93 \pm .09^\circ\text{C} / 9$ years and $1.17 \pm .15^\circ\text{C} / 6$ years. Mean annual air temperatures and ground temperatures calculated with a conduction model assuming direct air-ground coupling do not display any significant trends.

The effect of snow cover duration on air-ground temperature exchange was tested by comparing average winter air-ground temperature differences ($T_{5\text{cm}} - T_{\text{air}}$) with annual duration of snow cover. The correlation coefficients between these variables are: **Bottineau:** $r^2 = .84$ (6 years), **Fargo:** $r^2 = .71$ (9 years), **Langdon:** $r^2 = .56$ (6 years), **Minot:** $r^2 = .79$ (6 years), and **Streeter:** $r^2 = .87$ (6 years). Best-fit latent energy of ground freezing values were determined with a conduction model and compared with total fall precipitation. The correlation coefficients between these variables are: Bottineau: $r^2 = .38$, Fargo $r^2 = .66$, Langdon: $r^2 = .69$, Minot: $r^2 = .95$, and Streeter: $r^2 = .01$.

A least-squares linear regression of mean annual air temperatures recorded in northwestern North Dakota from 1895 to 1995 indicates a warming magnitude of $1.57 \pm .23^\circ\text{C}$ per century. This temperature time series was forced into the ground with direct coupling to generate a synthetic temperature-depth profile. Inversion of this profile yielded a ground-surface warming magnitude of 1.7°C per century. Total fall precipitation is used as a proxy for latent energy of ground freezing. Latent energy effects were modeled with direct coupling of the regional air temperature record and a temperature dependent constraint for snow cover insulation. This generated a 0.4°C per century signal.

CHAPTER 1

INTRODUCTION

During the last two decades there has been a growing interest in the impact of human activities on the composition of the atmosphere and its effect on climate. Climate models project that the mean annual global surface temperature will increase by 1-3.5°C by 2100, that global mean sea level will rise by 15-95cm, and that changes in the spatial and temporal patterns of precipitation would occur (IPCC, 1997). The average rate of warming probably would be greater than any seen in the past 10,000 years (IPCC, 1997). Because of the social, economic and scientific significance of such effects, the study of climate change has become increasingly important in order to derive predictive models. Unfortunately, few instrumentally acquired surface air temperature records that would test the models exist prior to the 20th century (Harris and Chapman, 1997). However, ground surface temperature histories inferred from boreholes extend farther back than recorded air temperatures without any statistical noise due to interannual variability. The solid earth continually records a thermally averaged and robust transient signal of long-period temperature variations at the ground surface. Analyses of 358 subsurface temperature measurements indicate that the average surface temperature of the Earth has increased by about 0.5°C in the 20th century and that the 20th century has been the warmest of the past five centuries (Pollack et al., 1998). The superposition of the climatic effect and anthropogenic activity effect upon ground warming is a very complicated process requiring additional research (Majorowicz, 1993).

Most borehole paleoclimate studies have been based on the assumption that a consistent 1:1 relationship exists between air and ground surface temperatures. However, the number of processes governing the energy transfer between the ground surface and the near-surface air layer is large, and the interrelationship between processes is extremely complex (Oke, 1987). A continual exchange of energy occurs between the Earth surface and the air layer near the ground involving incident solar radiation, emitted long and short wavelength radiation, energy flow within the ground, diffusion and mass exchange, and latent energy effects, mainly evaporation (Geiger et al., 1995). Boundary layer variables influencing the energy exchange include snow cover, soil moisture, inundation, latent energy due to moisture phase changes, vegetation, wind exposure, ground-surface albedo, proximity to urban structures, and topographic and terrain effects (Farouki, 1981; Majorowicz, 1993). Local variations of ground temperatures and differences in mean annual air and ground temperatures are due to microclimatic and boundary layer factors (Geiger et al., 1995). Therefore in addition to climatic data, records of air and ground temperatures are needed to study the variations of ground temperatures in relation to the changing climatic environment (Majorowicz, 1993). Changing boundary layer factors can produce anomalous subsurface temperatures similar to those expected from climatic changes (Lewis and Wang, 1992). If these effects are not recognized, climatic changes inferred from subsurface temperatures may be incorrect (Lewis and Wang, 1992).

Recent climate change studies in areas of North America subject to snow cover and ground freezing have revealed regional discrepancies in warming magnitudes inferred from borehole temperatures and statistical analyses of recorded air temperatures

(Beltrami and Mareschal, 1991, Gosnold et al., 1997, Majorowicz and Skinner, 1997). In a study of climate change in the Northern Plains, Gosnold et al. (1997) observed that ground surface temperatures underwent significantly greater warming in the last century than recorded air temperatures north of 46° N latitude. Because this region was not subject to any deforestation or terrain effects, the discrepancies are attributed to ground temperatures retaining a record of temperature, combined with the thermal effects of snow cover and latent energy of ground freezing and thawing.

The goal of this dissertation is to better understand the factors that cause separation of air and ground temperatures on a seasonal to inter-annual time scale. Factors examined in this study include vegetation, snow cover, total daily precipitation, and latent energy associated with moisture freezing and thawing processes in the subsurface. The following hypotheses are tested: 1) Ground-surface factors are capable of generating trends in mean annual ground temperatures that do not occur in mean annual air temperatures during 6 and 9-year periods; 2) Annual air-ground temperature differences averaged during winter months are mainly controlled by total duration of winter snow cover; 3) Modeled latent energy of ground freezing is a function of precipitation totaled 2-3 months prior to the onset of ground freezing; 4) The thermal effects of latent energy of ground freezing determined by observed fall precipitation values are capable of generating a transient subsurface temperature signal in a 100-year period.

CHAPTER 2

GROUND-SURFACE TEMPERATURE EXCHANGE

Ground-surface temperature exchange in soils and rock is a complex interaction of radiation absorption and emission, conduction, moisture exchange, moisture phase changes, and vegetation cover (Farouki, 1981). Heat transfer in soils is complicated by embedded stones, tree roots, dead organic matter, soil organisms, ionic concentration, and water passages (Geiger et al., 1995). Thermal properties of soils are strongly affected by the presence of water and air in pore spaces (Farouki, 1980). Soil water can be transported by gravity, capillary action, soil water tension, and differences in vapor pressure (Geiger et al., 1995). Moisture content of soil varies in response to climatic events, varying ground surface albedo, density, permeability, porosity, and thermal diffusivity (Geiger et al., 1995). Not only does the variable water content of soil determine its temperature, the temperature regime of the soil affects the water distribution in it (Geiger et al., 1995). Surface air temperatures vary much more during the day than ground temperatures. This is because the thermal capacity of soil is 1000-3000 times that of air, depending on the moisture content of the soil (Geiger et al., 1995).

Although ground surface temperature indirectly controls the boundary condition for the conductive flow of heat into the earth, the interactions at the ground surface are greatly influenced by the type of surfaces (Roy et al., 1972, Geiger et al., 1995). These may produce lateral variations in the ground surface temperature of several degrees over tens of meters (Blackwell et al., 1980). Lateral variations in air-ground temperature

exchange can either be abrupt due to deforestation, vegetative cover changes, inundation, groundwater advection, proximity to urban structures, or gradual due to long-term changes in variables at the ground surface. These factors are considered terrain effects and influence the relation of “effective” ground surface temperature to the air temperature (Lewis and Wang, 1992). Secular changes in average snow cover or precipitation also influence the average ground surface temperature even if the average air temperature remains constant (Lewis and Wang, 1992). Unfortunately, screening the thermal effects of the boundary layer and terrain from the transient component of the geothermal gradient is difficult.

In the case of gradual changes in ground-surface variables, the time scale and magnitude of change are main determinants of whether or not the Earth records a spurious or accurate climatic signal. Depth and time are linked nonlinearly by thermal diffusivity. High frequency signals diffuse with time, leaving a temporally “smeared” direct signal of long-wavelength temperature variations at the Earth’s surface. The temporal resolving power of the borehole inversion scheme to past climatic events contains inherent uncertainties that increase with time, due to the diffusive nature of heat conduction (Clow, 1992). The propagation depth of a signal from the ground surface is proportional to thermal diffusivity and duration of the signal. Thermal diffusivity in soils is largely a function of moisture content and varies from 3×10^{-4} to $8 \times 10^{-7} \text{m}^2/\text{s}$ (Farouki, 1981). Thermal diffusivity of rock varies from 6×10^{-6} to $1 \times 10^{-7} \text{m}^2/\text{s}$ (Touloukian et al., 1981). Diurnal and annual signal waves are attenuated in the upper 20 – 30m of the ground. For example in bedrock having a thermal diffusivity of $1 \times 10^{-6} \text{m}^2/\text{s}$, a 10°C annual signal is attenuated to $.012^\circ\text{C}$ at 20m and $.0002^\circ\text{C}$ at 30m depth.

Regional description of study area

The Northern Plains region is semi-arid and experiences a wide range of seasonal temperatures. The topography of North Dakota has a minimal effect on the state climate. Although the soils at all temperature sites in North Dakota were formed from glacial tills, the boundary layers from all sites exhibit different temperature exchange properties due to varying moisture content, organic matter, grain size, porosity, mineral composition, surface roughness, elevation, slope and vegetative density.

Thermal properties of the Northern Plains

Most of the central and northern Great Plains is underlain with Pierre Shale. The Minot borehole in this study is in the eastern facies of Pierre Shale, a clay-rich Upper Cretaceous marine shale having an effective thermal conductivity of $1.2 \text{ Wm}^{-1}\text{K}^{-1}$ (Gosnold, 1990). The conductivity of shales in the Northern Plains ranges from about 1.0 to $2.4 \text{ Wm}^{-1}\text{K}^{-1}$, due to differences in quartz content (Gosnold, 1990). Shales with higher quartz content have a higher thermal conductivity. In general the thermal conductivity and diffusivity of sedimentary material is lower than igneous and metamorphic material (Touloukian et al., 1981). A typical granite has a conductivity of 2.5 to $3.5 \text{ Wm}^{-1}\text{K}^{-1}$ (Turcotte and Schubert, 1982).

Site descriptions

Continuous records of air and ground temperatures from five NDAWN (North Dakota Agriculture Weather Network) stations in North Dakota are used in this study, including Fargo, Bottineau, Langdon, Minot, and Streeter (Figure 1). Air and ground

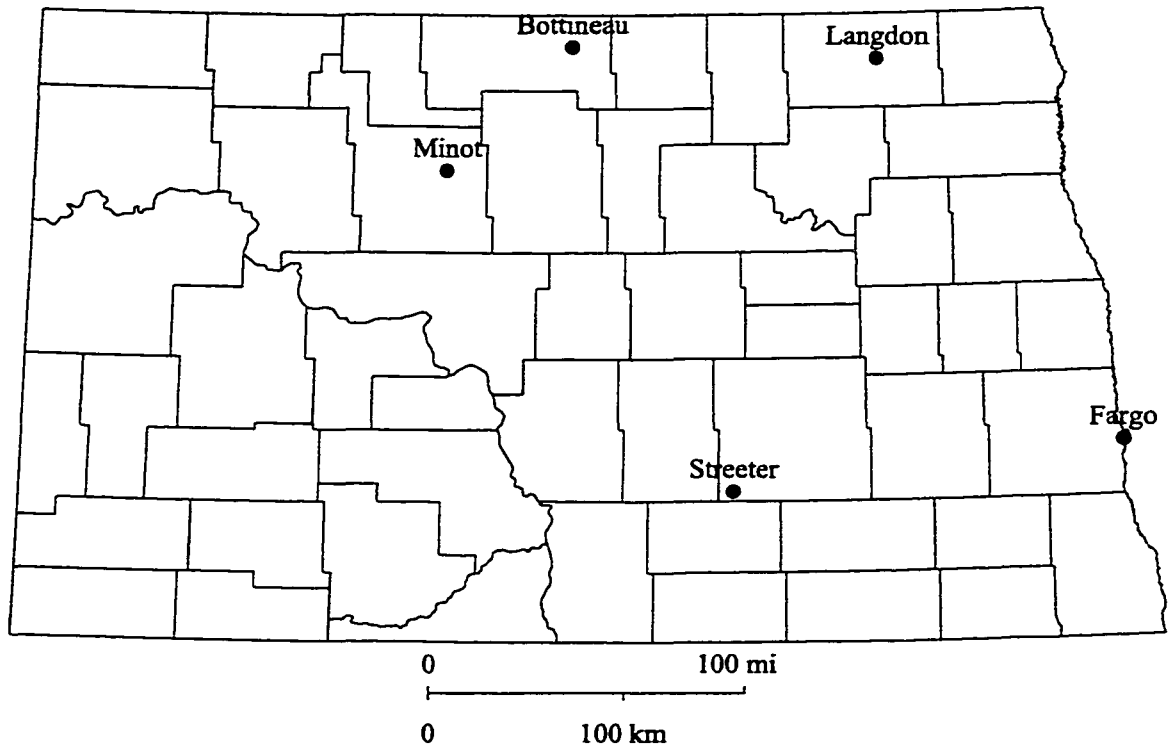


Figure 1. Map of North Dakota showing the location of data recording sites, including Fargo, Bottineau, Langdon, Minot, and Streeter.

temperatures at Fargo were recorded from October 10, 1980 to April 21, 1989 at 19 depths (Table 1). Ground temperatures at the remaining sites were recorded from October 5, 1992 to Jan 1, 2000 at 13 depths (Table 1). All temperatures were recorded hourly and averaged into a single daily-mean value. Air temperatures at all sites were recorded at heights of 1.5m.

Data recording

Ground temperatures were recorded by sets of two thermocouples wired in parallel for determining the average temperature at each depth. The thermocouples were attached to a wooden rod placed into a hole made with a 4cm-diameter soil-coring device. After placement of the rod in the ground, the holes were filled and packed with soil slurry. Wooden rods were chosen as a thermocouple attachment due to the low thermal conductivity of wood. The approximate uncertainty in thermocouple measurements is $\pm 0.2^{\circ}\text{C}$ (Enz, personal communication).

Climatic data, including total daily precipitation and daily measured snow cover, were recorded and archived at National Climatic Data Center stations (NCDC, NOAA). Daily percent sunlight was recorded at the Fargo NCDC station. Four of the five NCDC stations were within 1-4km of the NDAWN stations. The NDAWN station at Bottineau is 38km from the NCDC station, creating the possibility of a different microclimate at the NDAWN and NCDC stations. All five NDAWN stations are on grass-covered sites in areas of level to gently sloping topography. Soil parent material is glacial till and salinity levels are low at all sites. All soils are greater than 20m deep and well drained with low to moderate permeability ranges of 0.5 - 5 cm/hr (USDA, 1992). Low annual rainfall and

Table 1. Thermocouple depths and vertical spacing between thermocouples from Fargo and Bottineau, Langdon, Minot, and Streeter sites.

Thermocouple depth Fargo (cm)	Vertical spacing (cm)	Thermocouple depth Bot, Lan, Min, Strt (cm)	Vertical spacing (cm)
1	1	5	5
5	4	10	5
10	5	20	10
20	10	30	10
30	10	40	10
50	20	50	10
60	10	60	10
80	20	80	20
125	45	100	20
150	25	125	25
200	50	150	25
250	50	175	25
270	20		
300	30		
370	70		
470	100		
770	300		
970	200		
1170	200		

cold temperatures have in resulted in a vegetation cover of mixed grasses and favored the accumulation of organic matter in the soils of North Dakota (USDA). Site elevations and properties are given in Table 2 (USDA, 1990).

Table 2. Elevation and soil properties of temperature recording sites.

Site:	Elevation (m)	Soil description
Bottineau	494	clay loam
Fargo	273	black silty-clay loam
Langdon	542	fine clay loam
Minot	590	fine loam
Streeter	650	fine sand and silt loam

Site:	Available water capacity	Water table depth (m)
Bottineau	high	> 2
Fargo	high	0 - 3
Langdon	high	> 2
Minot	moderate	> 2
Streeter	high	1 - 2

CHAPTER 3

SEPARATION OF AIR AND GROUND TEMPERATURES

Observed air and ground temperature differences

The tracking and decoupling of air and ground temperatures can be closely studied during all times of the year with continual records of air and ground temperatures. Seasonal trends in air and ground temperature differences are observable in one year of daily mean air and 50cm-depth temperatures from all five NDAWN sites (Figs. 2-6). These data reveal a significant insulation of ground temperatures during winter periods and a varied separation of air and ground temperatures during non-freezing periods. The complete 6 and 9-year time series of daily mean air and 50cm-depth ground temperatures from all sites are shown in Figures 7-11.

To quantify differences between air and 50cm-depth ground temperatures at specific times of the year, temperature differences ($T_{\text{air}} - T_{50\text{cm}}$ residual temperatures) were averaged for each month. Daily mean air and 50cm-depth temperatures at Fargo recorded from January 1, 1981 to December 31, 1981 are plotted with monthly-averaged residual temperatures to show how the separation of air and ground temperatures varies during the year (Fig. 12).

To understand the relationship of air and ground temperatures on an intra-annual time scale, monthly-averaged residual temperatures were calculated for the 6 and 9-year measurement periods. These periods include 1981-1989 at Fargo and 1994-1999 at Bottineau, Langdon, Minot, and Streeter. Figures 13-17 show monthly averaged air and

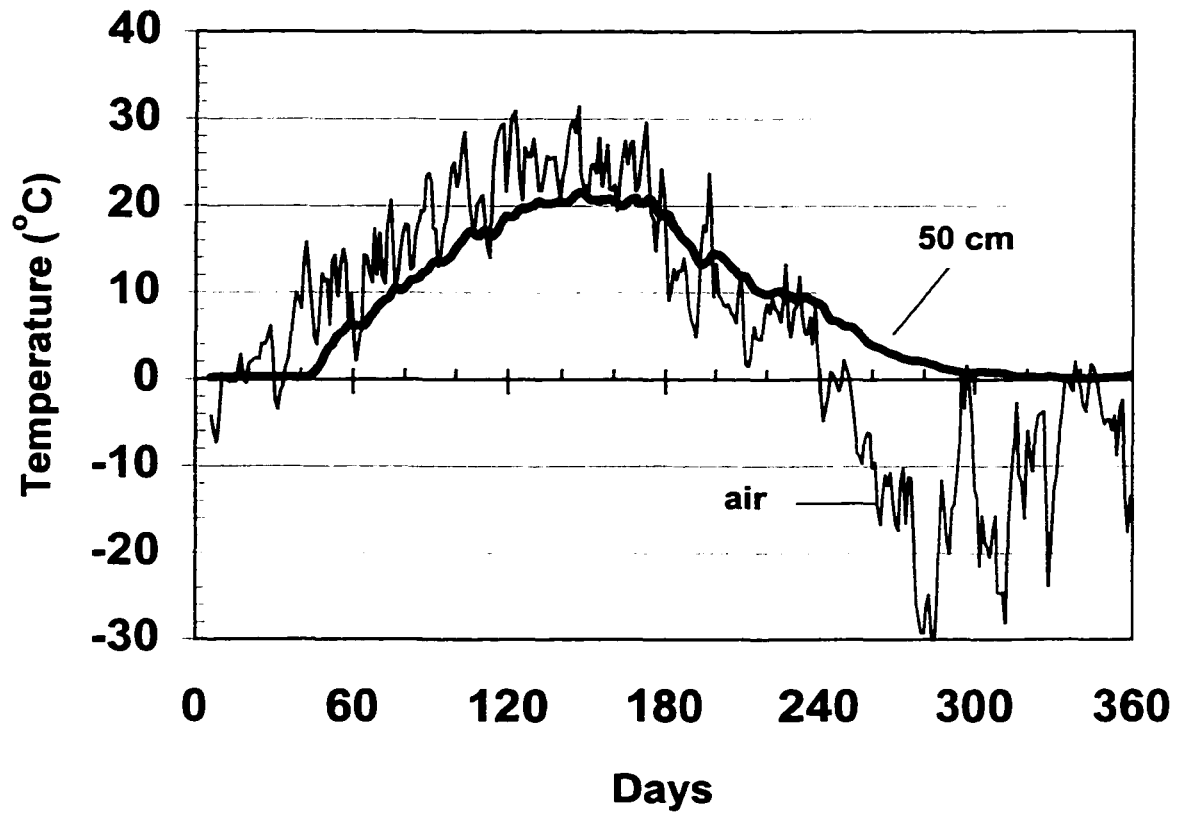


Figure 2. Daily mean air and 50cm depth temperatures recorded at Fargo from 3/15/82 to 3/10/83.

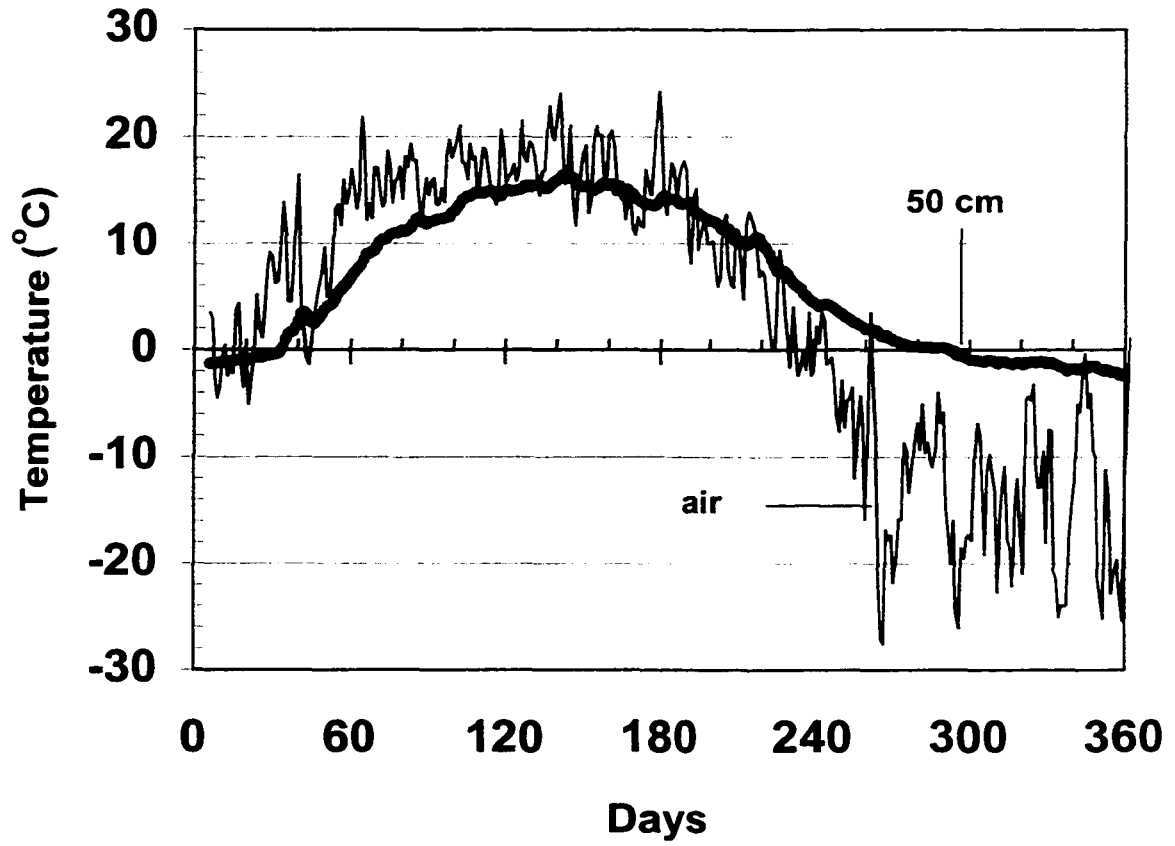


Figure 3. Daily mean air and 50cm depth temperatures recorded at Bottineau from 3/15/94 to 3/10/95.

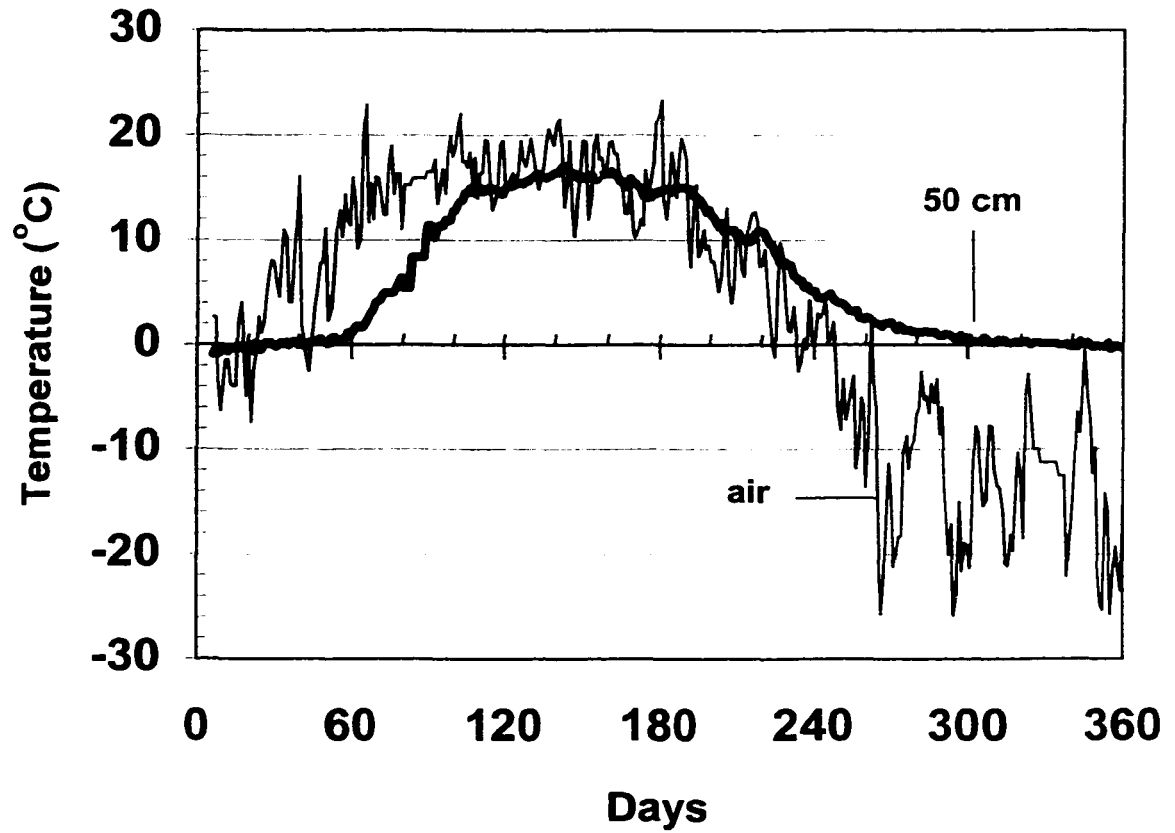


Figure 4. Daily mean air and 50cm depth temperatures recorded at Langdon from 3/15/94 to 3/10/95

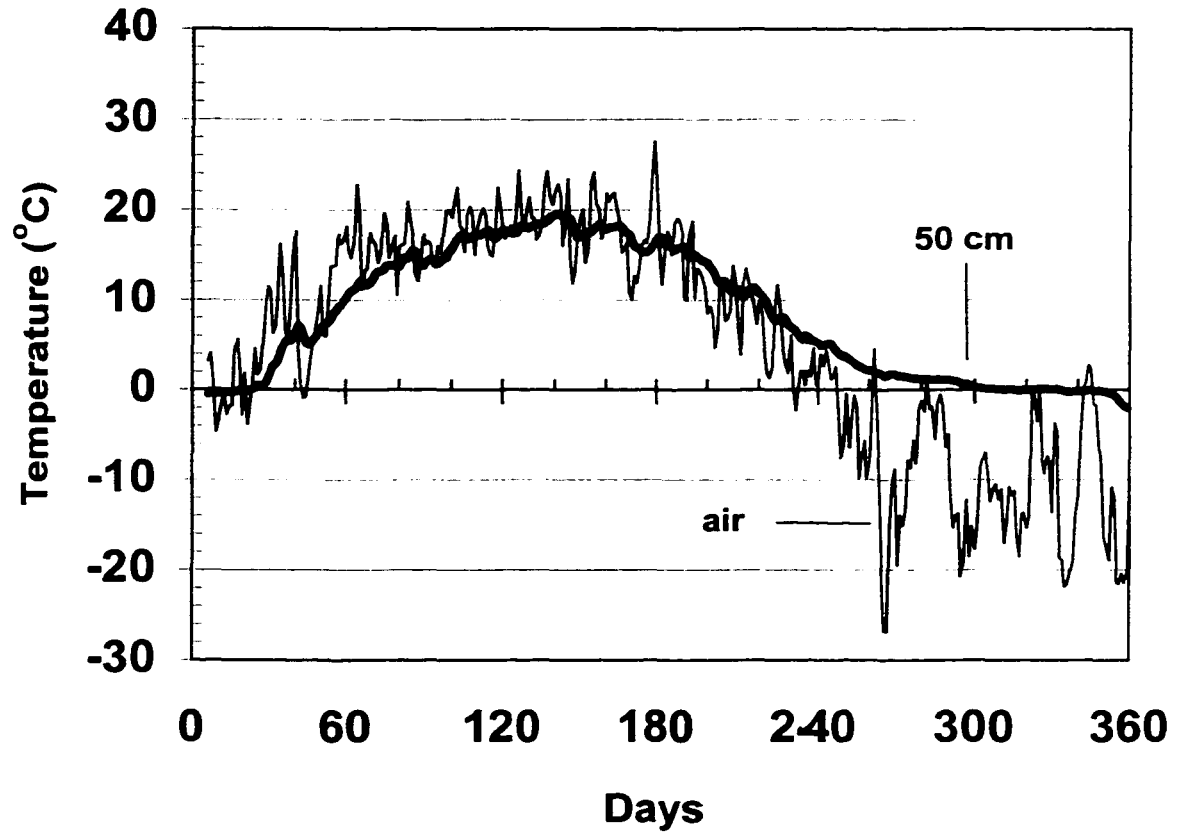


Figure 5. Daily mean air and 50cm depth temperatures recorded at Minot from 3/15/94 to 3/10/95.

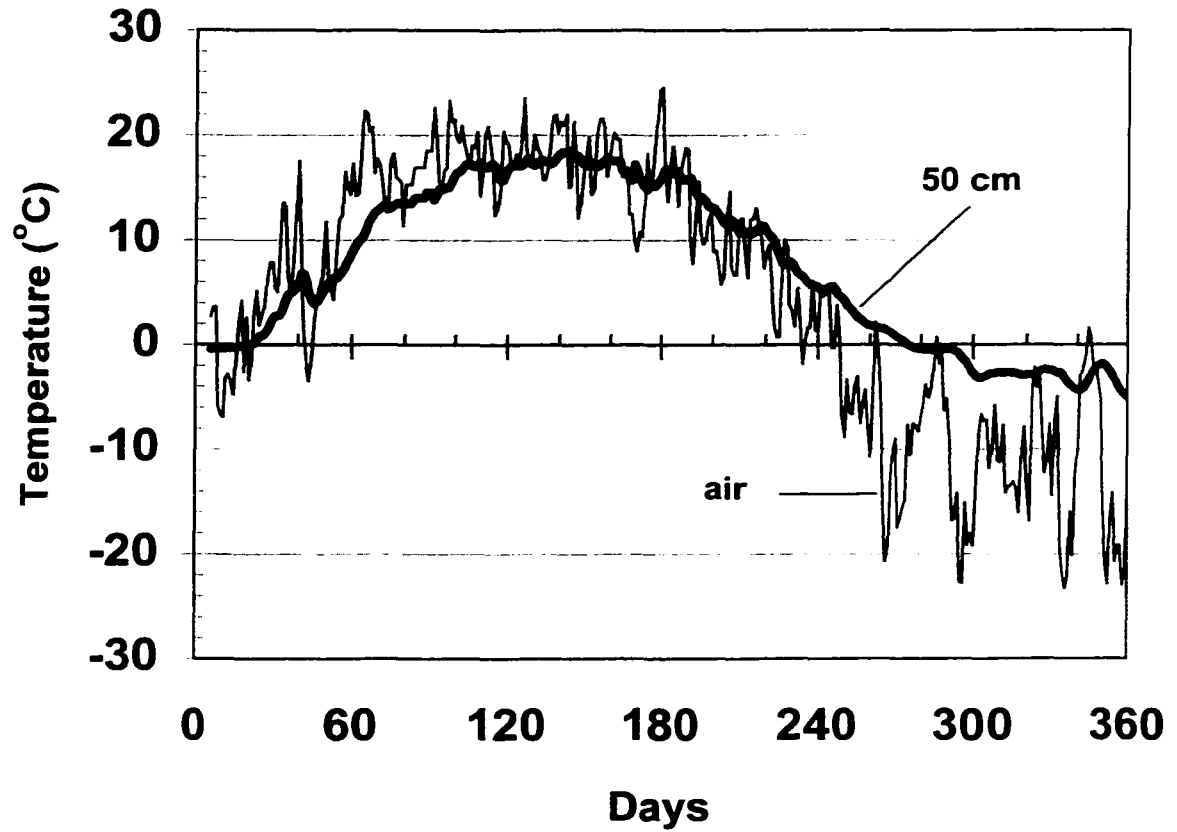


Figure 6. Daily mean air and 50cm depth temperatures recorded at Streeter from 3/15/94 to 3/10/95.

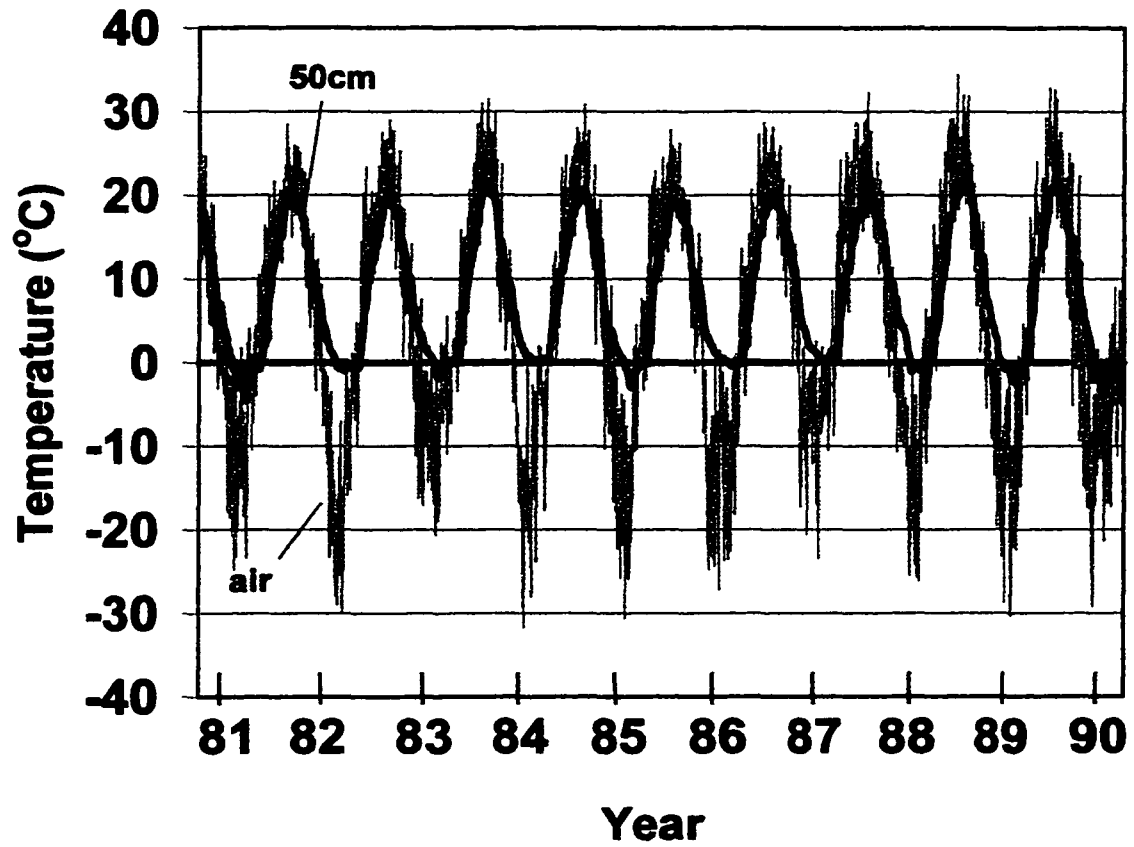


Figure 7. Daily mean air and 50cm depth temperatures recorded from 10/10/1980 to 4/16/1990 at Fargo showing annual separation of air and ground temperatures.

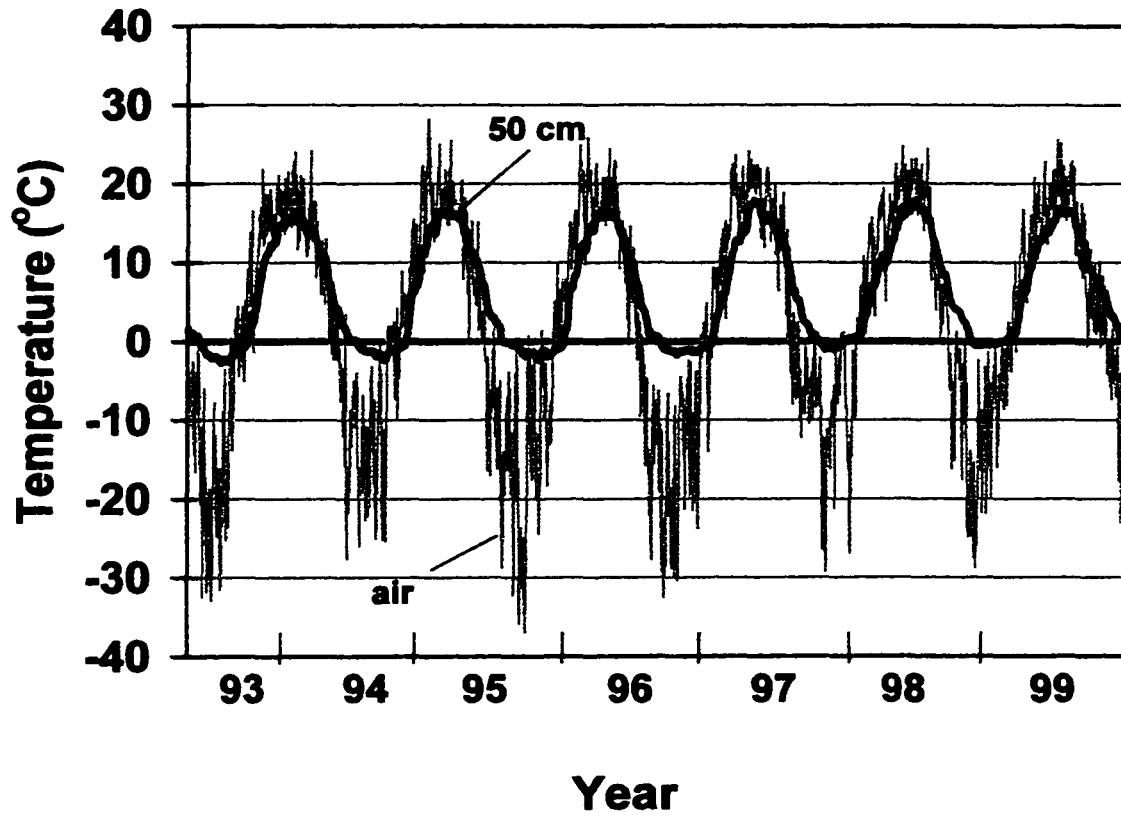


Figure 8. Daily mean air and 50cm depth temperatures recorded from 11/25/1993 to 1/1/2000 at Bottineau showing annual separation of air and ground temperatures.

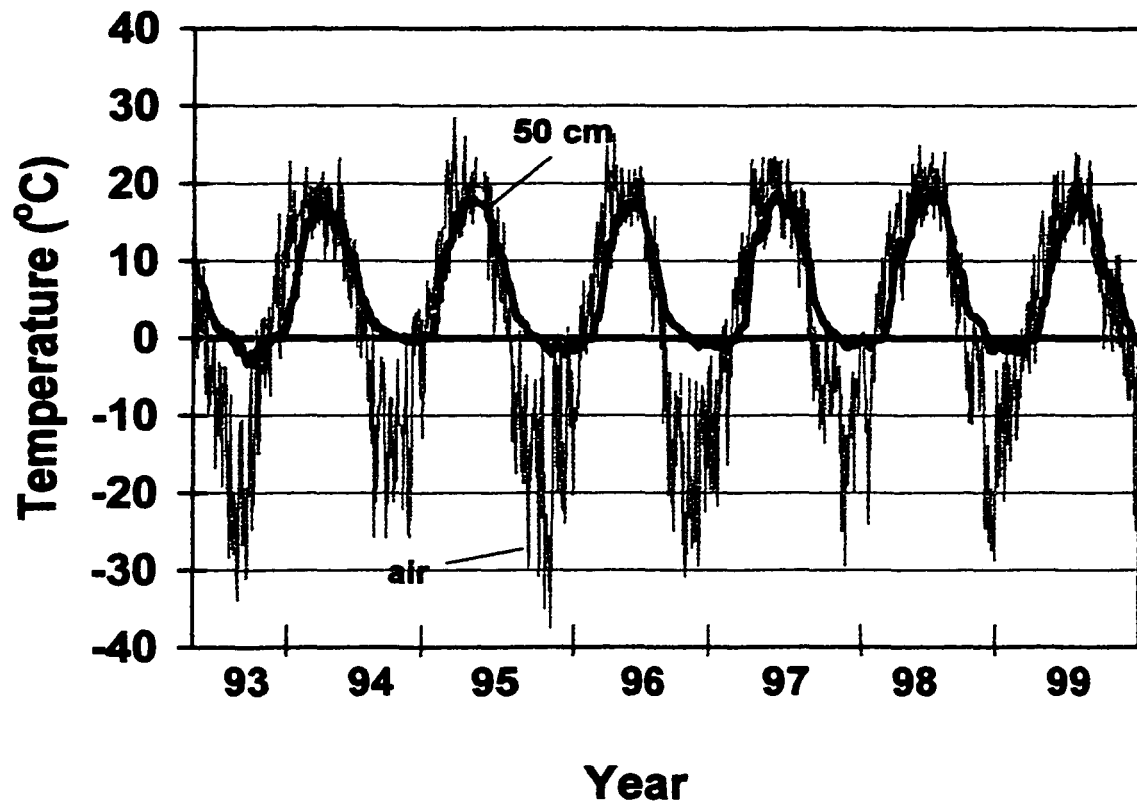


Figure 9. Daily mean air and 50cm depth temperatures recorded from 10/1/1993 to 1/1/2000 at Langdon showing annual separation of air and ground temperatures.

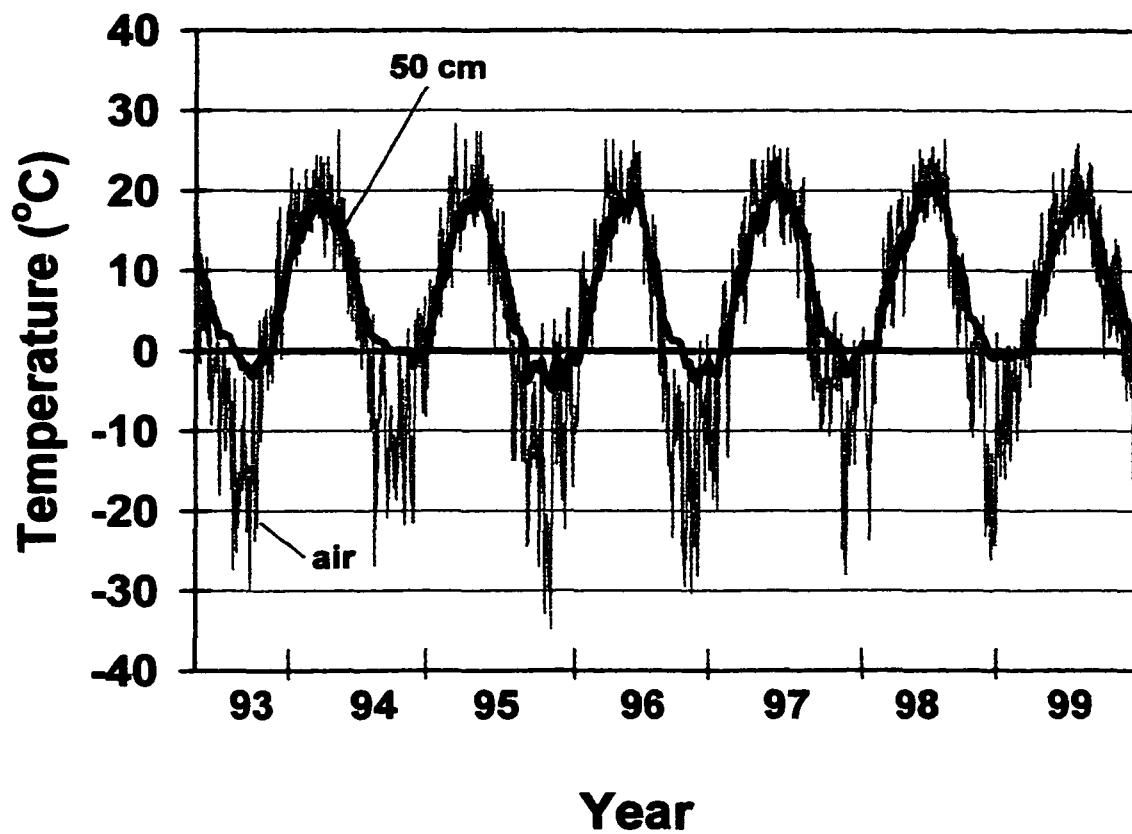


Figure 10. Daily mean air and 50cm depth temperatures recorded from 10/1/1993 to 1/1/2000 at Minot showing annual separation of air and ground temperatures.

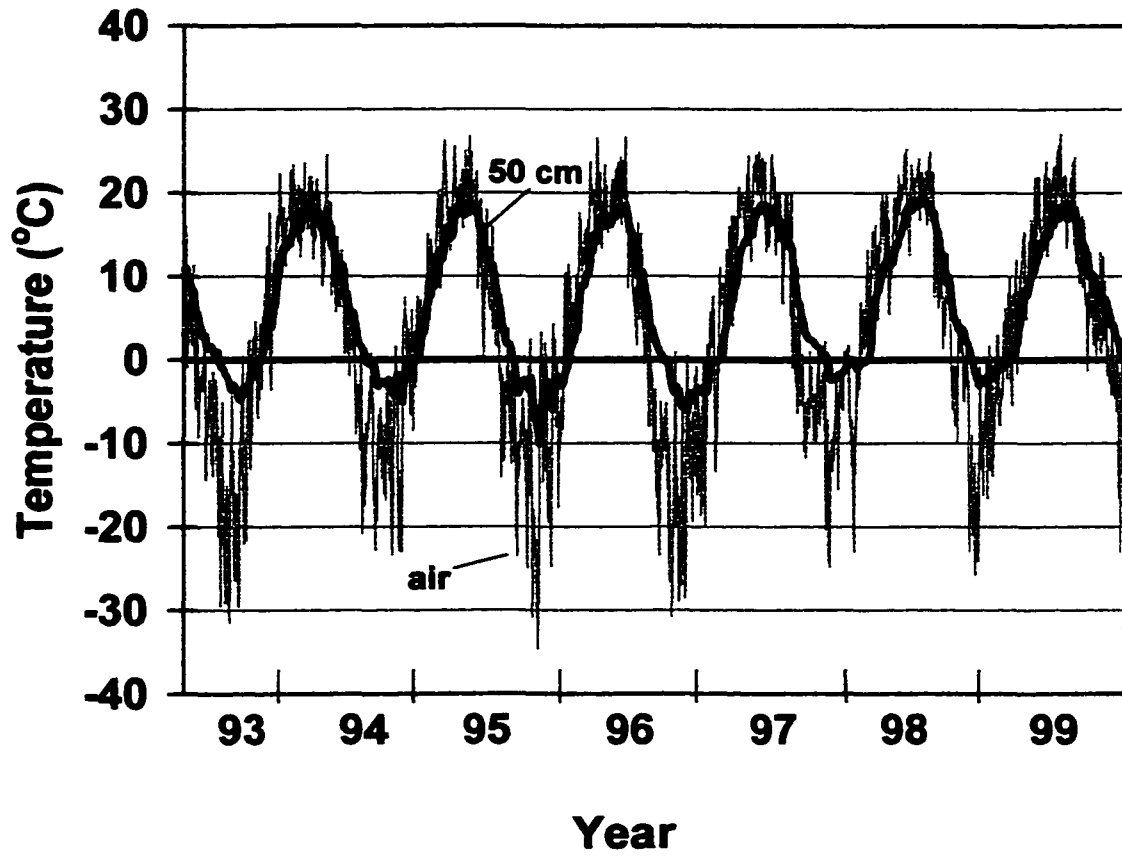


Figure 11. Daily mean air and 50cm depth temperatures recorded from 10/1/1993 to 1/1/2000 at Streeter showing annual separation of air and ground temperatures.

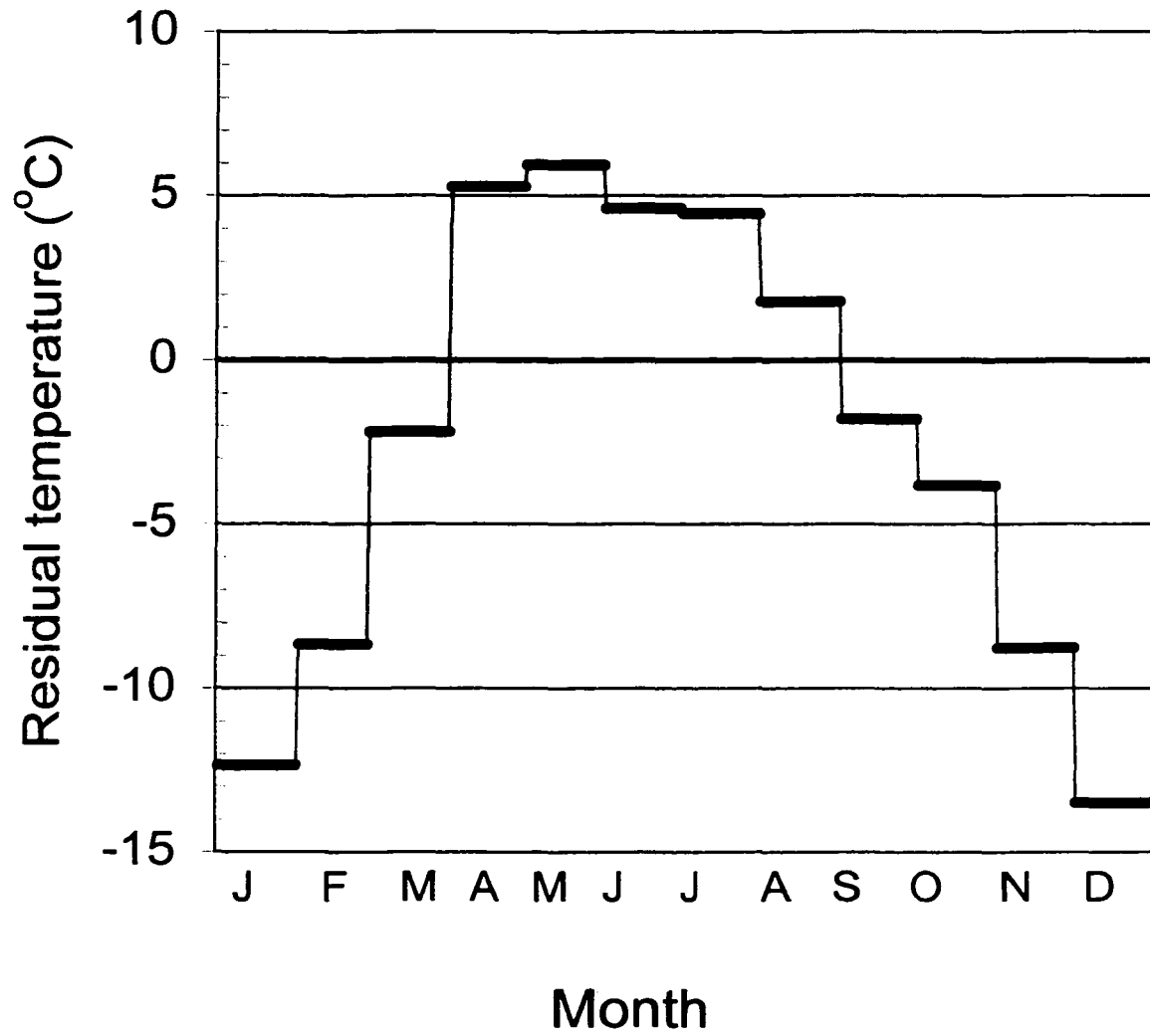


Figure 13. Monthly air and 50cm-depth temperature differences from Fargo averaged from 1981 to 1989.

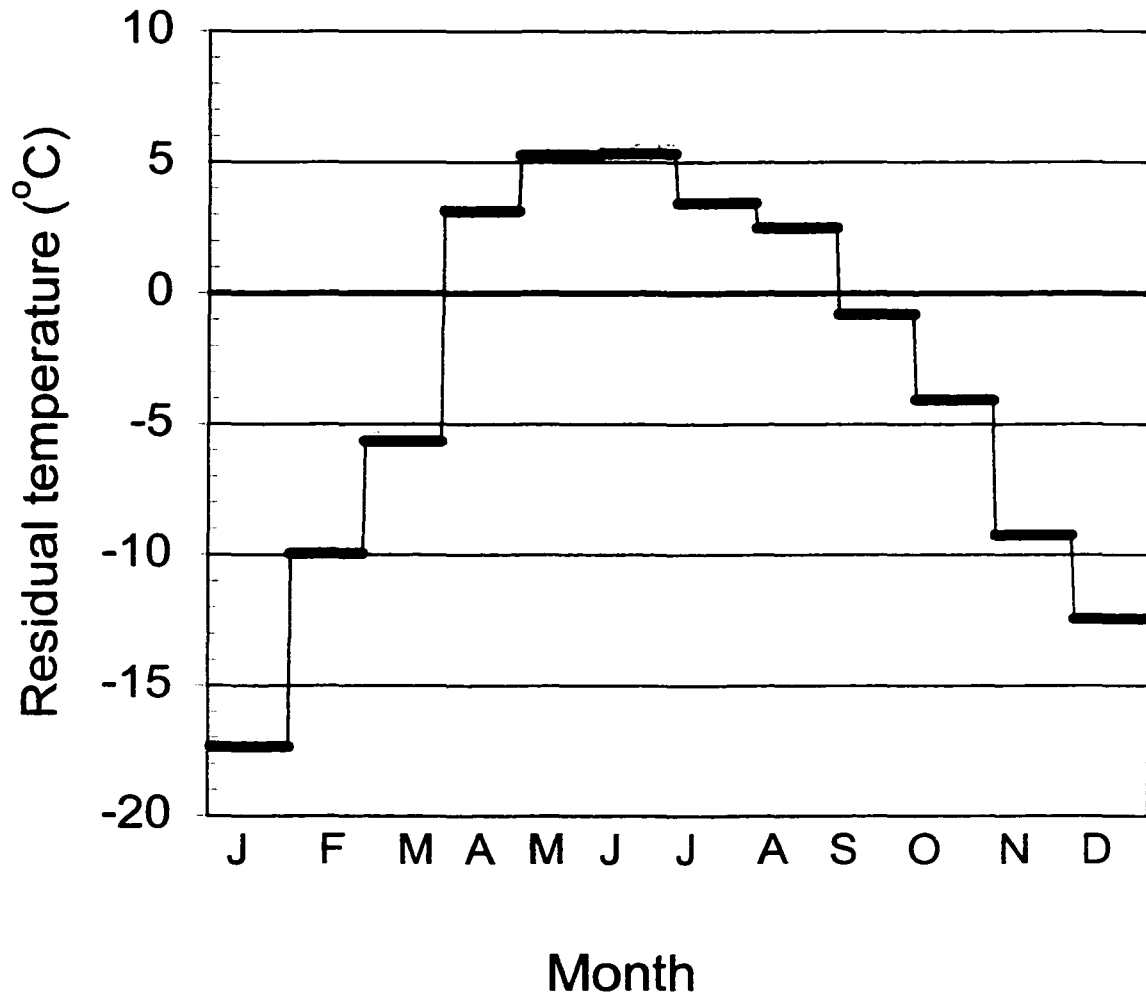


Figure 14. Monthly air and 50cm-depth temperature differences from Bottineau averaged from 1994 to 1999.

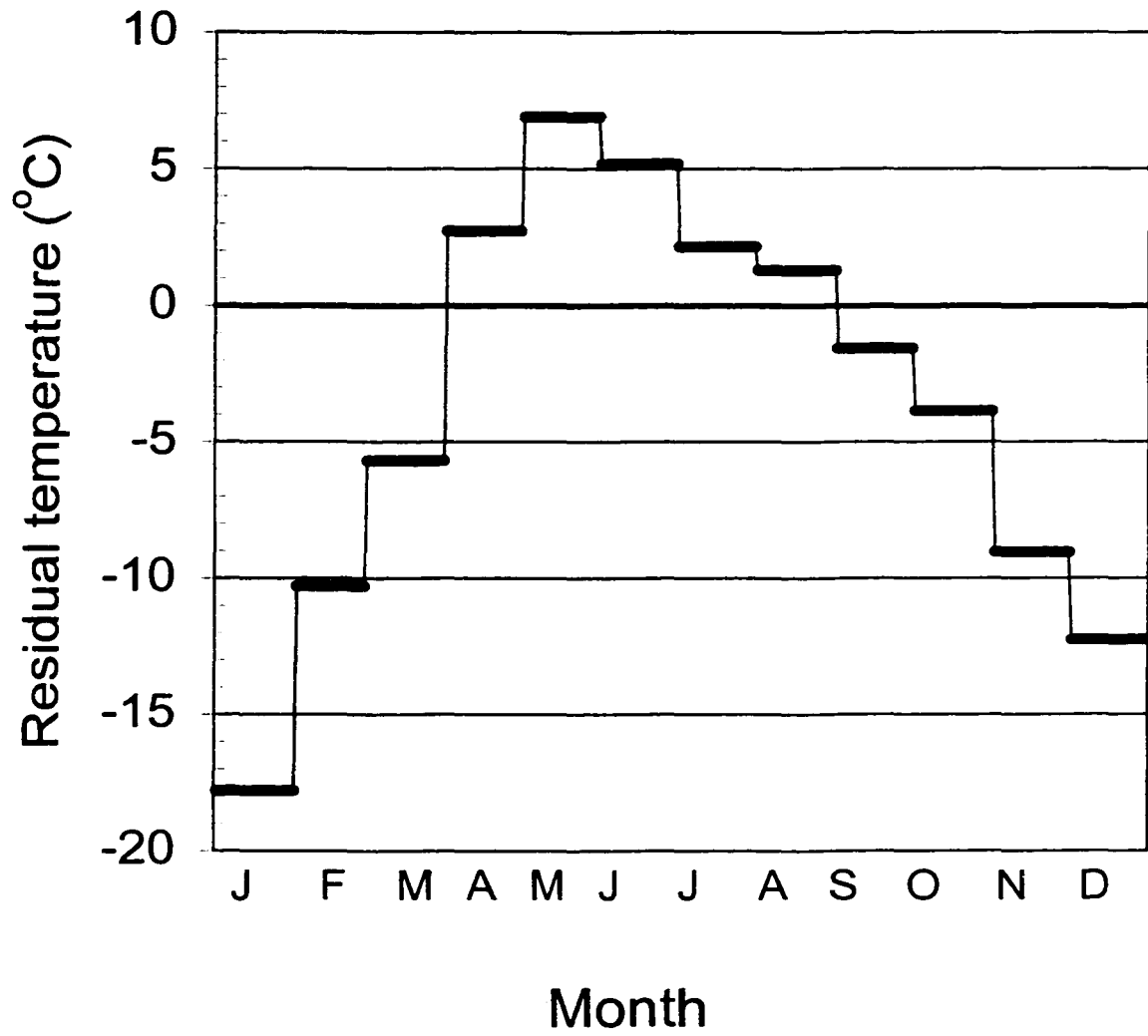


Figure 15. Monthly air and 50cm-depth temperature differences from Langdon averaged from 1994 to 1999.

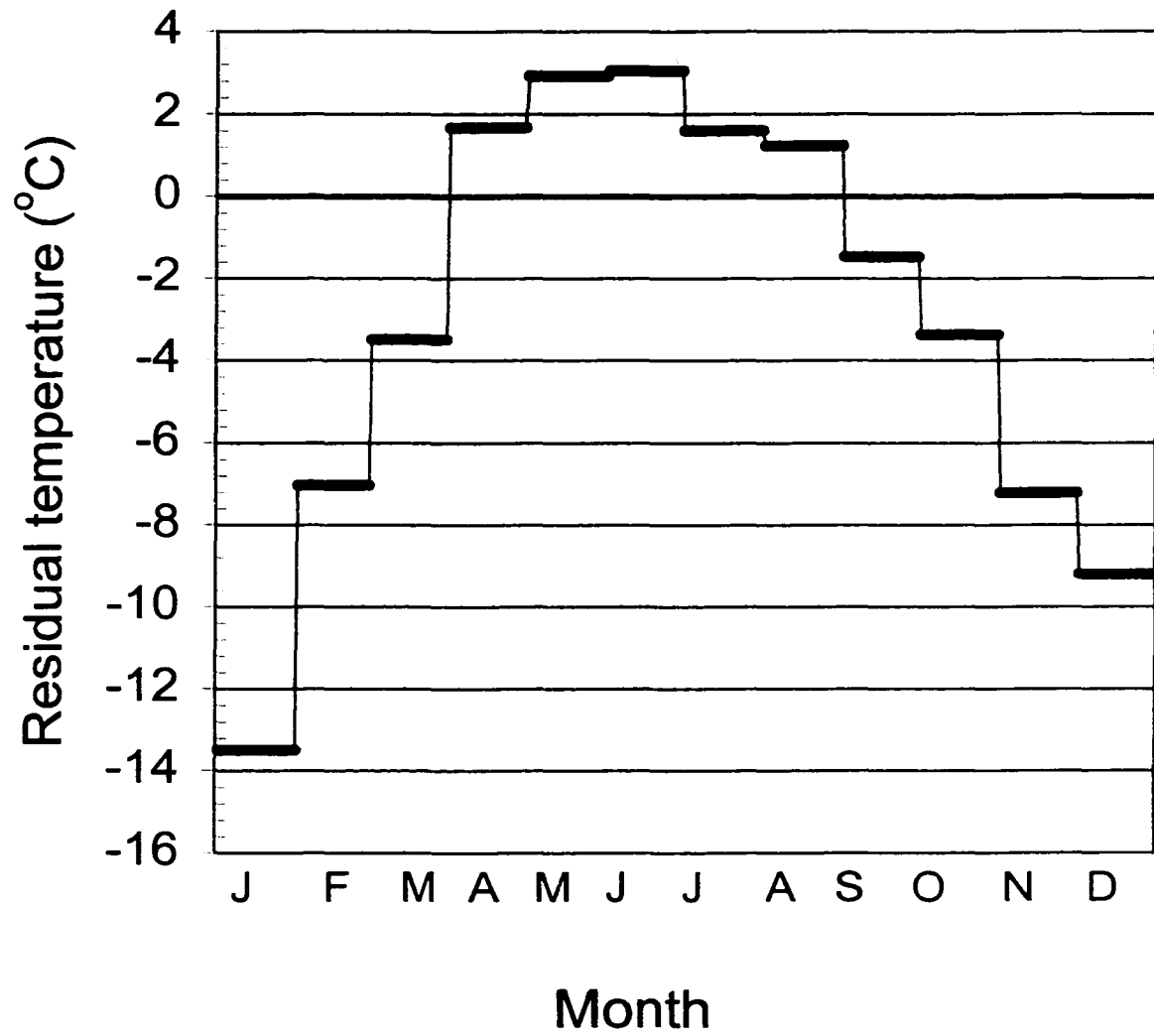


Figure 16. Monthly air and 50cm-depth temperature differences from Minot averaged from 1994 to 1999.

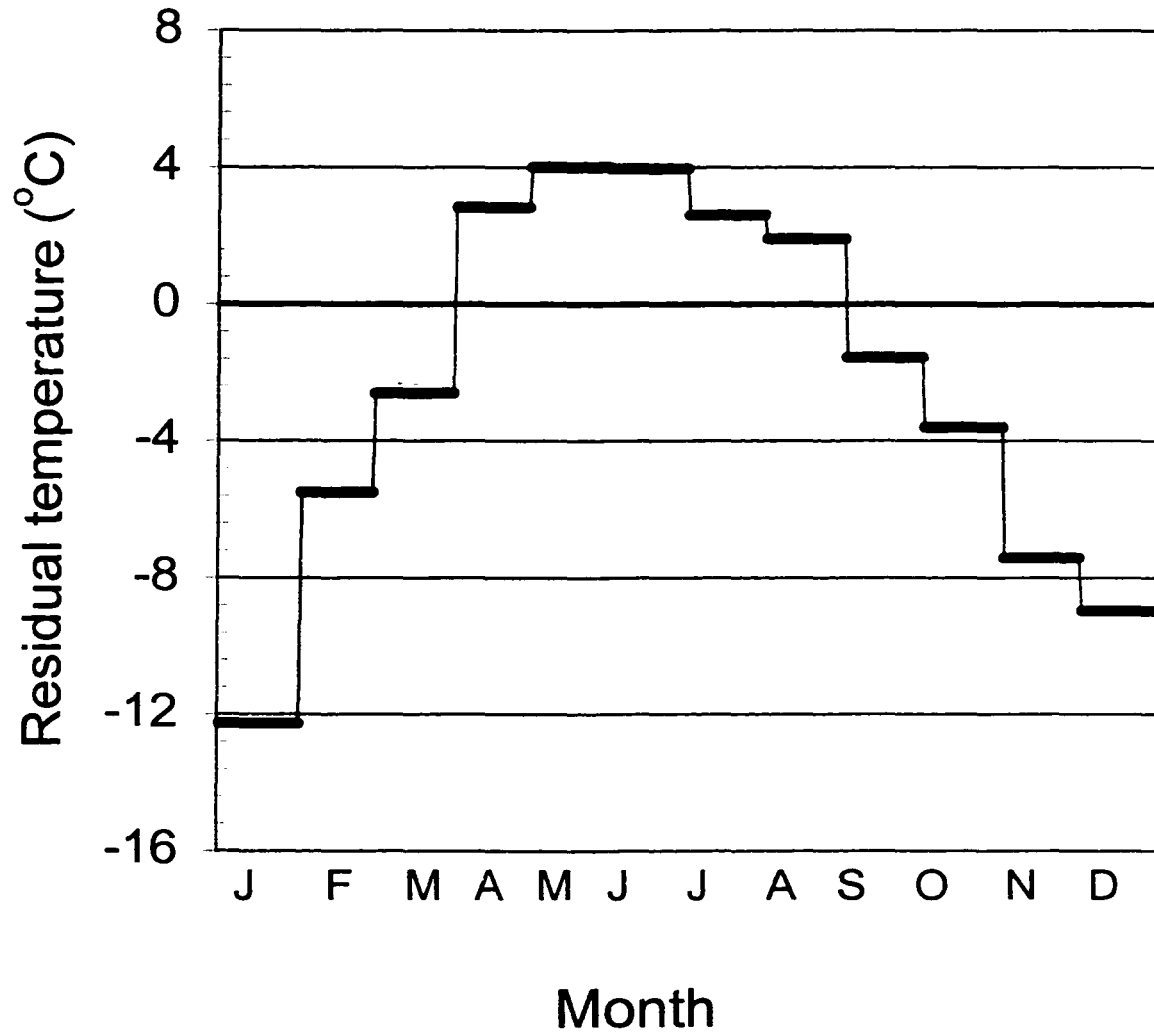


Figure 17. Monthly air and 50cm-depth temperature differences from Streeter averaged from 1994 to 1999.

50cm-depth temperature differences from all sites. The seasonal reversal of net ground-surface energy from negative (winter) to positive (summer) is recognizable in the sinusoidal trend of monthly mean residual temperatures (Figs. 13-17).

Factors decoupling air and ground temperatures

Vegetation and snow cover significantly influence air-ground temperature exchange by introducing an energy-absorbing layer between the air and ground surface. Fresh snow cover often reflects more than 90% of incident radiation (Enz, 1985). Vegetation adsorbs incident energy and takes part in radiative, conductive and moisture exchange processes (Geiger et al., 1995). There is a general decrease in mean annual ground temperatures with increasing vegetation (Smith, 1975). The total surface area of vegetation in a meadow is 20-40 times the area of the ground on which it grows (Geiger et al., 1995). The quantity of solar radiation penetrating the ground depends upon the density and structure of the plant cover (Oke, 1987).

The Fargo NDAWN site has a 4-12cm-high grassy cover. All other NDAWN sites are covered by moderate-density prairie grass. The onset of vegetative cover at all sites varies seasonally depending on temperature, sunlight, cloud cover, humidity, moisture conditions, and the timing of spring thawing (Geiger et al., 1995). Active vegetation at these sites occurs from about April to September (Enz, personal communications). However, resolving the effects of vegetation on daily-mean air-ground temperature differences is difficult for the following reasons: 1) Vegetation effects are cumulative over periods of several months. The onset and decrease of vegetative activity is very gradual compared to the diurnal averaging period; 2) The diurnal averaging period

includes night times with no photosynthesis or evaporation effects; and 3) Because vegetation adsorbs a significant amount of energy at the boundary layer, its influence is not completely restricted to either air or ground temperatures.

Incident solar radiation

Incident solar radiation is susceptible to changes in cloud cover, solar angle, and seasonal changes (Enz, 1985). The ground surface does not store energy, but a considerable exchange of energy occurs across it (Geiger et al., 1995). Air temperatures during the summer are warmer than ground temperatures because of higher incident radiation causing an excess of net energy in the ground surface (Geiger et al., 1995). The excess energy during the summer is conducted into the soil, re-radiated into the atmosphere, and involved in water phase changes at the boundary level (Geiger et al., 1995). Winter ground temperatures are warmer than air temperatures because of a net energy deficit at the ground surface (Geiger et al., 1995). Winter ground temperatures are insulated by the snow layer and latent energy of freezing effects. The deficit of ground surface energy during the winter means that heat is conducted upward toward the boundary layer.

A plot of monthly averaged incident solar radiation recorded from 1953 – 1975 in Bismarck, ND shows the annual radiation variability ranging from maximum during July to minimum during December (Fig. 18, Enz, 1985). Average incident radiation values during June and July are four times that of December and January (Fig. 18). Average annual incident radiation recorded in Bismarck during 1985 was $14277 \text{ KJ m}^{-1} \text{ day}^{-1}$.

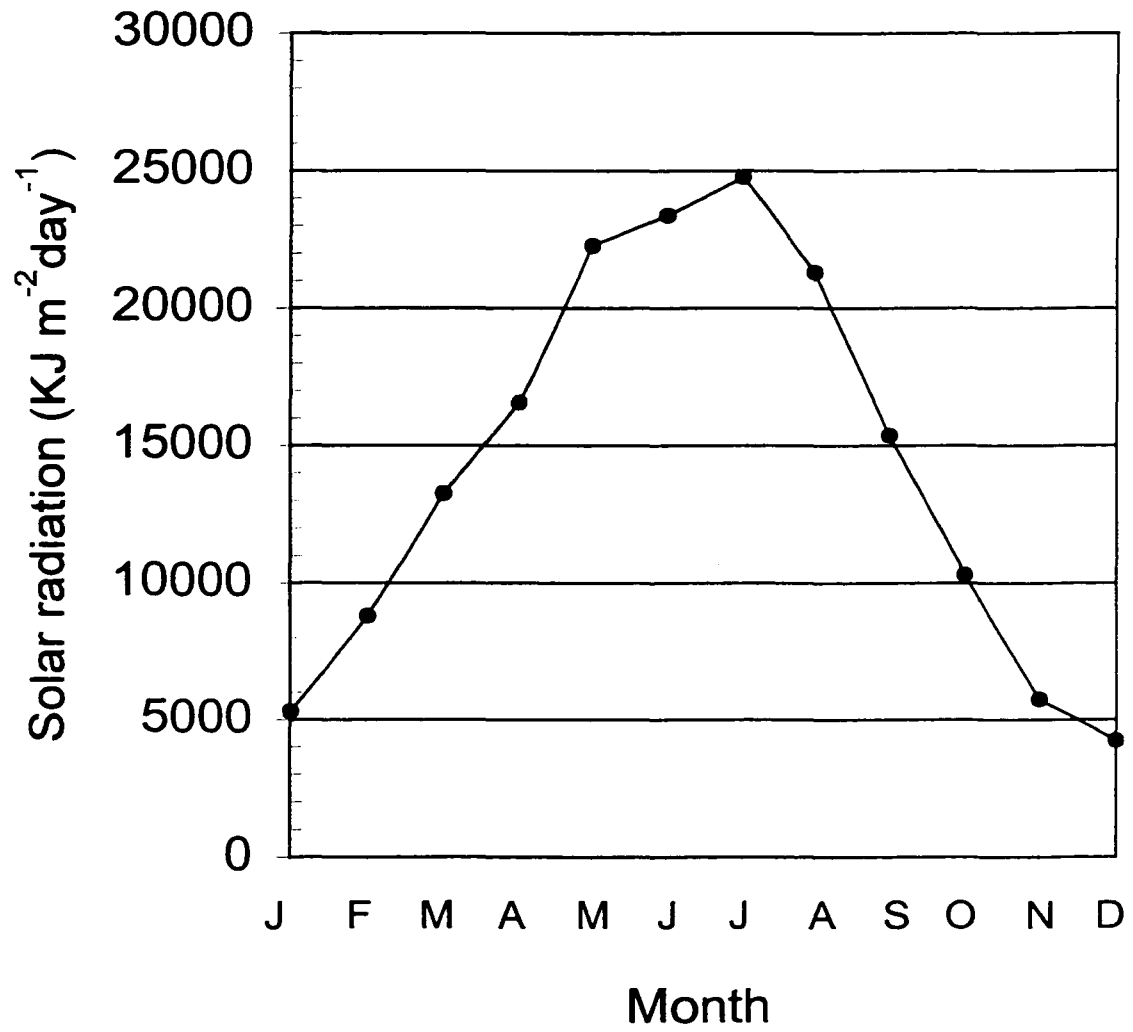


Figure 18. Monthly averaged incident solar radiation recorded from 1953 to 1975 in Bismarck, ND.

The relationship between daily mean air temperatures and daily solar radiation values recorded at Bismarck shows significant seasonal variation (Enz, 1985). During the period May to October, there is a direct correlation between daily mean air temperatures and average daily solar radiation (Enz, 1985). The days with high solar radiation tend to be the warmest because of intense surface heating. High radiation days during the winter are associated with cold dry air from the arctic and clear skies. However, because of reflection from snow cover, radiation causes little surface heating and air temperatures remain low (Enz, 1985). Winter storm periods are associated with warm, humid air moving up from the south. These conditions produce maximum cloudiness, low solar radiation, and temperatures near freezing (Enz, 1985). If there is little or no snow cover on the ground and a dry, mild air mass present, skies are usually clear. The combination of clear skies and high solar heating causes relatively high air temperatures (Enz, 1985).

Daily mean air and 50cm-depth temperatures (Figs. 7-11), monthly averaged residual temperatures (Figs. 13-17), and monthly average incident radiation (Fig. 18) are referenced for the following points:

- 1). The magnitude of winter separation of air and ground temperature significantly exceeds the separation during any other time of the year. The magnitude of residual temperature in January is more than twice that of any summer month. Monthly averaged ground temperatures are higher than monthly averaged air temperatures at all sites for the period September to March. All sites have been subject to annual snow cover and ground freezing effects from November to April. Winter factors causing insulation of ground

temperatures are susceptible to secular changes, including snow cover, latent energy of phase changes, and changes in thermal parameters of the subsurface due to the presence of pore ice (Farouki, 1981). The 9 percent volumetric increase in converting water to ice causes soils to expand and reduces the volume of air in pore spaces (Farouki, 1981). When soil freezes, its thermal diffusivity will typically increase from 20 to 50 percent (Geiger et al., 1995). The observed separation of winter air and ground temperatures at all sites is attributed to a combination of these insulating factors. Snow cover and latent energy of freezing effects are examined more closely in Chapters 5-7.

2). Monthly ground temperatures are cooler than monthly air temperatures from April to August. This period coincides with the time of highest monthly-averaged incident radiation. Net ground surface energy as well as vegetation effects are therefore highest during these months. The highest monthly residual temperatures during a non-winter period occur during May and June. Most residual temperatures are closest to 0°C during September. This is also the first fall month when average ground temperatures exceed average air temperatures. Average incident radiation during September ($15,377 \text{ KJ m}^{-2} \text{ day}^{-1}$) is about halfway between minimum ($4,229 \text{ KJ m}^{-2} \text{ day}^{-1}$ during December) and maximum ($24,782 \text{ KJ m}^{-2} \text{ day}^{-1}$ during July). The ground surface during September is subject to lower incident radiation and vegetative effects than during summer months. It's normal for vegetation in North Dakota to have extracted all the available water from the root zone by late summer (Fanning et al., 1981). Soil moisture content tends to be lowest in Fargo during the fall, depending on summer precipitation (Enz, personal communication).

3). The greatest increase in residual temperatures occurs between the months of March and April at all sites. Spring periods are times of high radiation adsorption, moist, dark, low albedo soils, and no vegetation effects (Geiger et al., 1995). Dark surfaces tend to adsorb more radiation than light surfaces. Several nonconductive effects occur during the spring, including meltwater infiltration effects, latent energy effects of freezing and refreezing, thawing, condensation, evaporation, and sublimation, and ionic diffusion due to melting of pore ice (Oke, 1987, Outcalt, 1990). These factors are controlled by the timing of spring snowmelt (Geiger et al., 1995). Spring is the time of highest soil moisture with a gradual decrease occurring during summer and fall (Enz, personal communications). The combination of these factors causes the abrupt increase in monthly-averaged residual temperatures.

Residual temperatures and precipitation

Because of the influence of water on soil temperatures and thermal properties, the correlation between daily residual temperatures and daily total precipitation was tested for one to five-month periods with data from all sites. This correlation was also tested with monthly mean residual temperatures and monthly precipitation totals. No correlation coefficient greater than $r^2 = .1$ was determined for either time scale. Possible explanations for this are: 1) The timing of infiltration effects on ground temperatures may not coincide with the 24-hour temperature averaging periods. The influence of precipitation infiltration on ground temperatures can extend for several days depending on the precipitation event (Fanning et al., 1981). Infiltration occurring during the last few hours of the averaging period could significantly influence the daily mean temperature.

The thermal effects of precipitation infiltration would be more easily discerned with continually recorded hourly temperatures; 2) Antecedent moisture content influences infiltration rates and amounts (Fanning et al., 1981). If the water table is already at the ground surface, it is possible that little to no infiltration of precipitation will occur; and 3) Precipitation may cause a gain or loss of energy, depending on the relative temperature of the ground (Geiger et al., 1995). Because of their interconnectedness, air and ground temperatures can be simultaneously influenced by precipitation. In this case daily mean temperature differences would not indicate any anomalous event.

CHAPTER 4

AN ANALYSIS OF AIR AND GROUND TEMPERATURES

Fargo

Because the Fargo data extend longer and contain deeper ground temperatures than the other sites, they are described separately. The surface air temperature record from the NCDC station in Fargo extends to 1884, with a 4.75°C average mean-annual air temperature for the period 1884-1999 (Fig. 19). A least-squares linear regression of mean annual air temperatures during this time indicates a slope of $+1.61 \pm .24^\circ\text{C}$ during the period of record (Fig. 19). Three of the four highest mean annual air temperatures occurred in the past 13 years, including 7.97 (1987), 7.69 (1931), 7.56 (1998), and 7.17°C (1999). The average mean annual temperature from 1981 to 1989 was higher than the average mean-annual air temperature from 1884 to 1999 (6.02 versus 4.75°C).

Attenuation of seasonal temperature fluctuations and successive phase lag with depth can be seen in the time series plot of daily mean temperatures at depths of 80, 250, 470, and 1170cm (Fig. 20). The annual temperature signal of about 35° at 1cm depth is attenuated to 1° at 1170cm depth. The thermal diffusivity that generates this attenuation of the annual temperature wave at 1170cm depth is $3.62 \times 10^{-7} \text{m}^2/\text{s}$. The 1170cm-depth temperature displays a visible warming trend during the period of record (Fig. 20). Seasonal ground freezing was confined to the upper 1m of the soil for all winters.

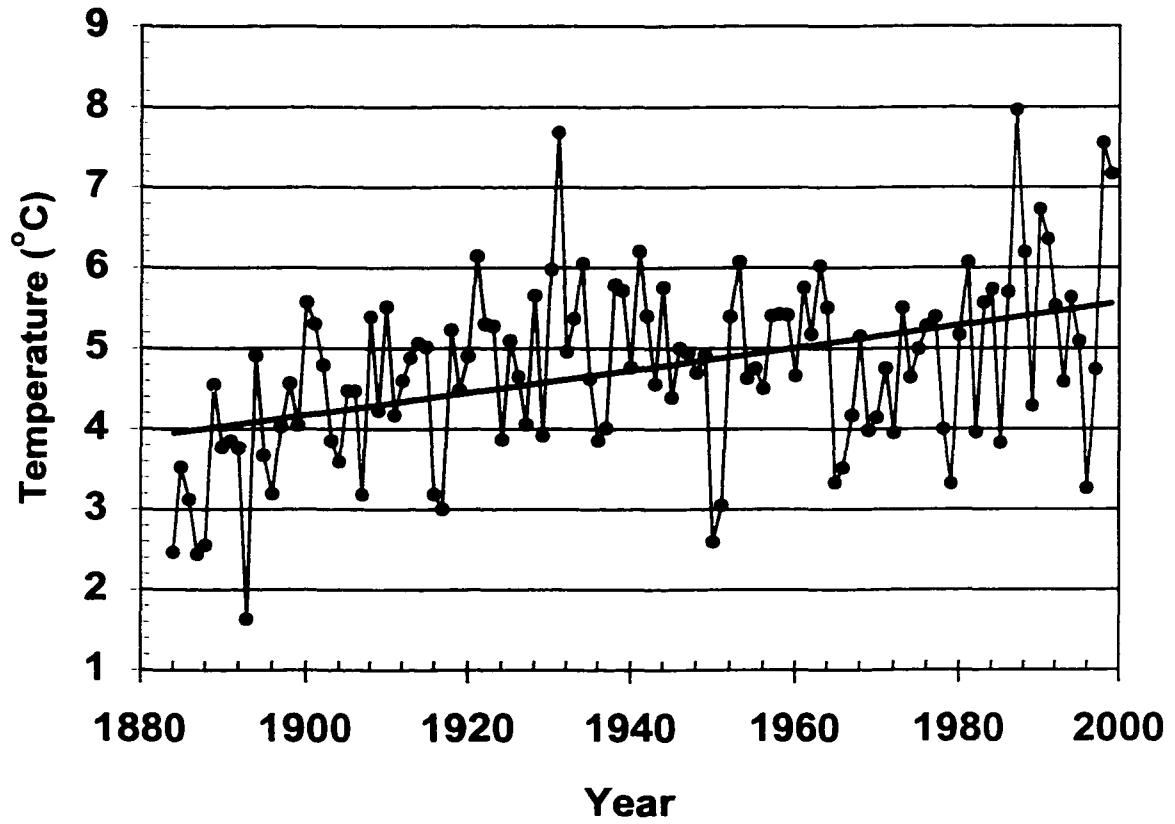


Figure 19. Mean annual air temperatures recorded at Fargo from 1884 to 1999. A least-squares linear regression line is shown.

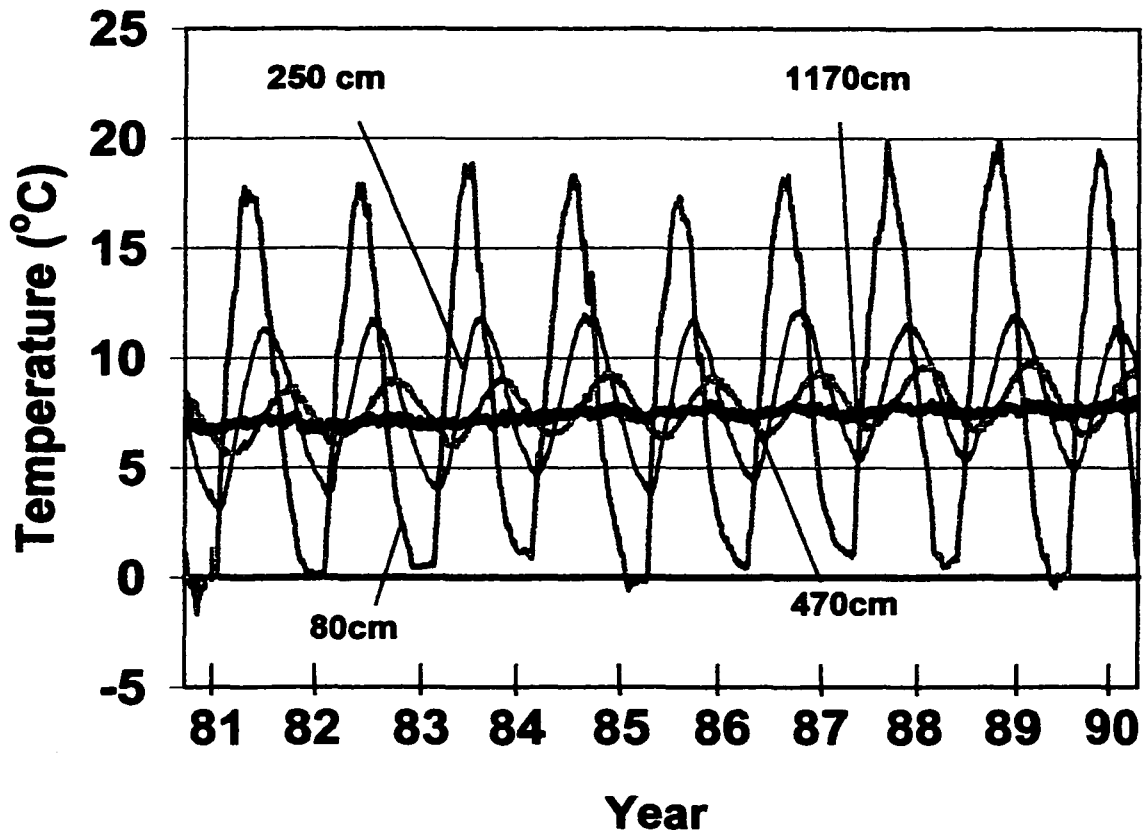


Figure 20. Daily mean 80cm, 250cm, 470cm, and 1170cm depth temperatures recorded at Fargo from 10/10/1980 to 4/16/1990. Phase lag and attenuation of the annual temperature signal with depth are observable.

To better understand soil temperatures at varying depths on a decadal scale, air and individual ground temperatures were averaged over the period January 1, 1981 to December 31, 1989. These values are given in Table 3 and plotted as a function of depth in Figure 21. All average ground temperatures were higher than the average air temperature (6.02°C) (Fig. 21). The highest average temperature for the 9-year period (9.54°C) occurred at the 1cm depth (Fig. 21). The greatest energy adsorption and emission occurs at this depth in the soil column. The differences between average air and ground temperatures decrease with increasing depth (Table 3).

Integrated heat flux

Average ground temperatures in the upper 50cm of Figure 21 are plotted with a steady-state background heat flow measured at a borehole within 75km of Fargo (Fig. 22, Scattolini, 1978). The 60m-deep borehole was logged in 1976 and indicated a measured temperature gradient of 15.8°C/km (Scattolini, 1978). The borehole is located at 46° 15.75' N latitude and 96° 56.75' W longitude. The total amount of heat retained in the upper 50cm of the soil column during the period of record at Fargo is the area between the curves in Figure 22. The total amount of heat, Q , retained by the soil column during the period of record is

$$Q = \int_0^z \rho c T(z) dz \quad (1)$$

Table 3. Air and ground temperatures averaged from 1/1/81 to 12/31/89. Differences between air and ground temperatures and warming magnitudes per decade determined by least-squares linear regression lines are also shown.

Depth (cm)	Average temp	$T_{\text{ground}} - T_{\text{air}}$ (deg. C)	Warming magnitude
	1/1/81-12/31/89 (deg.C)		per decade (deg. C)
Air	6.15	-	-
1	9.54	3.39	-
5	8.79	2.65	-
10	8.90	2.75	-
20	8.55	2.41	-
30	8.66	2.51	-
50	8.47	2.32	-
60	8.15	2.00	-
80	8.29	2.14	-
125	8.08	1.93	0.98 \pm .12
150	8.25	2.11	1.10 \pm .11
200	8.03	1.88	1.15 \pm .10
250	8.04	1.89	1.11 \pm .09
270	7.99	1.84	0.96 \pm .09
300	7.90	1.75	1.12 \pm .08
370	7.88	1.74	1.07 \pm .07
470	7.67	1.52	1.01 \pm .05
770	7.69	1.54	1.04 \pm .04
970	7.20	1.06	1.00 \pm .03
1170	7.39	1.24	0.75 \pm .03
Average	8.18	2.04	0.93\pm.08

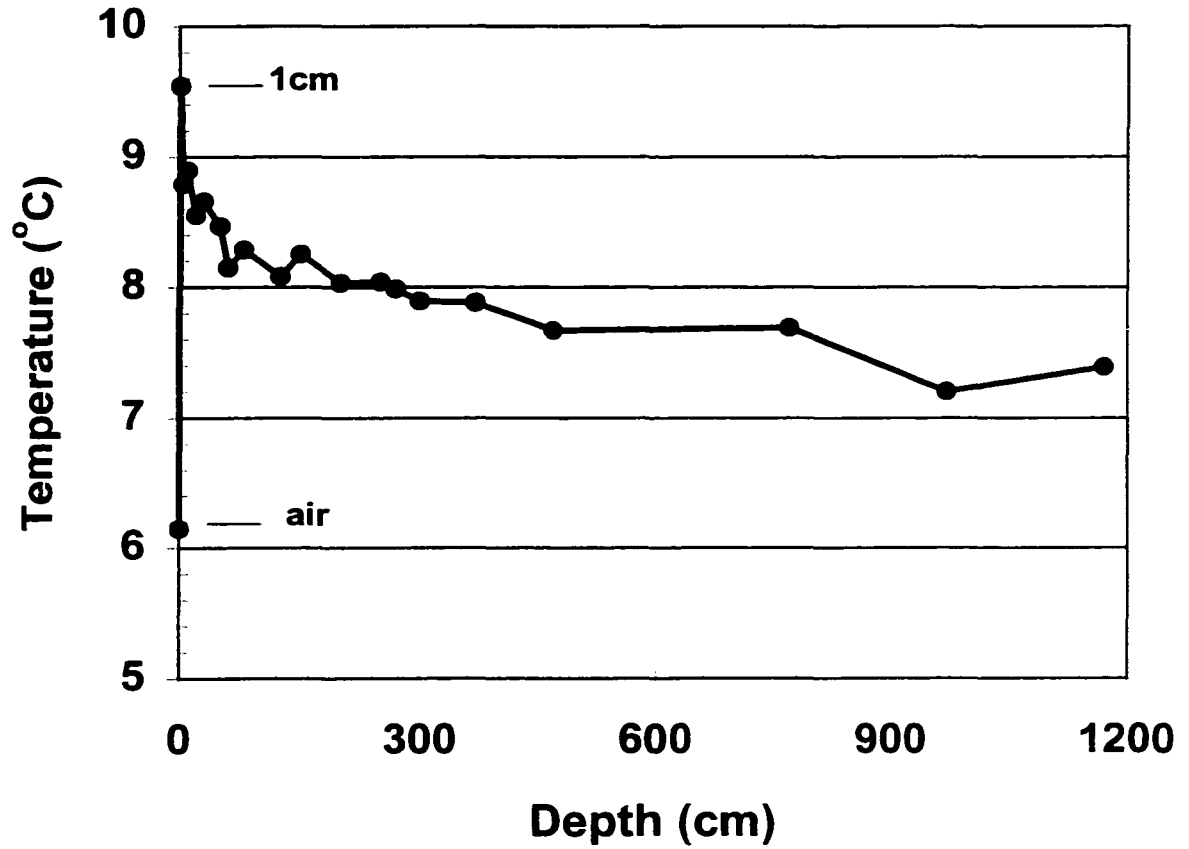


Figure 21. Air and ground temperatures from all measurement depths averaged over the period 1/1/81 to 12/31/89 and plotted as a function of depth.

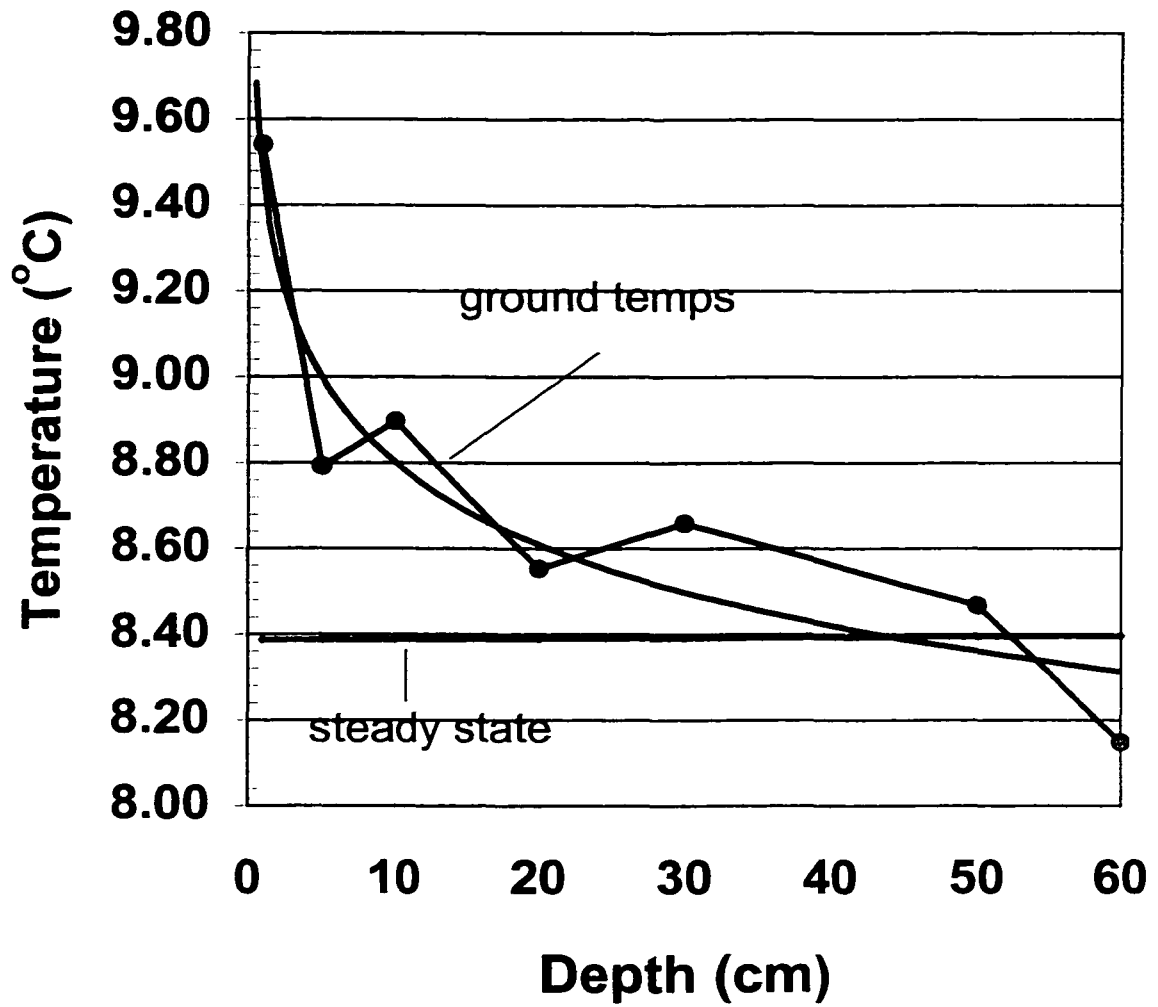


Figure 22. Ground temperatures in the upper 50cm of the ground at Fargo averaged over the period 1981 to 1989. An exponential smoothing curve is plotted for ground temperatures. The steady-state background heat flow from a 60m-deep borehole is shown.

where ρc is the volumetric heat capacity and z is the depth to which the anomalous temperature extends (Lachenbruch and Marshall, 1986). In this case $T(z)$ is not a known function, but is an average temperature at given depths representing the 9-year period. To graphically approximate the area between the curves an exponential smoothing curve is added to Figure 22. Assuming $\rho c = 0.5 \text{ cal cm}^{-3} \text{ K}^{-1}$ (Lachenbruch and Marshall, 1986), the total heat retained by the soil during the period of record is $3 \times 10^5 \text{ J m}^{-2} \text{ s}^{-1}$, or $8 \times 10^{12} \text{ J m}^{-2} \text{ yr}^{-1}$. Assuming the steady-state heat flow and gradient used in this calculation is equivalent to that of the Fargo site, the upper 50cm of the ground recorded a net positive energy flux during the period of record. However, a 76m-deep borehole within 90km of Fargo logged in 1976 indicates a temperature gradient of 20.5°C/km with a surface intercept of 8.67°C (Scattolini, 1978). Therefore estimates of background heat flow values can vary significantly over short distances.

Linear regressions of mean annual temperatures

Mean annual ground temperatures from all depths were plotted for the 9-year period and analyzed with least-squares linear regressions. All 125-1170cm-depth temperatures displayed significant-fit regressions at the 95% confidence level. Warming per decade magnitudes are shown in Figure 23. The temperatures from 770-1170cm depths displayed low variation and nearly linear increases during the decade. Mean annual ground temperatures in the upper 80cm exhibited higher variability that reduced the reliability of the regression. The high variability of near-surface ground temperatures is due to low attenuation of the varying climatic signal and ground-surface effects including incident radiation, precipitation, wind speed, vegetation effects, runoff,

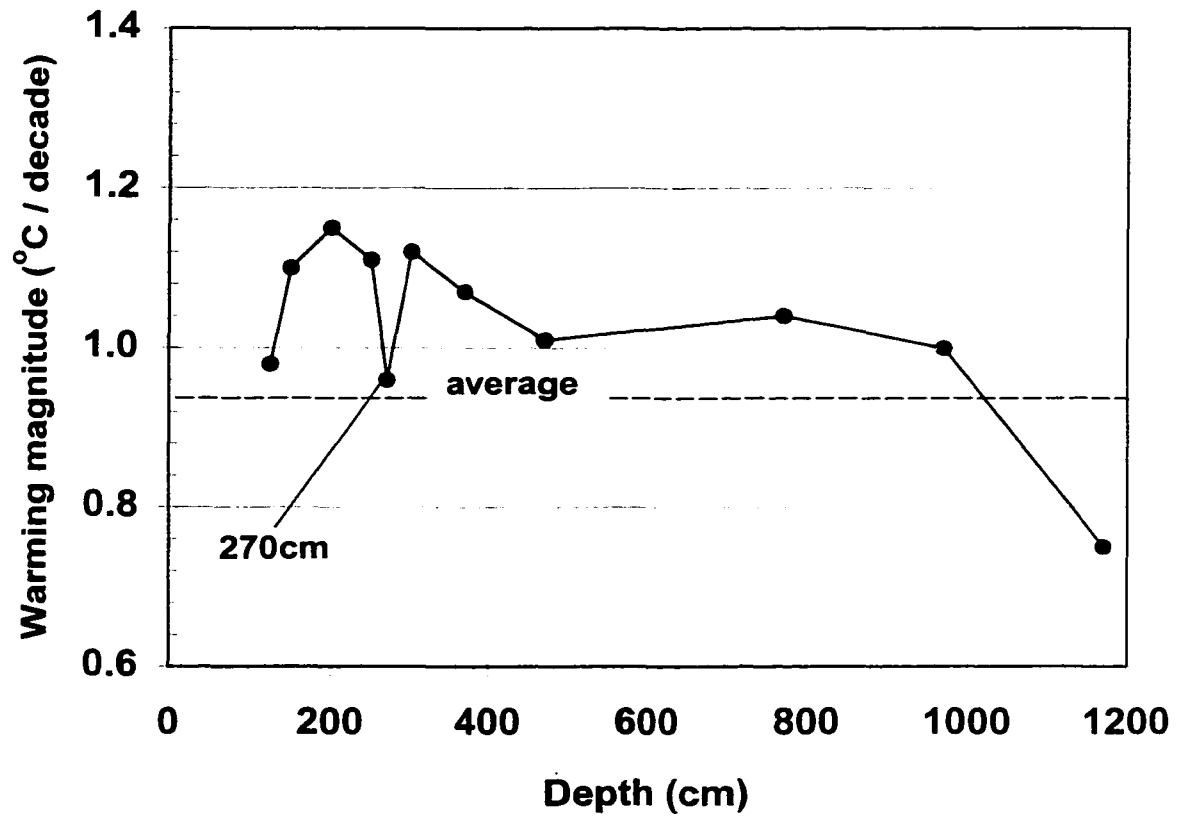


Figure 23. Warming magnitudes per decade of Fargo mean annual ground temperatures from 125-1170cm depths plotted as a function of depth.

infiltration, evaporation, condensation and soil cracking during extensive dry periods. The warming per decade magnitudes of mean-annual ground temperatures from 125-1170cm suggest inaccurate calibration of the 270cm-depth thermocouples (Fig. 23). The greatest temperature increase during the period of study ($1.15 \pm 0.10^\circ\text{C}$) occurred at 200cm depth. Warming rates per decade of individual depths from 125–1170cm are given in Table 3.

Mean annual ground temperatures from all measurement depths were averaged into a single mean annual value and plotted for the period 1981-1989 (Fig. 24). A least-squares linear regression of these temperatures yields a slope of $+0.93 \pm 0.09^\circ\text{C}$ per decade (Fig. 24). Mean annual air temperatures plotted from 1981-1989 do not generate a significant-fit regression line at the 95% confidence limit due to high variability. The hypothesis that mean annual air and ground temperatures yield different warming magnitudes per decade is tested. Mean annual air and ground temperatures are plotted to determine the confidence limits on the correlation coefficient of regression lines for each data set. This test did not generate a significant-fit correlation at the 95% confidence limit. The hypothesis that mean annual air and ground temperatures show *different* trends during the 9-year period is therefore rejected. Although mean annual ground temperatures display a significant-fit trend during the period of record, the high variability in the linear regression of air temperatures yields too much uncertainty to state that warming during the decade occurred only in ground temperatures.

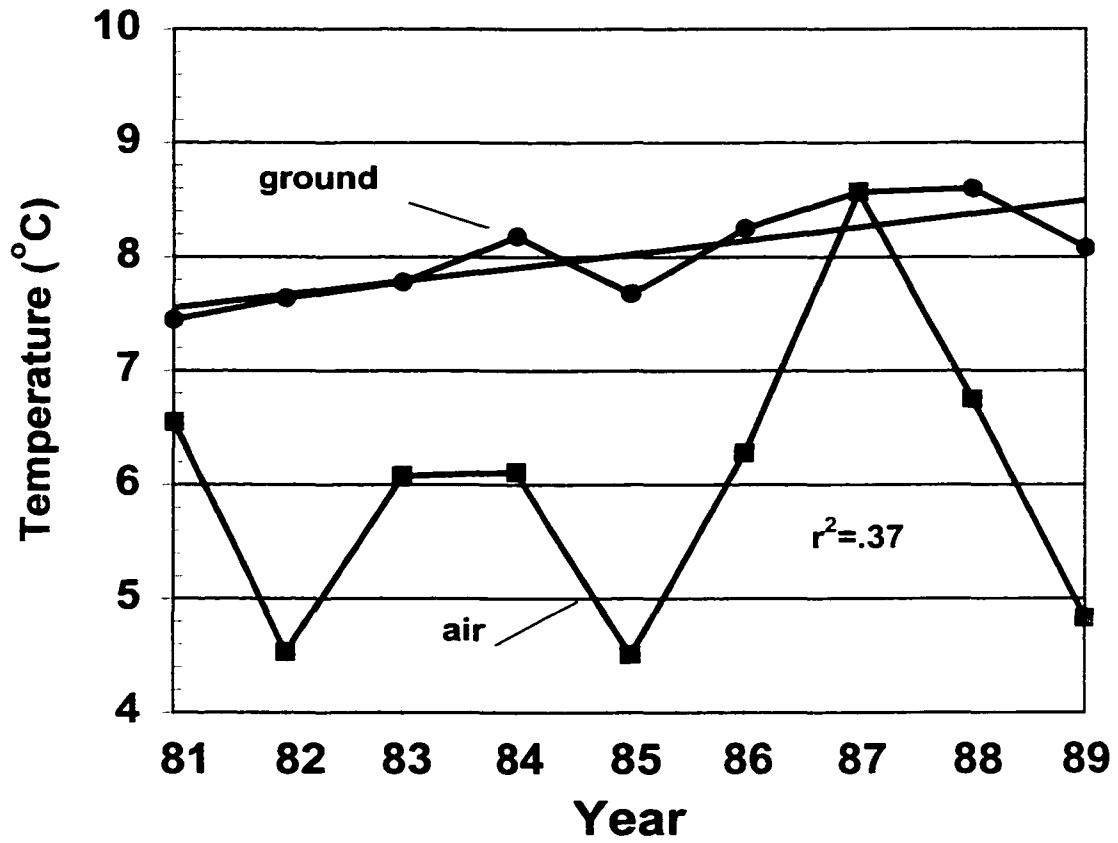


Figure 24. Mean annual air and ground temperatures averaged from all depths from Fargo. A least-squares linear regression line is shown on ground temperatures.

Ground-surface influence

To test the influence of ground-surface factors, recorded air temperatures were forced into the ground using a conduction model with direct air-ground surface coupling (see Appendix and Chapter 6 for a model description). Nodal spacing was set at ground temperature measurement depths. The model was run from January 1, 1981 to December 31, 1989 with the observed temperature profile of January 1, 1981 used as the initial profile. Best-fit thermal conductivity values averaged over all modeling periods were chosen ($k_{un} = 0.67$ and $k_{fr} = 1.30 \text{ Wm}^{-1}\text{K}^{-1}$). Mean annual modeled and observed temperatures averaged from 10-1170cm depths are shown in Figure 25. Similar to mean-annual air temperatures, air-temperature forced model temperatures are lower than recorded ground temperatures and show no significant-fit linear regression trend for the decade (Figs. 24 & 25). Mean annual surface air temperatures commonly display high variability (Oke, 1987). Modeled ground temperatures have too much intra-annual variability to accurately claim that linear regressions of modeled and observed temperatures display different slopes. Although linear regressions of modeled and observed ground temperatures do not show different trends, the fact that only observed ground temperatures show a definite warming trend is important. The incongruity of fit is due to nonconductive boundary-layer factors.

Analytical model

The warming trend present in mean annual ground temperatures is approximated by a 0.93°C per decade ramp-function ground-surface signal. To determine the effect of this 0.93°C signal on ground temperatures deeper than 12m an analytical model with a

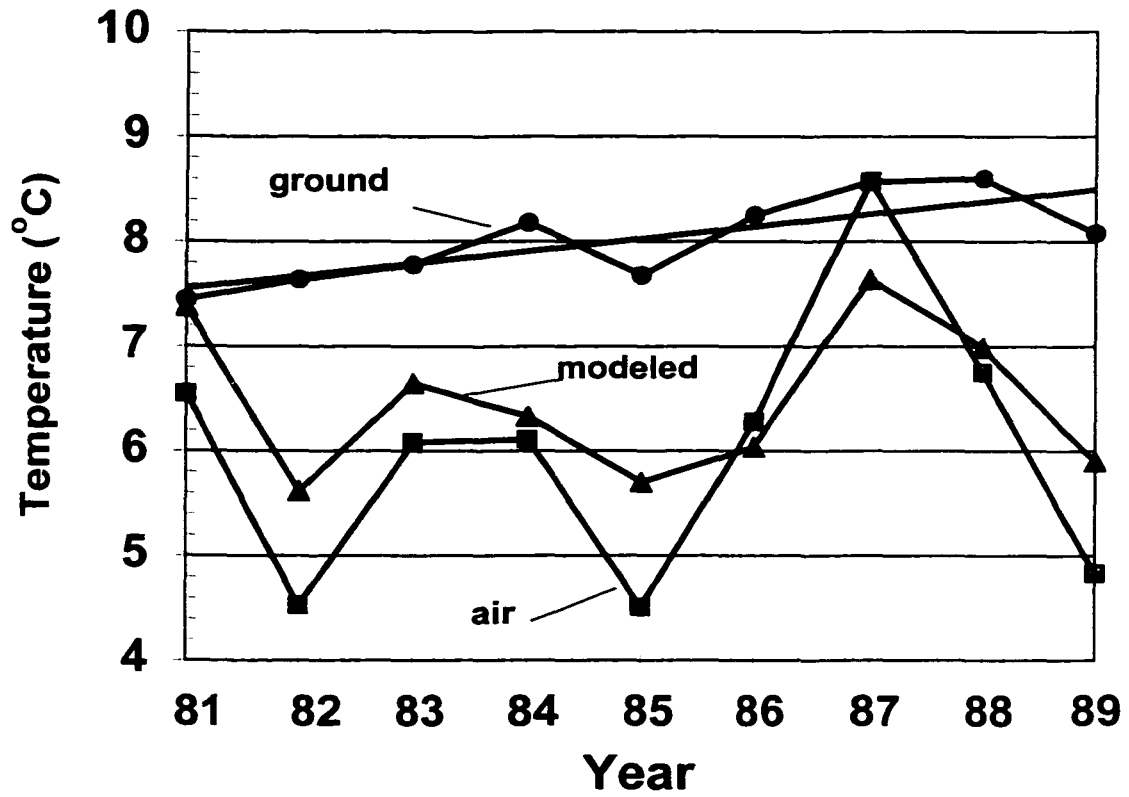


Figure 25. Mean annual modeled and recorded ground temperatures averaged from 10-1170cm depths at Fargo. Mean annual air temperatures are also shown.

10-year ramp-function increase in the ground-surface forcing signal was used. A thermal diffusivity of $1 \times 10^{-6} \text{m}^2/\text{s}$ was chosen (thermal conductivity = $2.2 \text{Wm}^{-1}\text{K}^{-1}$), giving an annual signal propagation depth of 13m. With a constant background heat flow, this transient signal has an effect of 0.16°C at 20m, 0.07°C at 30m, and 0.03°C at 40m-depth after 10 years.

Bottineau, Langdon, Minot, and Streeter

Compared to the last century, the period 1994-1999 was a time of high precipitation and above average air temperatures for Bottineau, Langdon, and Minot. Long-term air temperatures were recorded at Bottineau (1898-1999), Langdon (1896-1999), and Minot (1906-1999) (Figs. 26,27,28). Average mean-annual air temperatures from these periods are 2.87 (Bottineau), 1.81 (Langdon), and 3.47°C (Minot). Least-squares linear regressions of mean annual air temperatures indicate warming per century magnitudes of 1.15 ± 0.17 (Bottineau), 1.16 ± 0.17 (Langdon), and $0.49 \pm 0.07^\circ\text{C}$ per century (Minot) (Figs. 26,27,28). Two boreholes near Minot, ND, and one near Bottineau, ND (Fig. 1), indicate ground-surface warming magnitudes of 1.9, 2.4, and 2.7°C per century, respectively (Gosnold et al., 1997). The warmest year from the air temperature record was 1998 for Langdon, Minot, and Streeter, and 1999 for Bottineau. Average air temperatures during the period 1994-1999 are 3.15 (Bottineau), 2.71 (Langdon), 4.62 (Minot), and 4.37°C (Streeter). Average annual precipitation from the period 1931-1993 and 1994-1999 is 43.12 and 46.18 (Bottineau), 46.02 and 54.74 (Langdon), and 44.16 and 52.03 cm (Minot).

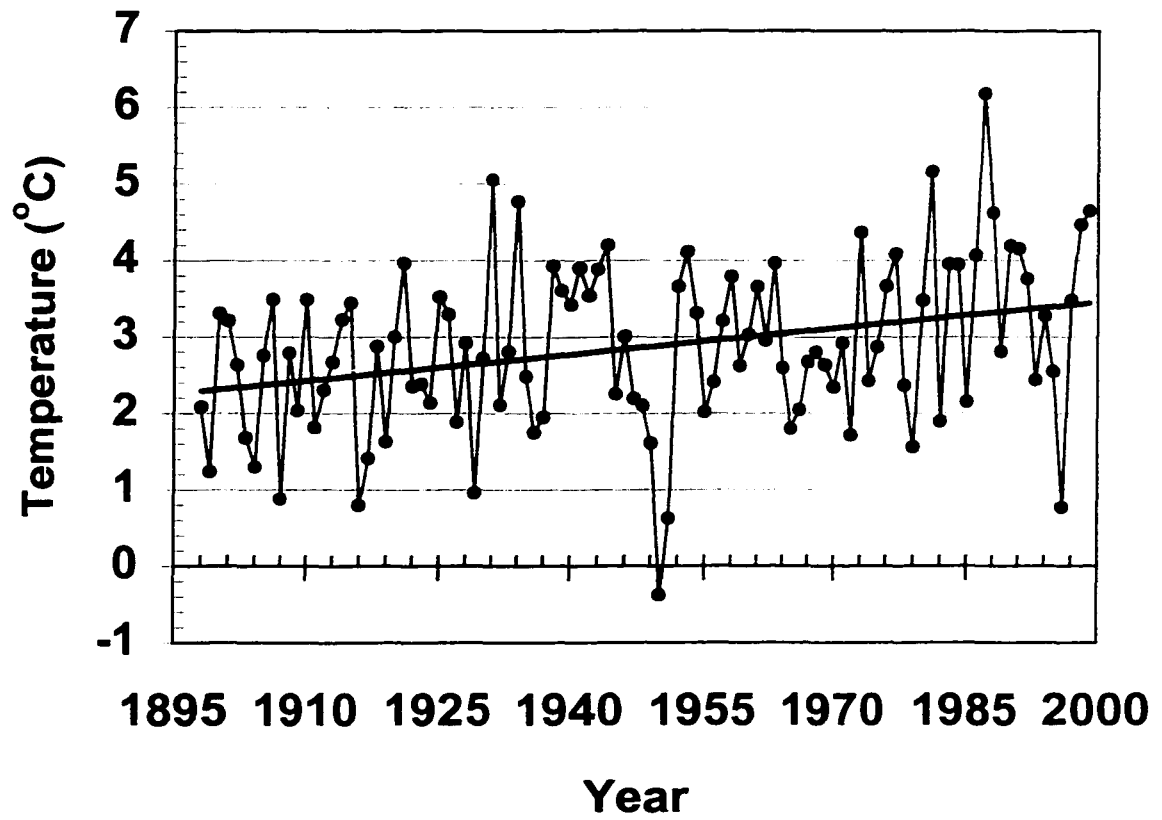


Figure 26. Mean annual air temperatures from Bottineau.

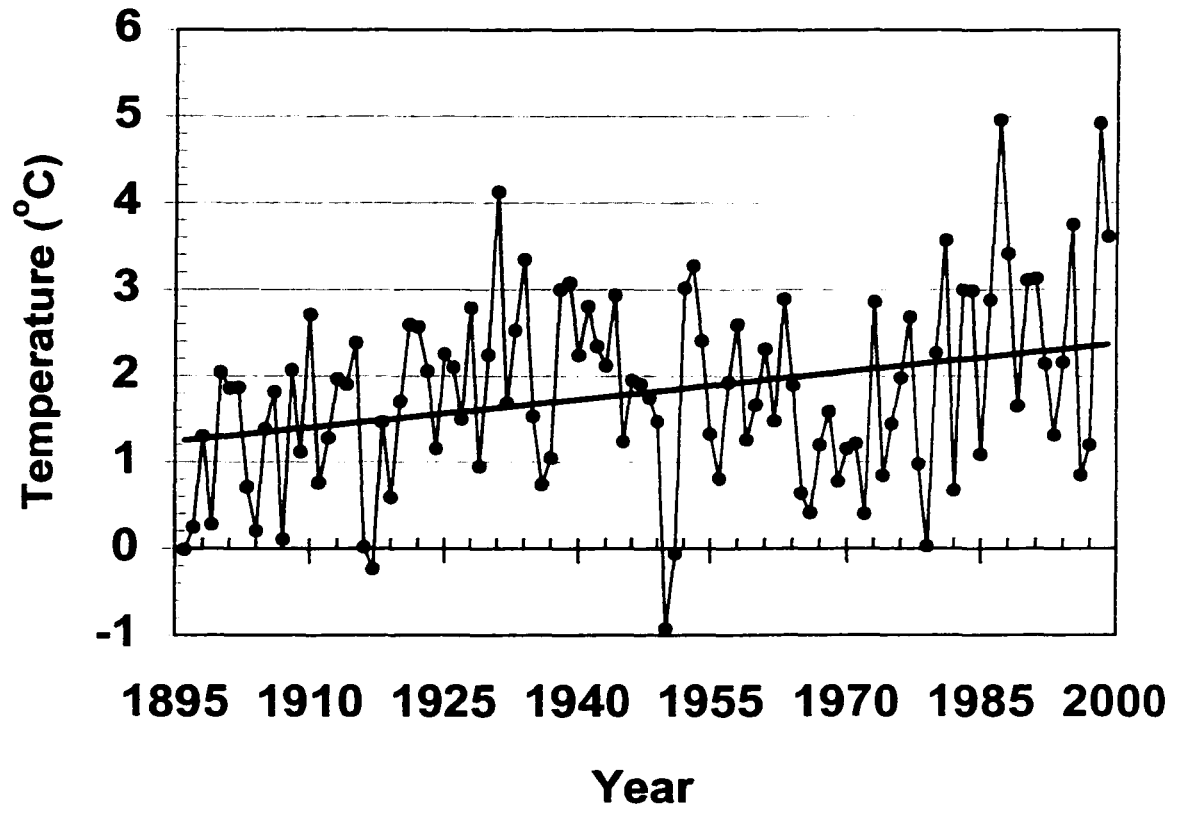


Figure 27. Mean annual air temperatures from Langdon.

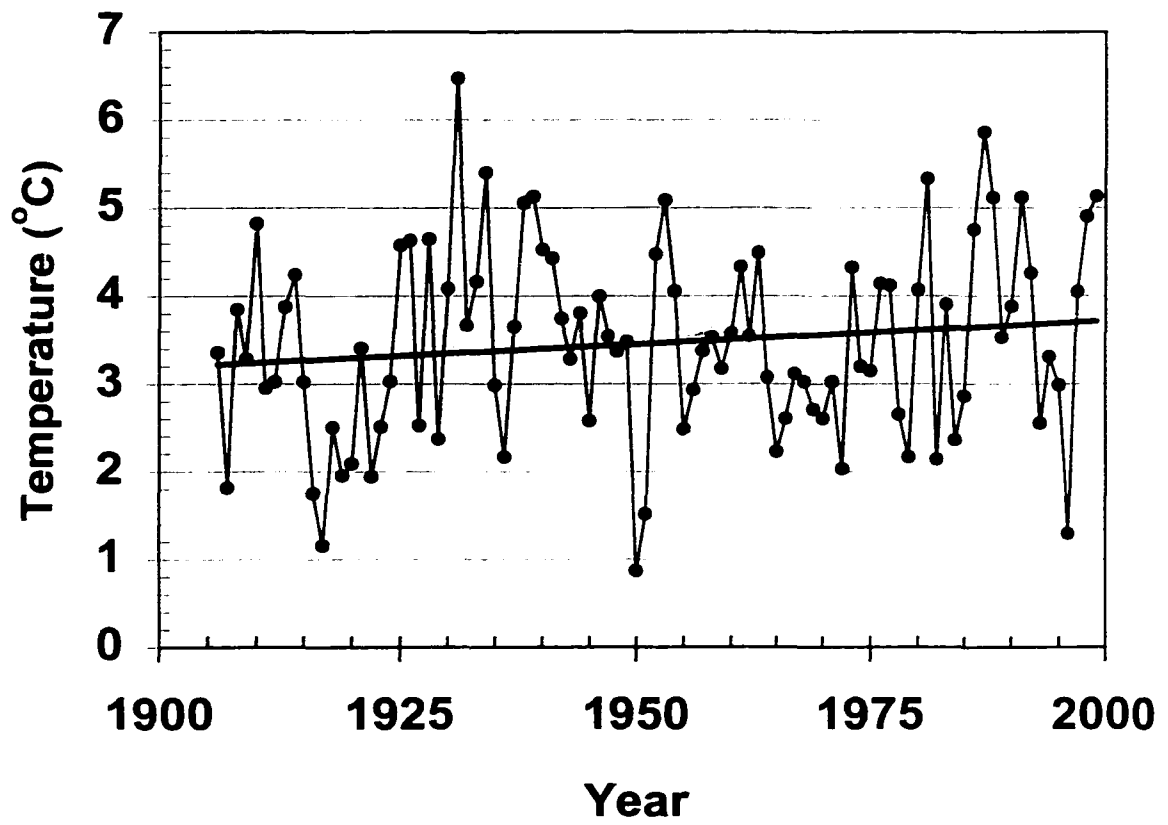


Figure 28. Mean annual air temperatures from Minot.

Mean annual air and ground temperatures averaged from all 12 depths are shown in Figures 29 - 32 for the period January 1, 1994 to December 31, 1999. All sites show a good correlation between mean annual air and ground temperatures (average $r^2 = .84$). Bottineau shows the best tracking between mean annual air and ground temperatures in this six year period ($r^2 = .91$). Bottineau is also the only site that shows a significant six-year increase in average ground temperatures (Fig. 29).

Bottineau

Mean annual ground temperatures from Bottineau were averaged from all depths to determine a single mean-annual ground temperature. Mean annual air and average ground temperatures from the 6-year period were plotted (Fig. 29). A least-squares linear regression of ground temperatures yields a slope of $+1.17 \pm 0.15^\circ\text{C}$ (Fig. 29). In an analysis similar to the Fargo data, the correlation coefficient of best-fit linear regression lines for air and ground temperatures was tested. As with the Fargo data, mean annual air and ground temperatures cannot be shown to have different best-fit regression lines.

Recorded air temperatures from January 1, 1994 to December 12, 1999 were forced into the ground with a conduction model assuming direct air-ground coupling. The observed subsurface temperature profile from January 1, 1994 was the starting profile. Average best-fit thermal conductivity values of $k_{un} = 0.67 \text{ Wm}^{-1}\text{K}^{-1}$ and $k_r = 1.30 \text{ Wm}^{-1}\text{K}^{-1}$ were chosen for the model and nodal spacing was set at temperature measurement depths. Mean annual modeled and observed temperatures averaged from all depths are shown in Figure 33. Modeled temperatures are lower than observed

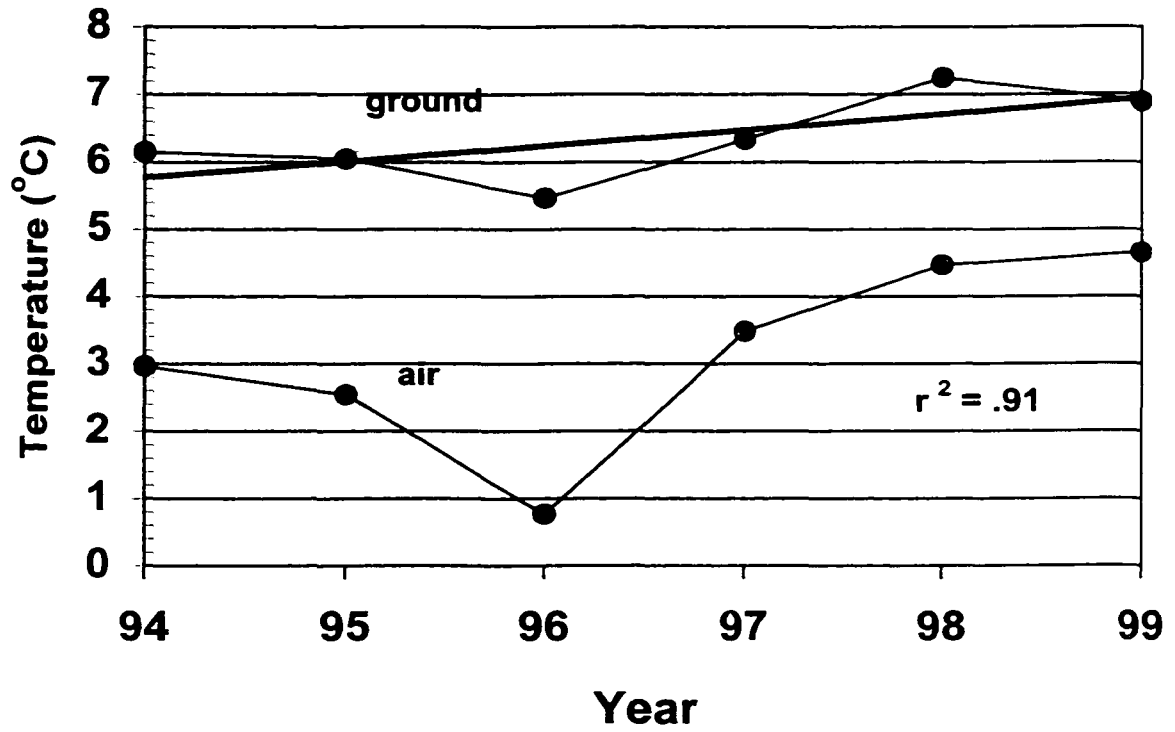


Figure 29. Mean annual air and ground temperatures averaged from all depths at Bottineau. A least-squares linear regression line is shown on ground temperatures.

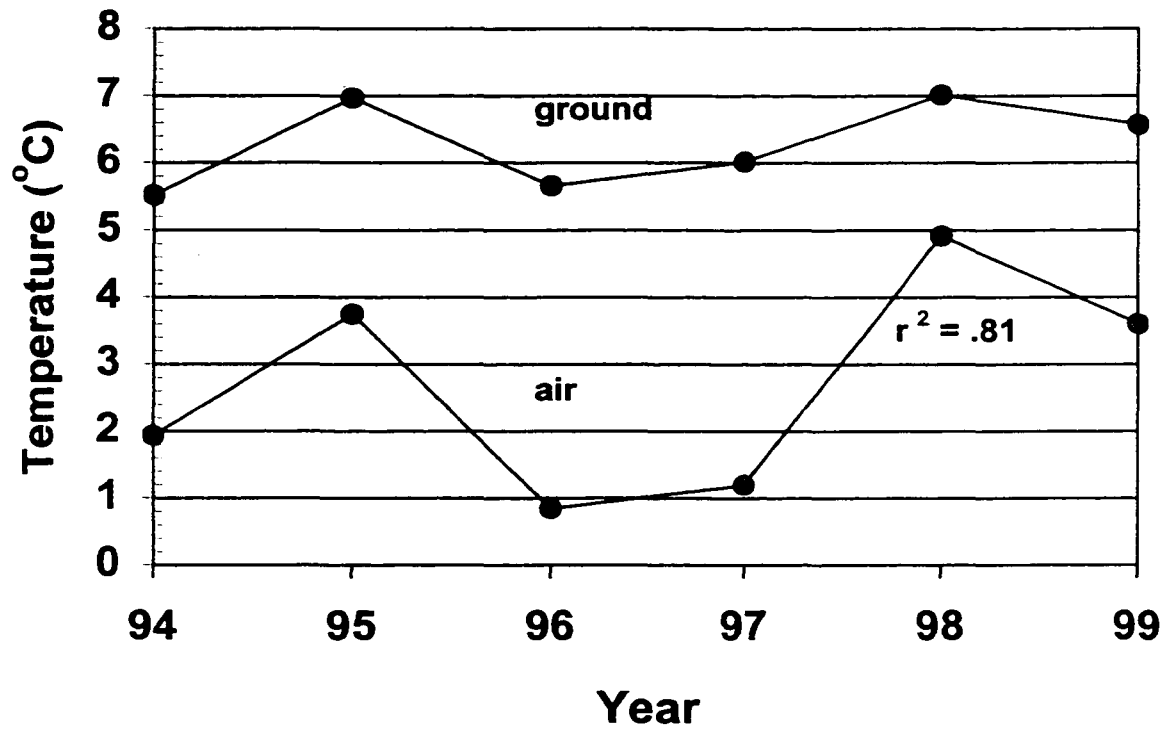


Figure 30. Mean annual air and ground temperatures averaged from all depths at Langdon.

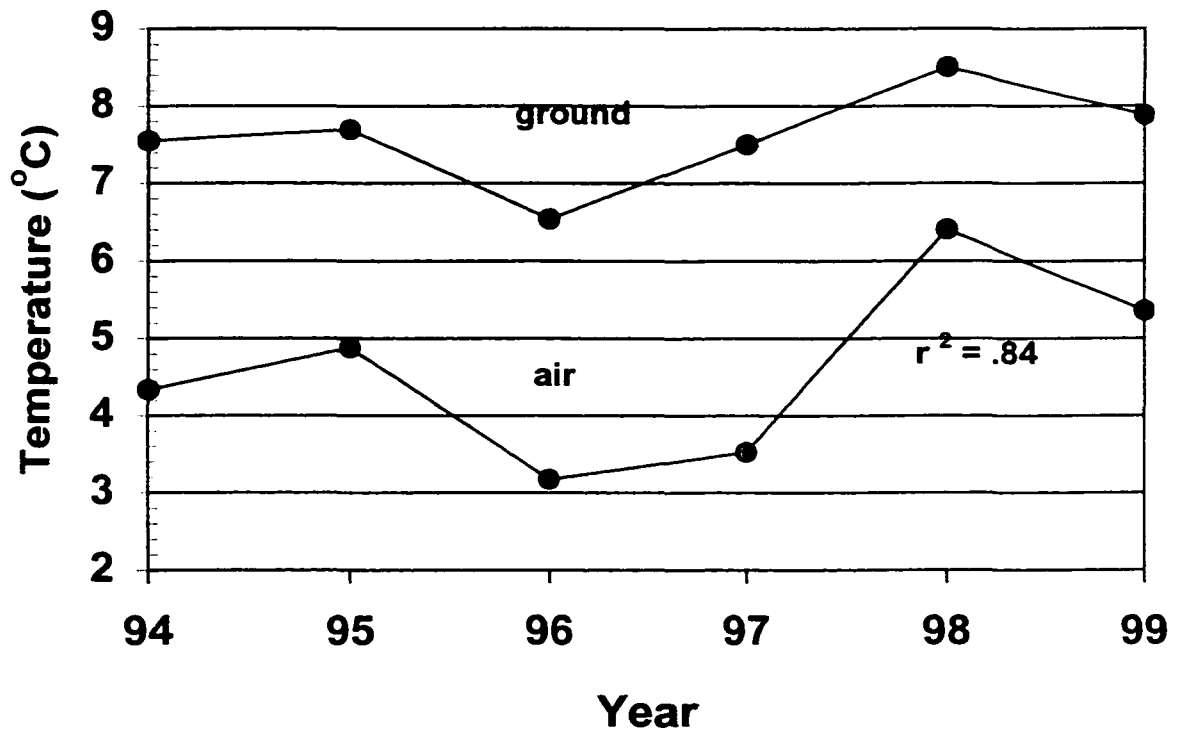


Figure 31. Mean annual air and ground temperatures averaged from all depths at Minot.

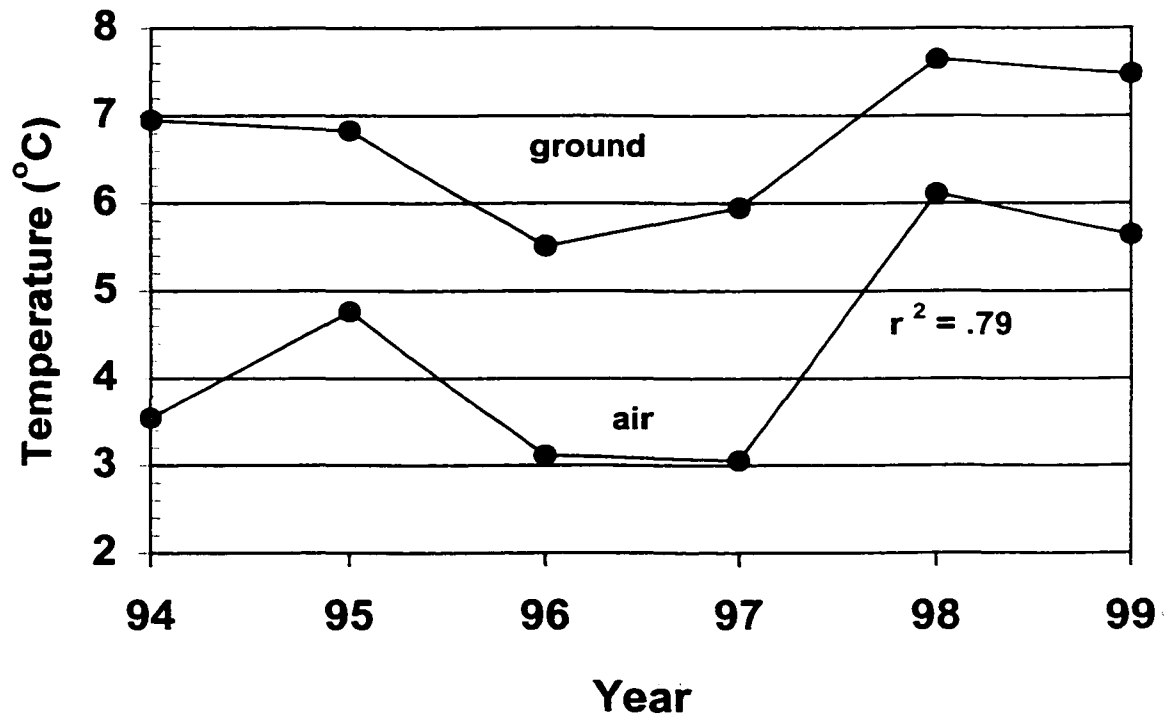


Figure 32. Mean annual air and ground temperatures averaged from all depths at Streeter.

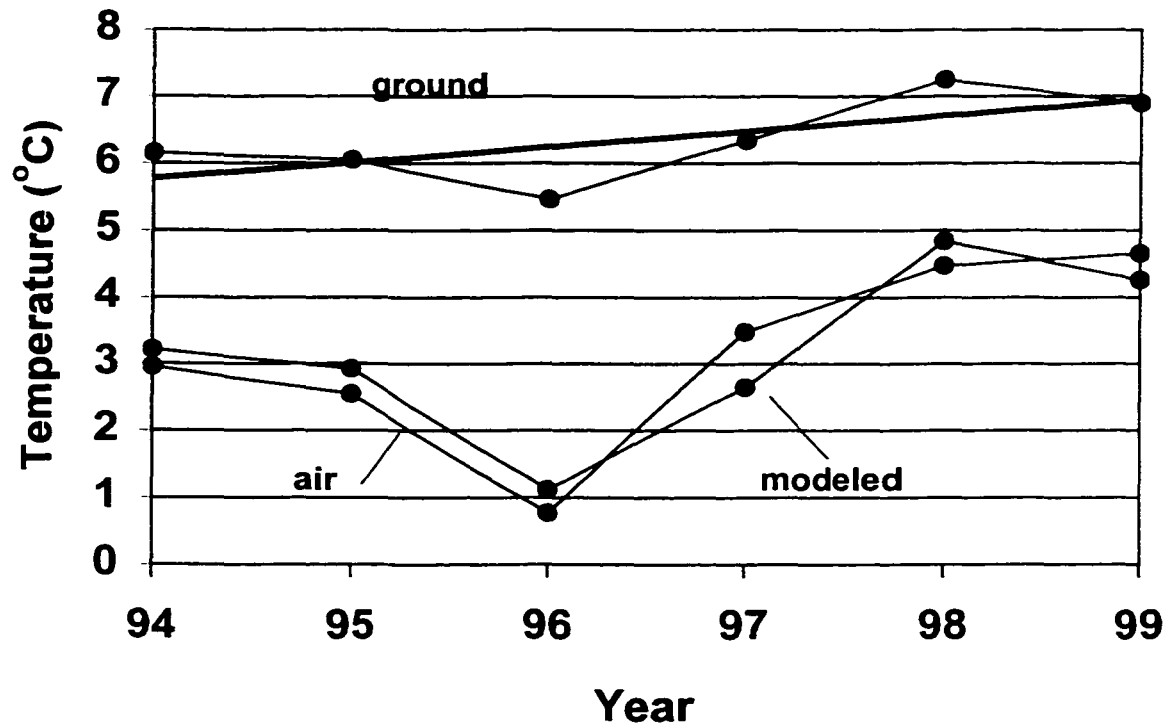


Figure 33. Mean annual recorded air and ground and modeled ground temperatures averaged from all depths at Bottineau. The least-squares linear regression line shows the $1.17 \pm 0.15^\circ\text{C}$ warming trend in recorded temperatures during the 6-year period.

temperatures and show no significant warming trend for the decade (Fig. 33). Similar to the Fargo data, the significant-fit warming signal occurs only in observed ground temperatures, due to nonconductive boundary-layer factors.

CHAPTER 5

SNOW COVER EFFECTS

A number of snow cover effects influence air-ground temperature exchange. The high surface albedo and emissivity of snow cause a reduction in absorbed solar energy and insulate the ground from outgoing long-wave radiation (Zhang et al., 1996). The low thermal conductivity of snow insulates the ground from snow surface temperature changes and conserves latent heat released in the soil (Oke, 1987). Local and regional duration and areal coverage of snow cover are the largest factors accounting for variations in winter ground surface temperatures (Desrochers and Granberg, 1988). Ground temperatures in regions of snow cover are determined mainly by the number of days in the spring and fall with snow cover and by the air temperature regime (Beltrami and Mareschal, 1992).

Snow cover is susceptible to variations due to drift patterns, slope of the ground surface, vegetation, incident radiation, and topography. Density and water content of snow tend to increase as it becomes older (Geiger et al., 1995). Warmer winters involve more melting and refreezing of snow, causing a denser snowpack with a higher thermal conductivity and total water content. In general, this type of snowpack provides less insulation than a lower density snowpack containing more air (Geiger et al., 1995). A thicker snowpack usually restricts heat loss from the ground to a greater extent than a thinner snow cover (Smith and Riseborough, 1996).

The snow-related variable available during the time of record from all NDAWN sites is daily-measured snow depth. This variable includes any amount of measurable snow cover greater than 0.1 inches. Unfortunately no record of snow parameters (density, thermal conductivity, water content) was available. Days with measurable snow cover are summed to determine the annual duration of winter snow cover. The duration of winter snow cover at all sites ranged from 29 to 185 days / winter.

To study the influence of snow cover on air-ground temperature exchange, seasonal duration of snow cover is compared with air-ground temperature differences averaged from November 15 to April 1. This period is chosen because it encompasses all periods of measurable snow cover from all sites. The average air-ground temperature difference is an indicator of overall snow cover insulation during a given period.

Fargo

Total days of measurable snow cover per winter correlate ($r^2 = 0.71$) with temperature differences ($T_{5\text{cm}} - T_{\text{air}}$) averaged from November 15 to April 1 of each year (Fig. 34). This average air-ground temperature difference varied by as much as 6.52°C (Fig. 34). Although 1cm depth temperatures show a similar correlation ($r^2 = 0.69$), temperature differences between air and the 5cm depth were chosen to minimize ground-surface effects at the 1cm depth. The data points in Figure 34 diverge during the last four years of the decade, due to possible changes in snow cover properties, spring snowmelt effects, or winter air temperatures. A graph of seasonal temperature trends from Fargo indicates that winter air temperatures decreased by 0.51°C during the 9-year period (Fig. 35).

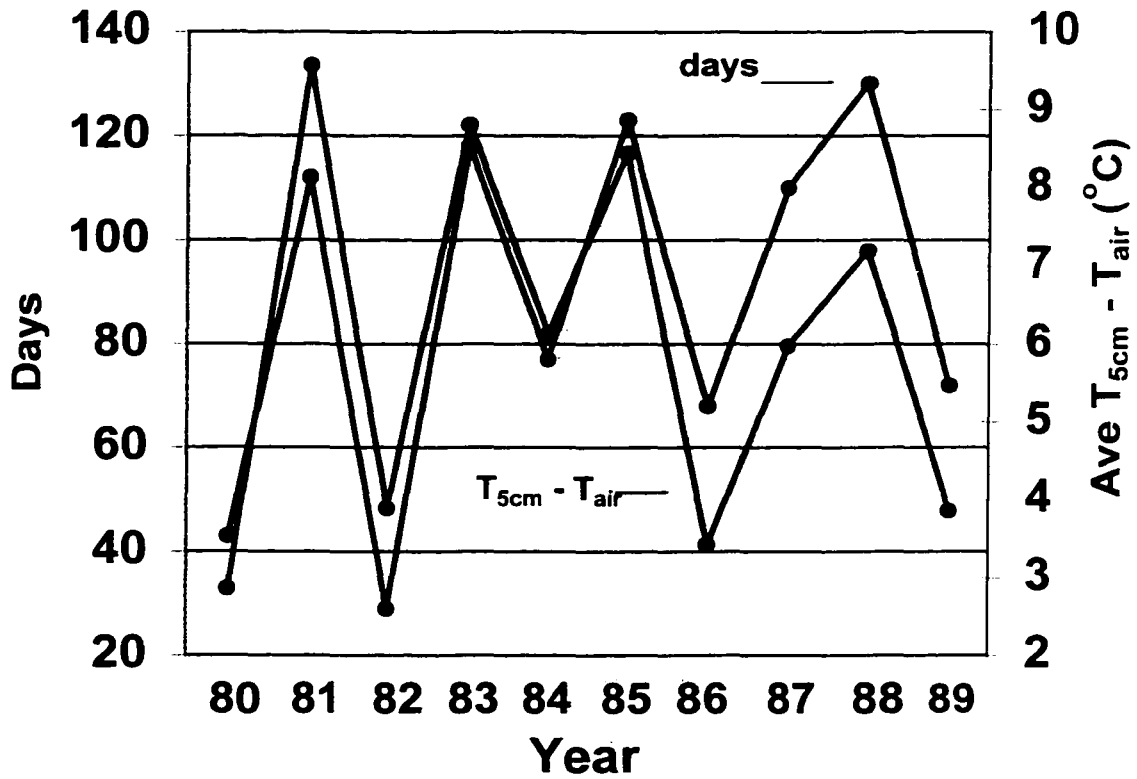


Figure 34. Total days with snow cover (days) and ground – air temperature differences ($T_{5cm} - T_{air}$) from Fargo averaged annually from November 15 to April 1.

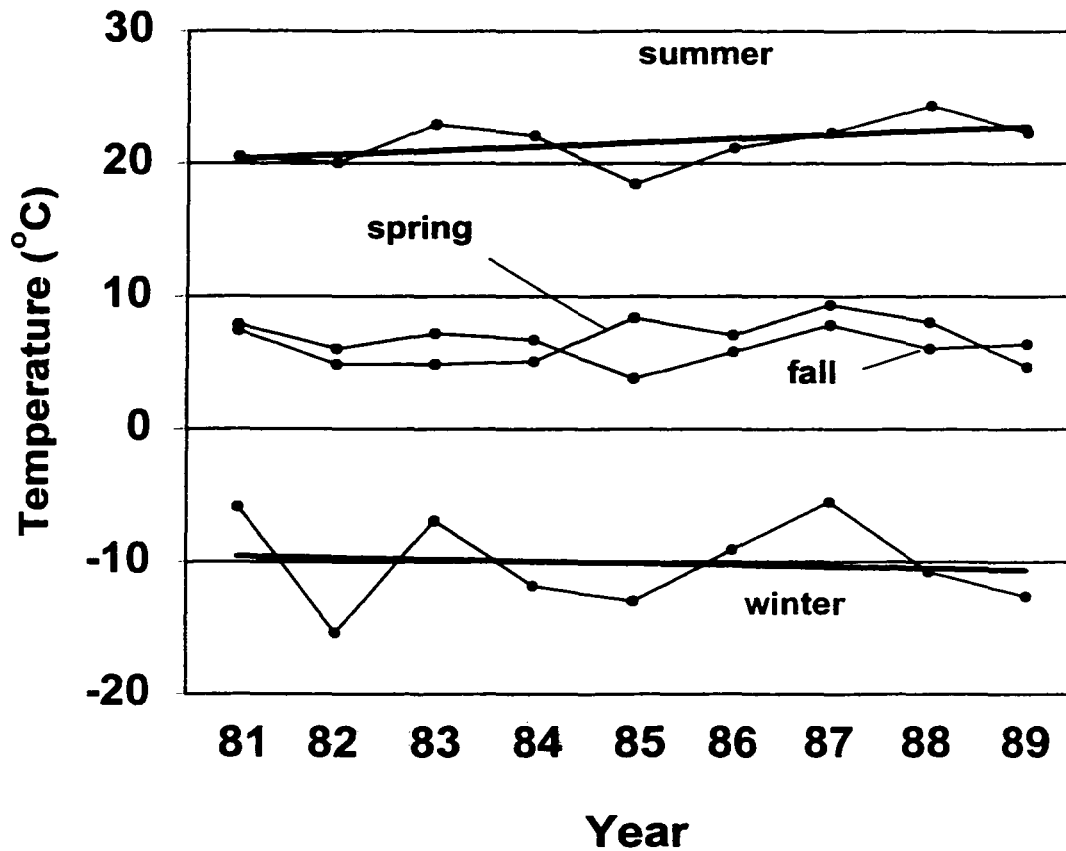
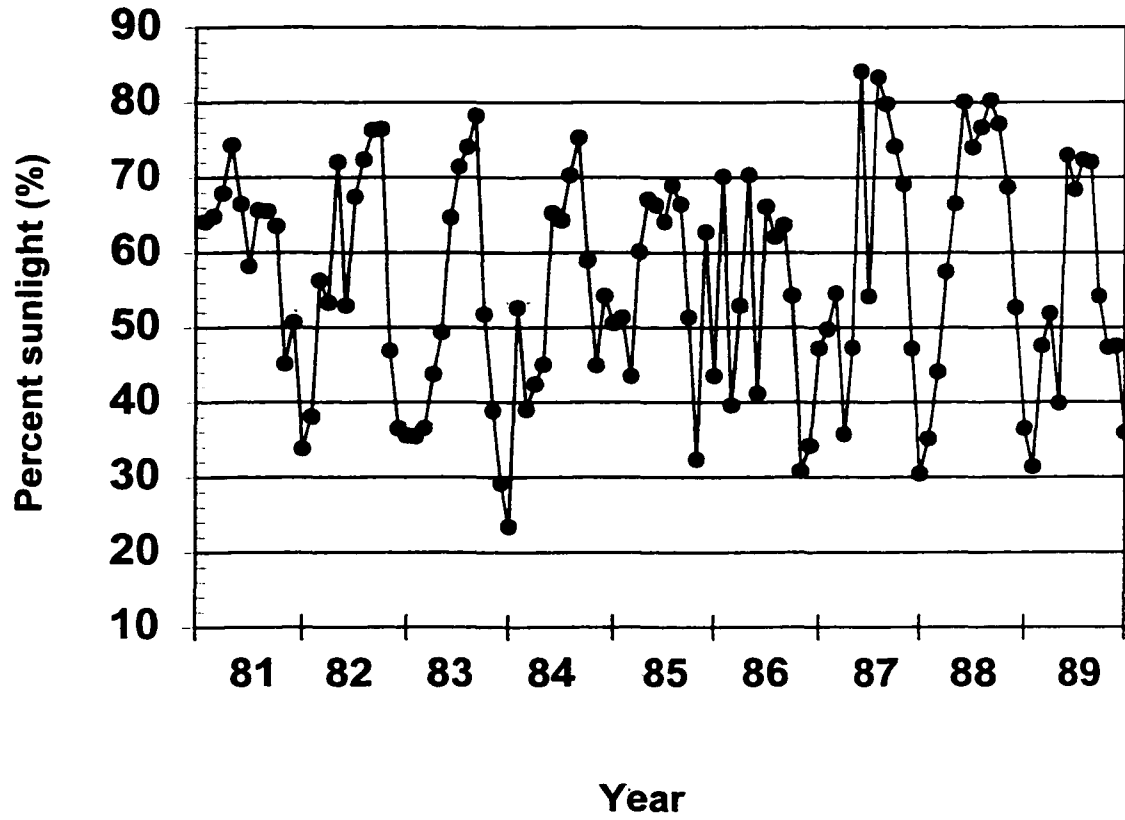


Figure 35. Seasonal air temperature trends, including summer (June-Aug), fall (Sep-Nov), winter (Dec-Feb), and spring (Mar-May). Changes per decade in mean seasonal temperatures are: $+2.43 \pm 0.78$ (summer), -0.75 ± 0.24 (fall), -0.51 ± 0.16 (winter), and $+1.26 \pm 0.41$ °C (spring). Least-squares linear regression lines are shown for winter and summer temperatures.

The numbers of days with any measurable snow cover for each winter averaged 82.2 days/winter including non-consecutive days (Fig. 34). An incremental sum of all greater-than-zero daily measured snow depth values was calculated for each winter in units of total meters per winter. These values are cumulative sums of daily-measured snow depth values. The cumulative measured snow depths ranged from 1.63m (43 day snow cover, 1981) to 32.36m (130 day snow cover, 1989), and averaged 15.03m for all winters during the decade.

Annual changes in winter percent sunlight values can affect the melting and refreezing and overall albedo of the snowpack. Monthly averages of daily percent sunlight values are plotted from January 1, 1981 to December 12, 1989 (Fig. 36). A linear regression of these monthly averages indicates no significant trend during the time of study. Winter averages of daily percent sunlight (Dec - Feb) during the time of study also indicate no significant trend.

The correlation between average air-ground temperature differences and duration of winter snow cover (Fig. 34) has some complicating factors. The period of average temperature difference also encompasses times of snowmelt and infiltration due to spring warming. Snow cover reduces spring warming effects and creates a competing effect with cold period insulation (Majorowicz and Skinner, 1997). Because the number of spring thawing days in this time period changes annually, the timing and magnitude of these competing factors change annually. Snowpack insulation properties can vary on time scales ranging from diurnal to monthly (Oke, 1987). However one-dimensional conduction models of temperature exchange through snow cover show that soil temperatures are more sensitive to the presence or absence of snow cover than to



variations in snow depth (Gosnold et al., 1997). Mean annual ground temperatures may be increased several degrees by changes in the duration of snow cover, but snow parameters have little effect on these increases (Goodrich, 1982). Mild winter air temperatures can lead to decreased ground-air temperature differences. Despite these factors, the observed correlation ($r^2 = .71$) between duration of winter snow cover and air-ground temperature differences demonstrates the influence of snow cover duration on winter air-ground temperature decoupling.

Bottineau, Langdon, Minot, and Streeter

Temperature differences ($T_{5\text{cm}} - T_{\text{air}}$) averaged from November 15 to April 1 are plotted with total days of winter snow cover from all NDAWN sites for the 6-year period (Figs. 37 - 40). Correlation coefficients are $r^2 = .84$ (Bottineau), $r^2 = .56$ (Langdon), $r^2 = .79$ (Minot), $r^2 = .87$ (Streeter), and $r^2 = .77$ (average) at the 95% confidence level (Figs. 37 - 40). Differences between mean annual air and 5cm depth temperatures ($T_{5\text{cm}} - T_{\text{air}}$) were also plotted with duration of snow cover for the four sites. However, mean annual temperature differences (average $r^2 = .63$) do not correlate as well as seasonal 5cm-air temperature differences (average $r^2 = .77$).

The high correlation between these variables with relatively few data points indicates that winter decoupling of air-ground temperatures is controlled mainly by duration of winter snow cover. These observations are consistent with the interpretations of Beltrami and Maraschel (1992), that ground temperatures in regions of snow cover are determined by the number of days with snow cover and the air temperature regime.

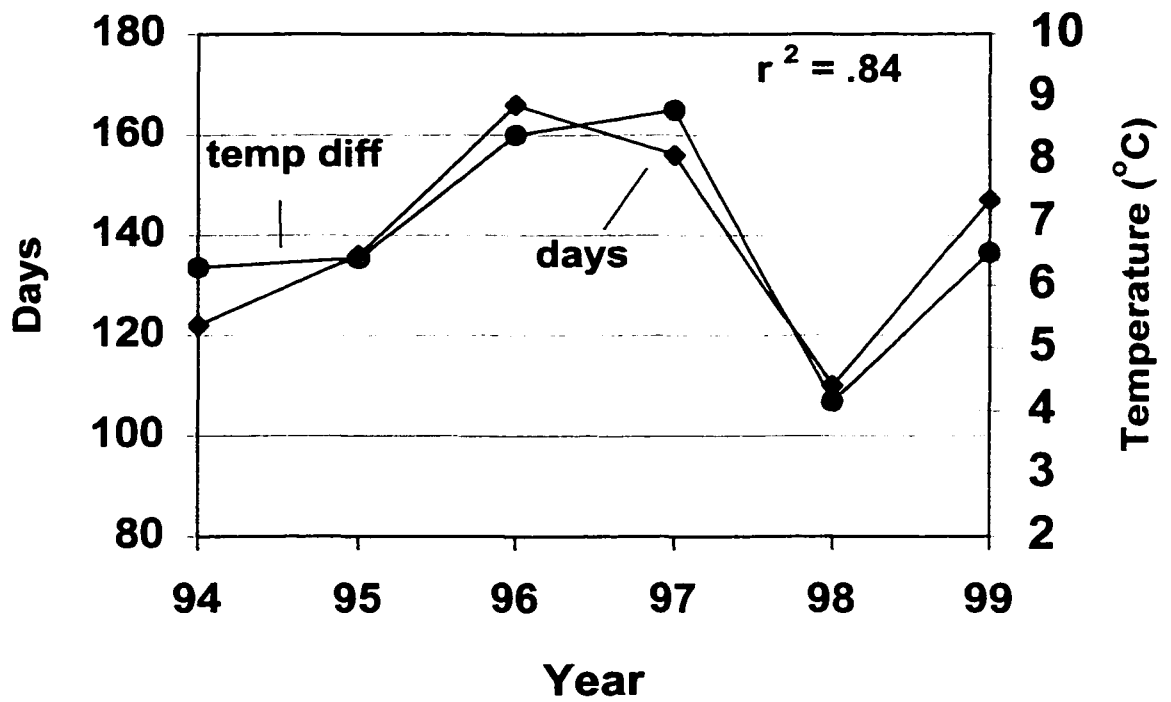


Figure 37. Total days of measurable snow cover per winter plotted with $T_{scm} - T_{air}$ values averaged from 11/15 to 4/1 at Bottineau.

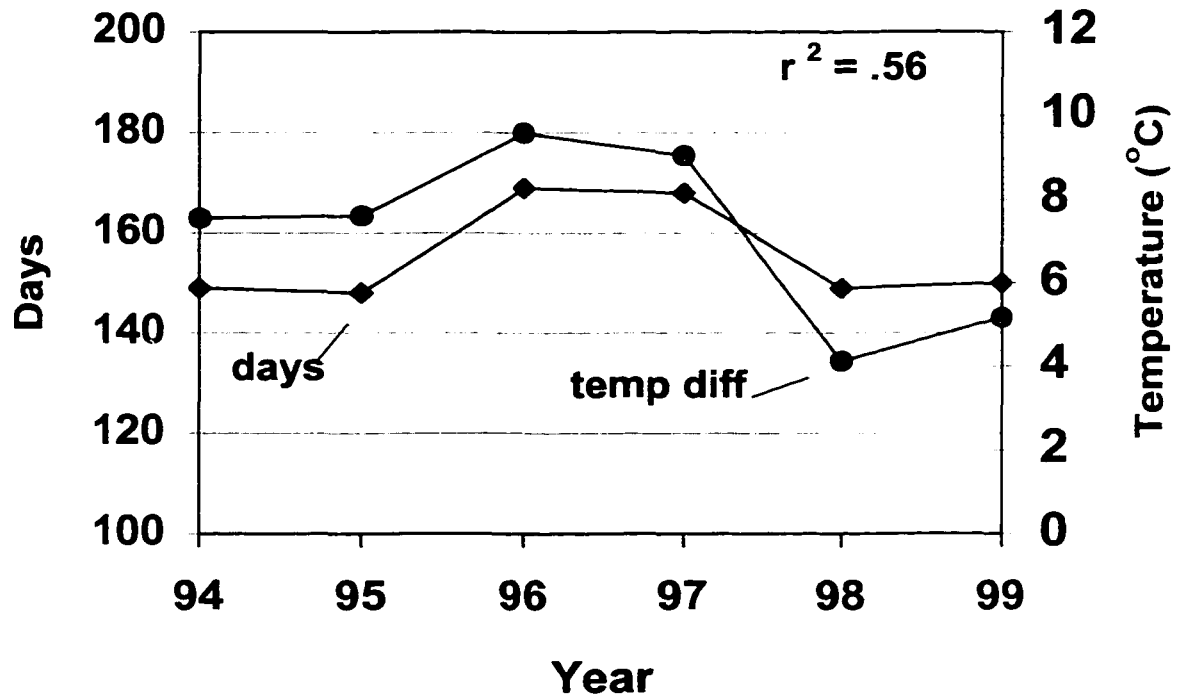


Figure 38. Total days of measurable snow cover per winter plotted with $T_{5cm} - T_{air}$ values averaged from 11/15 to 4/1 at Langdon.

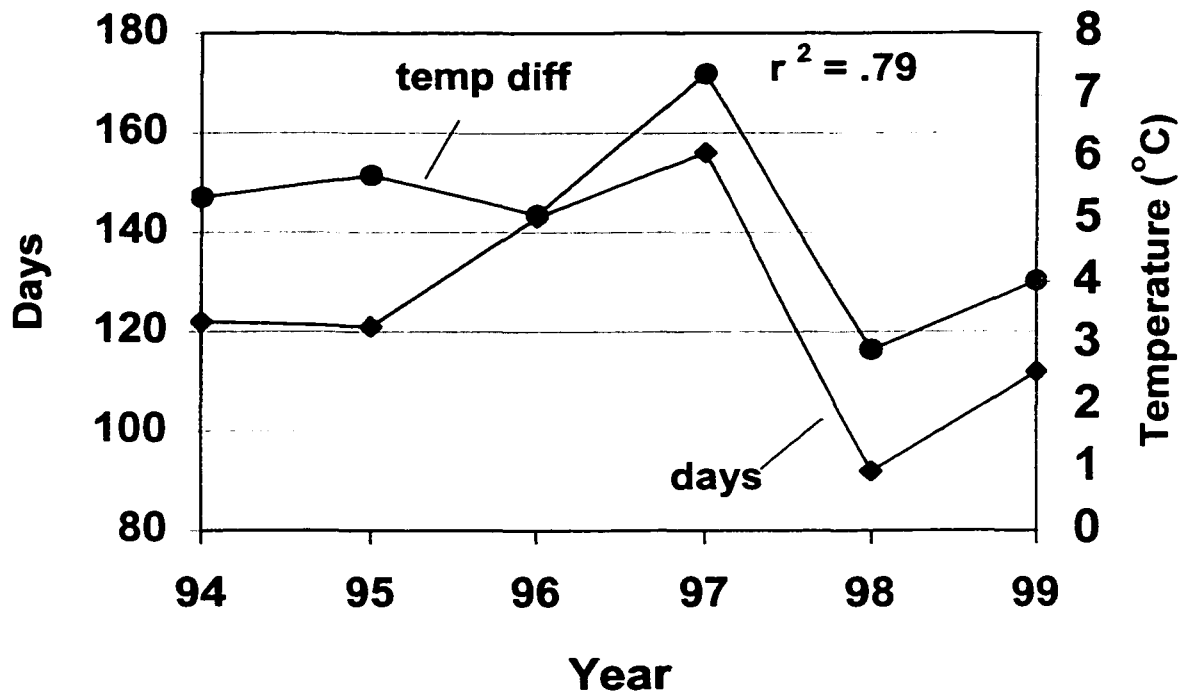


Figure 39. Total days of measurable snow cover per winter plotted with $T_{5cm} - T_{air}$ values averaged from 11/15 to 4/1 at Minot.

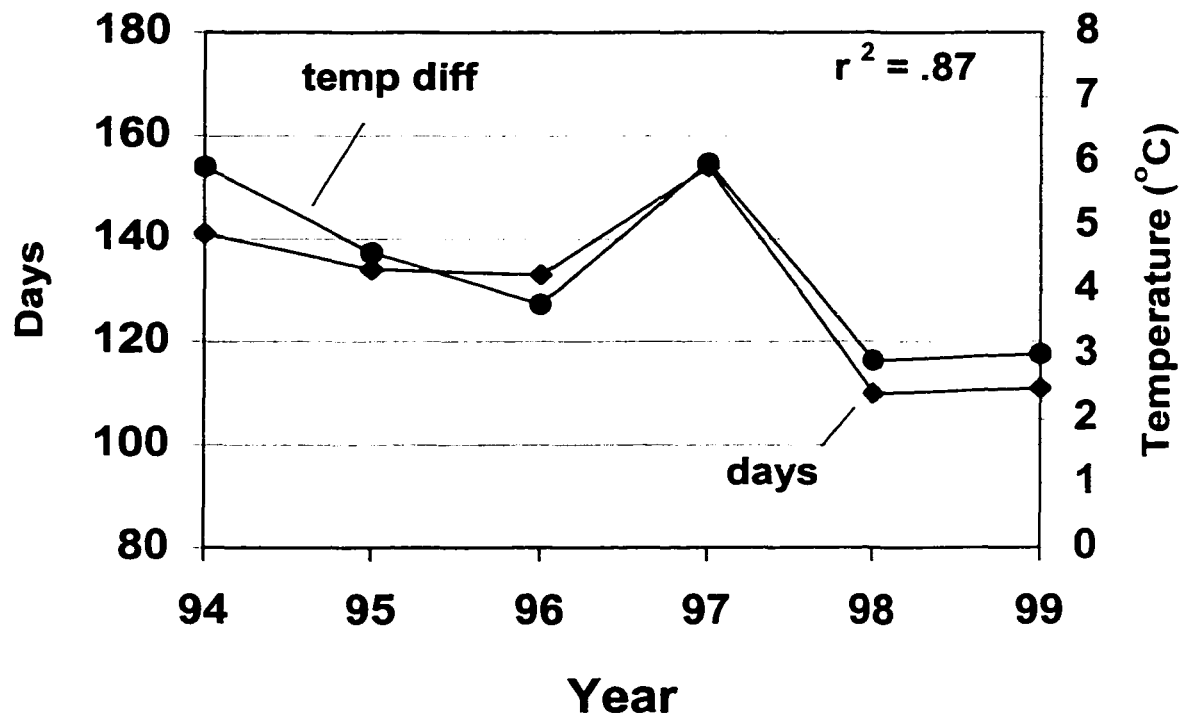


Figure 40. Total days of measurable snow cover per winter plotted with $T_{5cm} - T_{air}$ values averaged from 11/15 to 4/1 at Streeter.

CHAPTER 6

THE CONDUCTION MODEL

Modeling recorded ground temperatures enables the determination of best-fit thermal properties including thermal conductivity, latent energy of freezing and thawing, and evapotranspiration. This gives an understanding of how thermal properties vary on a seasonal scale and if the variation can be related to climatic variables. A one-dimensional finite-difference numerical heat conduction algorithm was used to model subsurface temperatures. Partial differential equations are expressed in finite difference form as a numerical implementation of the heat conduction equation.

The equation describing time dependent heat conduction in one dimension is:

$$\rho C_p \partial T / \partial t = \partial / \partial z (k \partial T / \partial z) \quad (2)$$

where z = depth, T = temperature, t = time, k = thermal conductivity, ρ = soil density, and C_p = specific heat (Carslaw and Jaeger, 1959). The heat flow Q from each node into an adjacent node is:

$$Q = k A \Delta T / L \quad (3)$$

where A = area per unit depth perpendicular to the direction of heat flow and L = vertical spacing between nodes.

An initial temperature is assigned to each node and the appropriate equation is solved to determine subsequent nodal temperatures based on the forcing signal at the ground surface. The resultant temperature profile is then used as an initial profile for the next set of calculations. The forcing signal is the incremental difference between successive recorded daily-mean air or 1 or 5cm-depth temperatures. Vertical nodal spacing was set at 10cm. For a more detailed description of the model, see Appendix.

Latent energy of freezing, thawing, and evapotranspiration is entered in the model as positive or negative heat production values as appropriate at specified nodes. The data sets were divided into seasonal modeling periods based on the latent energy requirement of the subsurface. These periods include freezing periods (positive latent energy at the freezing boundary), thawing periods (negative latent energy at the thawing boundary), and summers (negative latent energy for evapotranspiration in upper 40cm). Evapotranspiration was only modeled with the Fargo data. Freezing and thawing modeling periods are constrained by when the forcing signal goes below 0°C and decreases with time (freezing periods) to when the forcing signal begins increasing and all subsurface melting has occurred (thawing periods) (Fig. 41). The initial temperature profile ascribed to the model nodes is determined from the recorded temperature profile on the first day of each modeling period. Trial values of thermal conductivity and latent energy are entered in a best-fit 'tuning' method and remain constant throughout a modeling period.

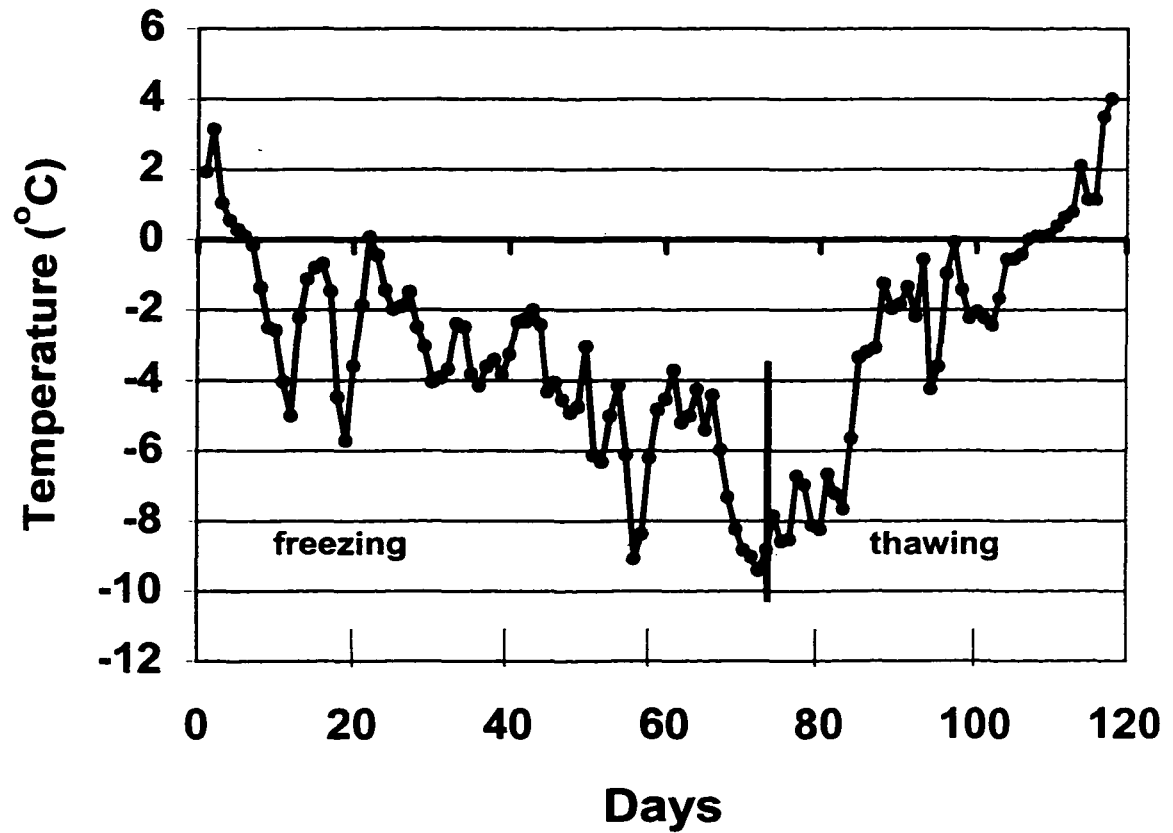


Figure 41. Daily mean 1cm-depth temperatures recorded from 11/25/84 to 3/22/85 at Fargo. The black line indicates the division between freezing and thawing periods.

A temperature-dependent step function is assumed for thermal conductivity. Thermal conductivity is homogeneous throughout the model and changes abruptly from k_{un} (unfrozen) to k_f (frozen) when nodal temperatures go below zero. Values held constant in the model include specific heat ($1000 \text{ J kg}^{-1}\text{°C}^{-1}$), and density (2200 kg m^{-3}).

Variations of the thermal conductivity distribution in the upper meter were tested for summer modeling periods with the Fargo data. Although increasing the number of variables in the modeling scheme decreases the total degrees of freedom, summer temperatures modeled with an upper (k_{up} : 1-40cm) and lower (k_{low} : 40-1170cm) thermal conductivity produced the best fit to recorded temperatures. A term for latent energy of evapotranspiration was also included in the upper 40cm of the ground. The 40cm depth does not represent any stratigraphic or soil discontinuity, but provides the best fit for a latent energy of evapotranspiration and thermal conductivity boundary at Fargo. The soils at all sites including Fargo are uniform for the entire depth of the measurement rods (Enz, 1998). Regardless of the choice of conductivity and evapotranspiration depths in the model, temperatures in the upper meter of the ground from Fargo were difficult to model accurately. Temperatures in the upper meter of the ground are influenced most by nonconductive effects such as water movement, air pressure changes, wind speed, vegetation, changes in solar radiation, evaporation and condensation. Although many factors can influence near-surface ground temperatures on an hourly scale, these factors also affect daily-mean temperatures.

Latent energy is constrained in the model by examining each node at the beginning of every iteration. If the temperature is negative above a node but positive below the node during a freezing period, the program activates a positive latent energy

value for the nodal temperature calculation *at* the solidification boundary to simulate freezing effects. A negative latent energy value is also activated when the temperature is positive above a node and negative below the node to simulate near-surface spring melting. The choice of an exact 0°C phase change in the model is an approximation. The presence of unfrozen water in frozen soils has a significant effect on the thermal properties of the soil, particularly influencing moisture migration to the freezing front (Farouki, 1981).

Best-fit residual temperatures

To determine how well modeled temperatures match recorded temperatures, residual temperatures ($T_{\text{calc}} - T_{\text{obs}}$) from each depth were averaged for entire modeling periods. Modeling heat conduction with two free parameters eliminates the possibility of a unique solution for both parameters. The two parameters are therefore continually adjusted until a minimum-average residual temperature is obtained for a modeling period. Thermal conductivity and latent energy values producing an average residual temperature closest to zero are considered best-fit values for a modeling period. Best-fit thermal conductivity values are considered 'effective' conductivities due to the nonconductive effects operating in the soil column, including advection, water vapor movement and phase changes.

Despite the non-unique nature of the conduction model, maximum-average residual temperatures for all modeling periods for all sites were as low as $\pm 0.18^{\circ}\text{C}$ (freezing), $\pm 0.30^{\circ}\text{C}$ (summer), and $\pm 0.70^{\circ}\text{C}$ (thawing) for depths greater than one meter. Recorded 1 and 5cm-depth temperatures are very effective model-forcing signals in spite

of any near-surface effects. These average residual temperatures are within the uncertainty of the thermocouples for freezing periods. Summer modeling periods were longest and included times of high incident radiation, giving the highest residual temperatures. Because nonconductive factors are not included in model calculations, the upper meter of the ground had a maximum-average residual temperature of $\pm 0.9^{\circ}\text{C}$ for all modeling periods.

Best-fit thermal parameters

Best-fit thermal conductivity values from winter periods in Fargo were low, ranging from 0.52-0.72 (unfrozen) to 1.07-1.57 $\text{Wm}^{-1}\text{K}^{-1}$ (frozen). The average thermal conductivities for all winter modeling periods were $k_{\text{un}} = 0.64$ and $k_{\text{fr}} = 1.33 \text{ Wm}^{-1}\text{K}^{-1}$ (Table 4). The average effective thermal conductivity values for all summer modeling periods were $k_{\text{up}} = 0.66$ and $k_{\text{low}} = 0.73 \text{ Wm}^{-1}\text{K}^{-1}$ (Table 4).

Best-fit thermal conductivity values from winter periods in Bottineau, Langdon, Minot, and Streeter were also low, ranging from 0.52-0.72 (unfrozen) to 1.01-1.57 $\text{Wm}^{-1}\text{K}^{-1}$ (frozen). The average effective thermal conductivity values for all winter modeling periods were $k_{\text{un}} = 0.62$ and $k_{\text{fr}} = 1.12 \text{ Wm}^{-1}\text{K}^{-1}$ (Table 5). The average thermal conductivity for all summer modeling periods was $k = 0.61 \text{ Wm}^{-1}\text{K}^{-1}$ (Table 5). Differences in seasonal thermal conductivity values at individual sites are attributed mainly to changes in *in situ* soil moisture. Thermal conductivity of a soil depends upon porosity, moisture content, and thermal properties of the soil particles, but moisture content is the only property that varies on short time scales (Oke, 1987). Thermal conductivity of frozen soil is greater than unfrozen soil, depending on porosity and

Table 4. Average best-fit thermal conductivity (**k**) and latent energy of freezing (**LE**) values from Fargo, including unfrozen (**unfr**), frozen (**fr**), upper (**up**) and lower (**low**) thermal conductivity and evapotranspiration (**evapotrans**).

Modeling period (year)	Winter best-fit k_{un} ($W m^{-1}K^{-1}$)	Winter best-fit k_{fr} ($W m^{-1}K^{-1}$)	Best-fit LE of freezing ($J s^{-1}m^{-3}$)	Summer best-fit k_{up} ($W m^{-1}K^{-1}$)	Summer best-fit k_{low} ($W m^{-1}K^{-1}$)	Best-fit LE of evapotrans ($J s^{-1}m^{-3}$)
1981	0.71	1.32	90	0.58	0.69	6
1982	0.60	1.23	195	0.62	0.72	9
1983	0.64	1.12	70	0.58	0.69	7
1984	0.72	1.57	205	0.70	0.77	11
1985	0.65	1.42	123	0.68	0.74	9
1986	0.65	1.38	115	0.72	0.78	7
1987	0.61	1.32	107	0.71	0.75	6
1988	0.52	1.07	115	0.66	0.72	6
1989	0.65	1.51	131	0.69	0.72	7
Average:	0.64	1.33	128	0.66	0.73	8

Table 5. Average best-fit thermal conductivity (**k**) and latent energy of freezing (**LE**) values from four sites, including unfrozen (**unfr**) and frozen (**fr**) thermal conductivity. These values are averaged over all modeling periods.

Site	k_{summer} ($W m^{-1} K^{-1}$)	$k_{winter, unfr}$ ($W m^{-1} K^{-1}$)	$k_{winter, fr}$ ($W m^{-1} K^{-1}$)	LE freezing ($W m^{-3}$)
Bottineau	0.57	0.58	0.67	88
Langdon	0.54	0.59	1.20	94
Minot	0.60	0.60	1.14	88
Streeter	0.72	0.71	1.45	84
AVERAGE	0.61	0.62	1.12	89

moisture content of the soil (Farouki, 1981). Thermal conductivity of an unfrozen soil increases with increasing soil moisture content (Farouki, 1981). Differences in effective thermal conductivity values may also be attributed to changes in nonconductive effects, including internal distillation, advection, evaporation, and condensation (Hinkel and Outcalt, 1994).

Saturated soils may have a latent energy budget during ground freezing in the upper 1m that is greater than the total solar daily flux (Putnam and Chapman, 1996). Saturated soils generally have higher thermal conductivity than dry soils but provide greater insulation from extreme cold temperatures due to latent energy extracted in the freezing process (Farouki, 1981). This insulating effect causes soil temperatures to be held at 0°C until all the moisture present freezes, isolating the region below the freezing front from subzero temperatures (Lewis and Wang, 1992). This “zero-curtain” effect initially is due to freezing effects but maintaining it involves internal evaporation, condensation and vapor transport processes (Outcalt et al., 1990). Water drawn from below the freezing front alters the thermal properties of the frozen and unfrozen zones (Farouki, 1981). Latent energy of freezing is known to have an insulating effect on subsurface temperatures (Goodrich, 1978), but the interannual variability and magnitude of this effect on subsurface temperatures is not well known.

Despite the complexity of ground freezing, the assumption of an abrupt conductivity change at the 0° isotherm and latent-energy terms in the model produce a good fit to observed temperatures. Figure 42 shows the modeled 125cm depth temperatures from the 1982-freezing season at Fargo calculated with and without a latent energy component. In addition to showing the necessity of the latent energy term in the

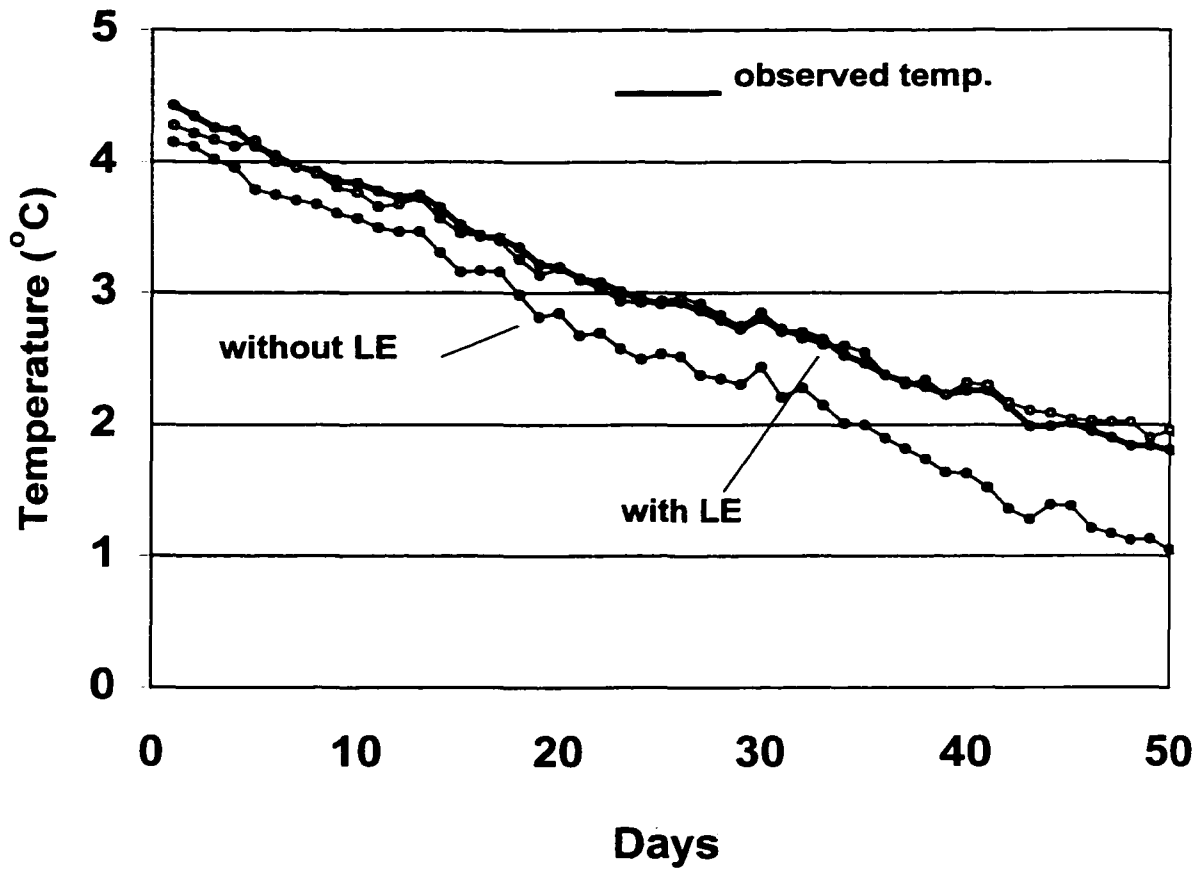


Figure 42. Observed 125cm-depth temperatures (observed temp.) for the 1982-freezing season at Fargo. Model temperatures shown are calculated with and without a term for latent energy.

modeling scheme, Figure 42 shows the discrepancy between 125cm depth temperatures calculated with and without latent energy increasing with time. This increase is due to the cumulative warming effects of latent energy release as the freezing isotherm reaches greater depths.

Model sensitivity

The freezing period extending from 12/10/81 – 2/9/82 was used to determine model sensitivity to choices of thermal conductivity and latent energy (**LE**). The best-fit thermal conductivity and latent energy of freezing values for this period are $k_{un} = 0.60$, $k_{fr} = 1.23 \text{ Wm}^{-1}\text{K}^{-1}$ and $LE = 195 \text{ Wm}^{-3}$, respectively. These best-fit parameters produce an average residual temperature from all depths of 0.005°C for this 58-day period.

Daily residual temperatures from all depths calculated with the best-fit latent energy value are plotted for three trial thermal conductivity values (Fig. 43). The $0.63 \text{ Wm}^{-1}\text{K}^{-1}$ difference between k_{un} and k_{fr} is maintained for all trial values of thermal conductivity. The average residual temperatures ($T_{av\ res}$) for this modeling period are $T_{av\ res} = 0.187^\circ\text{C}$ ($k_{un} = 0.50$, $k_{fr} = 1.13 \text{ Wm}^{-1}\text{K}^{-1}$), $T_{av\ res} = 0.005^\circ\text{C}$ ($k_{un} = 0.60$, $k_{fr} = 1.23 \text{ Wm}^{-1}\text{K}^{-1}$, best-fit k values), and $T_{av\ res} = -0.163^\circ\text{C}$ ($k_{un} = 0.70$, $k_{fr} = 1.33 \text{ Wm}^{-1}\text{K}^{-1}$).

Average residual temperatures from all depths are plotted as functions of trial thermal conductivity and latent energy values in Figures 44 and 45, respectively. Best-fit latent energy is held constant while trial thermal conductivity values are entered in the model (Fig. 44), and best-fit thermal conductivity values are held constant while trial latent energy values are entered in the model (Fig. 45). The linear regression line in Figure 44 indicates a thermal conductivity variance of $\pm 0.058 \text{ W m}^{-1} \text{ K}^{-1}$ ($\pm 9.7\%$),

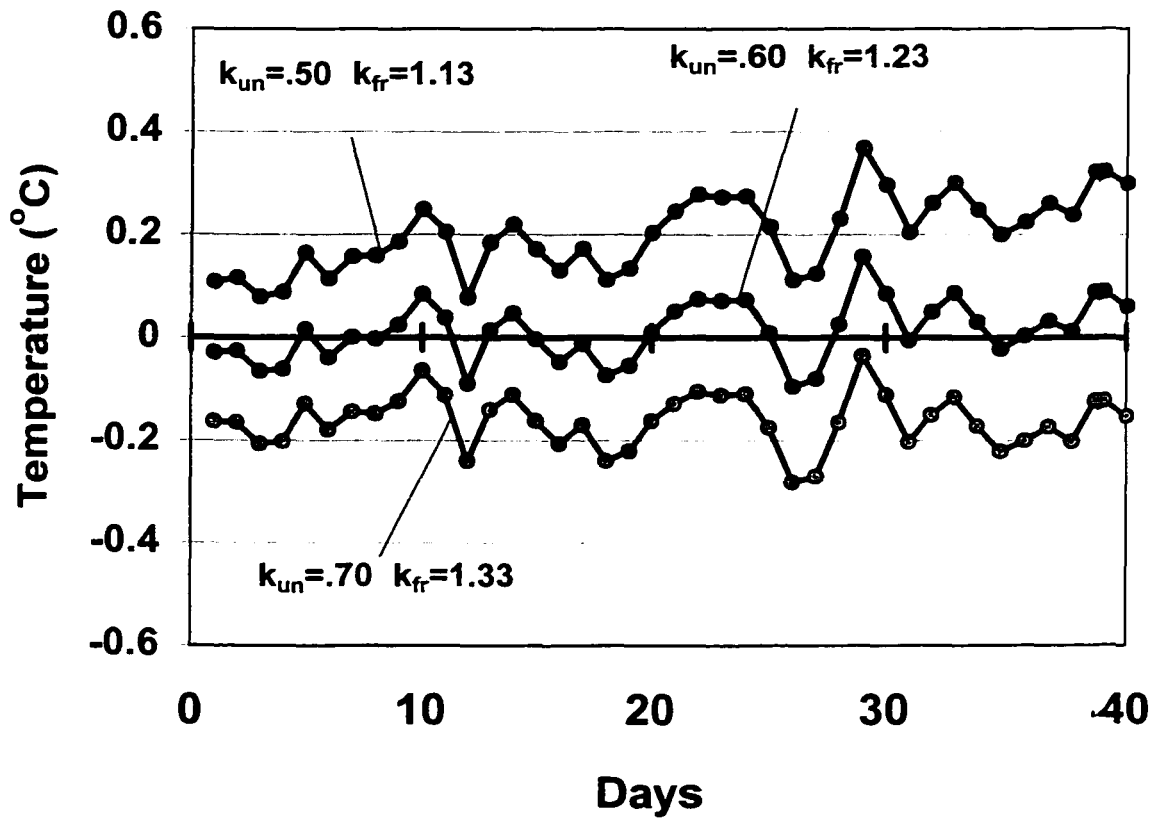


Figure 43. Daily residual temperatures calculated with three trial thermal conductivity values from the winter 1982 modeling period. Residual temperatures averaged during this modeling period are $T_{av\ res} = 0.187^{\circ}\text{C}$ ($k_{un} = 0.50$, $k_{fr} = 1.13\ \text{Wm}^{-1}\text{K}^{-1}$), $T_{av\ res} = 0.005^{\circ}\text{C}$ ($k_{un} = 0.60$, $k_{fr} = 1.23\ \text{Wm}^{-1}\text{K}^{-1}$), and $T_{av\ res} = -0.163^{\circ}\text{C}$ ($k_{un} = 0.70$, $k_{fr} = 1.33\ \text{Wm}^{-1}\text{K}^{-1}$).

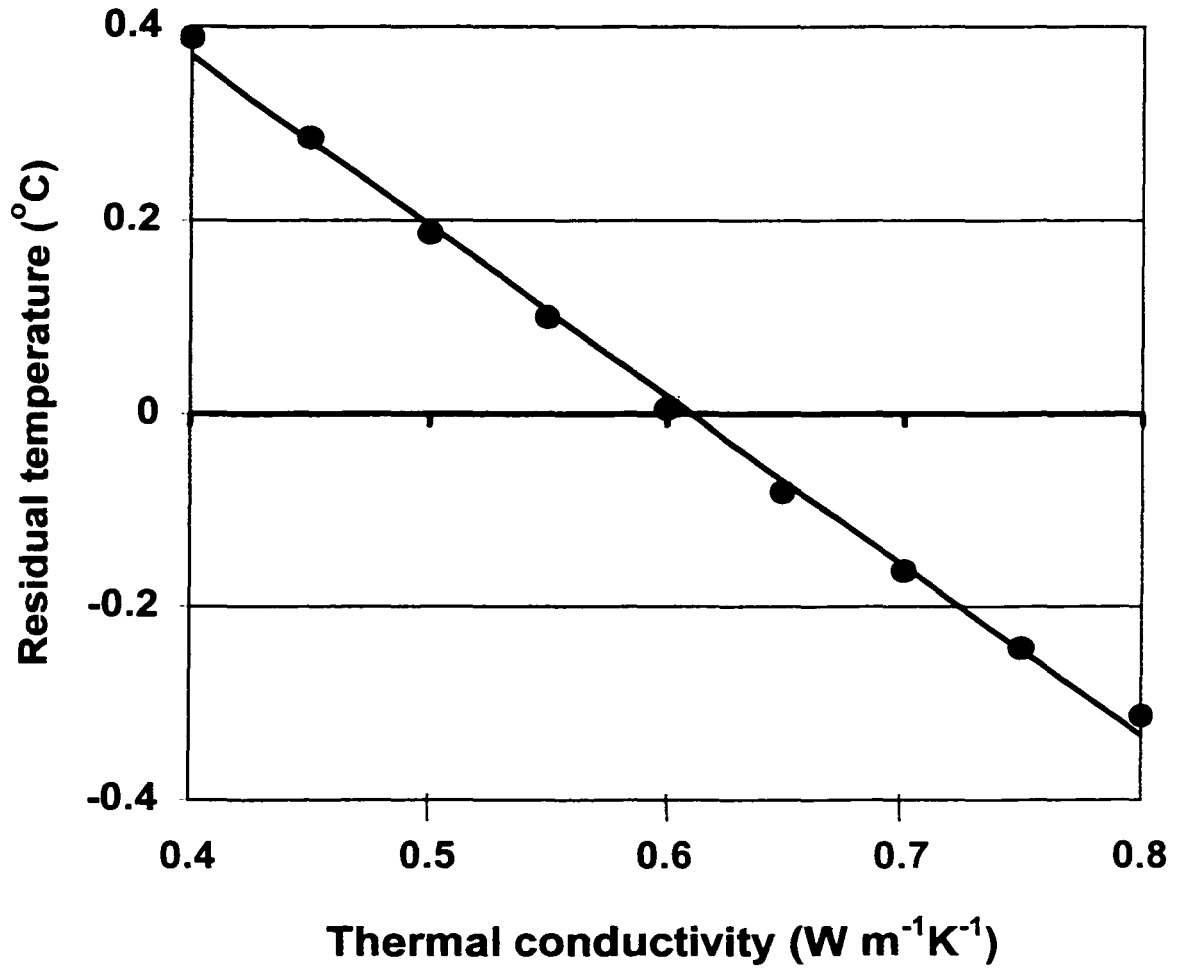


Figure 44. Average residual temperatures from all depths plotted as a function of trial thermal conductivity values with latent energy held constant at $LE = 195 \text{ Wm}^{-3}$. Thermal conductivity is varied around best-fit values of $k_{un} = 0.60$, $k_{fr} = 1.23 \text{ Wm}^{-1}\text{K}^{-1}$, with a constant difference of $0.63 \text{ Wm}^{-1}\text{K}^{-1}$ maintained between k_{un} and k_{fr} . A linear regression line is shown.

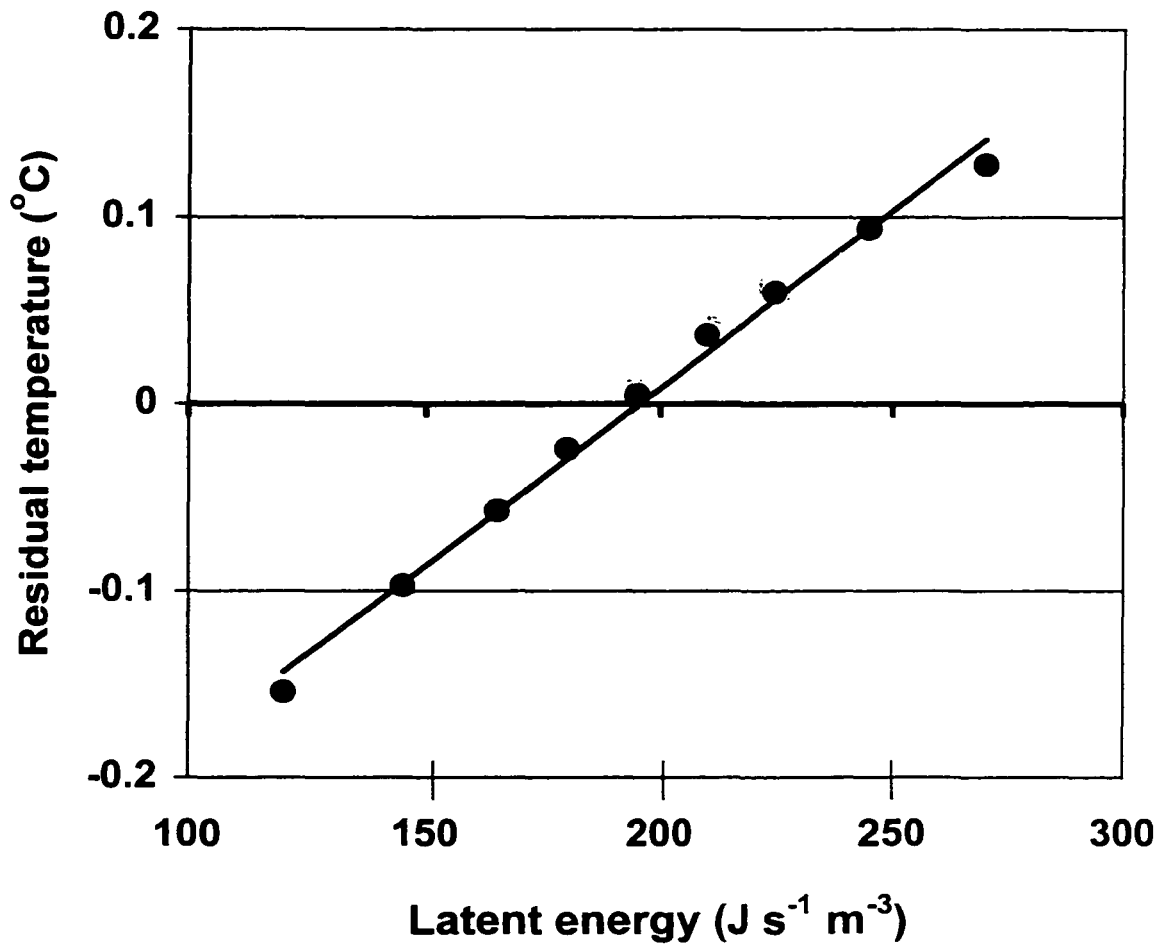


Figure 45. Average residual temperatures from all depths plotted as a function of trial latent energy. Thermal conductivity is held constant at $k_{\text{un}} = 0.60$, $k_{\text{fr}} = 1.23 \text{ Wm}^{-1}\text{K}^{-1}$. A linear regression line is shown.

corresponding to a $T_{av\ res}$ variance of $\pm 0.10^{\circ}\text{C}$. The linear regression line in Figure 45 indicates a latent energy variance of $\pm 52\ \text{W m}^{-3}$ ($\pm 26.7\%$), corresponding to a $T_{av\ res}$ variance of $\pm 0.10^{\circ}\text{C}$. The average residual temperatures for this modeling period show a much greater sensitivity to choices of thermal conductivity than to choices of latent energy. The choice of thermal conductivity influences temperature calculations at all nodes in the model, whereas latent energy is released only at the freezing isotherm.

When the model is run with and without a latent energy term for this period, the average residual temperature from all depths increases from $T_{av\ res} = 0.005^{\circ}\text{C}$ (with LE) to $T_{av\ res} = -0.578^{\circ}\text{C}$ (without LE). The influence of latent energy on calculated temperatures for this period occurs entirely within the upper 2.5m of the ground. The latent energy of fusion term in the model is necessary to match subzero temperatures near the freezing front accurately, but inclusion of this term does not change the magnitude of the average residual temperature greatly (0.58°C / 58-day period). Latent energy of fusion provides an insulating effect by holding soil temperatures near the freezing point, but does not seem to alter average residual temperatures significantly. A similar study of ground-surface temperature exchange using a numerical conduction model with latent energy of freezing and temperature dependent thermal conductivity produced similar results on subsurface temperatures (Goodrich, 1978). The nonlinear effects of snow cover and latent energy of freezing were shown to reduce the amplitude of ground temperature fluctuations with depth and increase mean annual ground temperatures (Goodrich, 1978).

Modeling spring temperatures

The thermal effects of spring thawing are influenced by several nonconductive factors, including gravity-driven infiltration, runoff, water table fluctuations, downward vapor migration, and latent energy of freezing, melting, evaporation, condensation, and sublimation (Outcalt, 1990). High-moisture soils freeze more slowly and to a lesser depth than dry soils, because of the latent heat released, but they also thaw more slowly in the spring (Geiger et al., 1995). Recorded ground temperatures tend to remain around 0°C for several weeks until all the subsurface ice melts. Average residual temperatures during spring modeling periods were as high as $\pm 0.70^\circ\text{C}$. Spring melting of pore ice occurs above and below the frozen section of the ground. Negative heat production terms for latent energy of melting are therefore entered both above and below the frozen section of the ground. The thermal effects of meltwater consistently exceeded modeled latent energy of thawing effects, and spring temperatures were impossible to model accurately.

Advective effects

A major difficulty in modeling near-surface ground temperatures is accounting for the thermal effects of water movement, including precipitation, infiltration, and changes in the depth of the water table. Figure 46 shows subsurface warming of almost 1°C due to infiltration of over 7.5cm of rainfall from May 24-27, 1984 at Fargo. The thermal effects of this infiltration extend beyond four meters in depth. It should be noted that this event might also be due to a malfunction in the thermocouple junction box relating to the rainfall (Enz, personal communications). Although this was the most significant precipitation event during the period of record, the effects of precipitation and water table

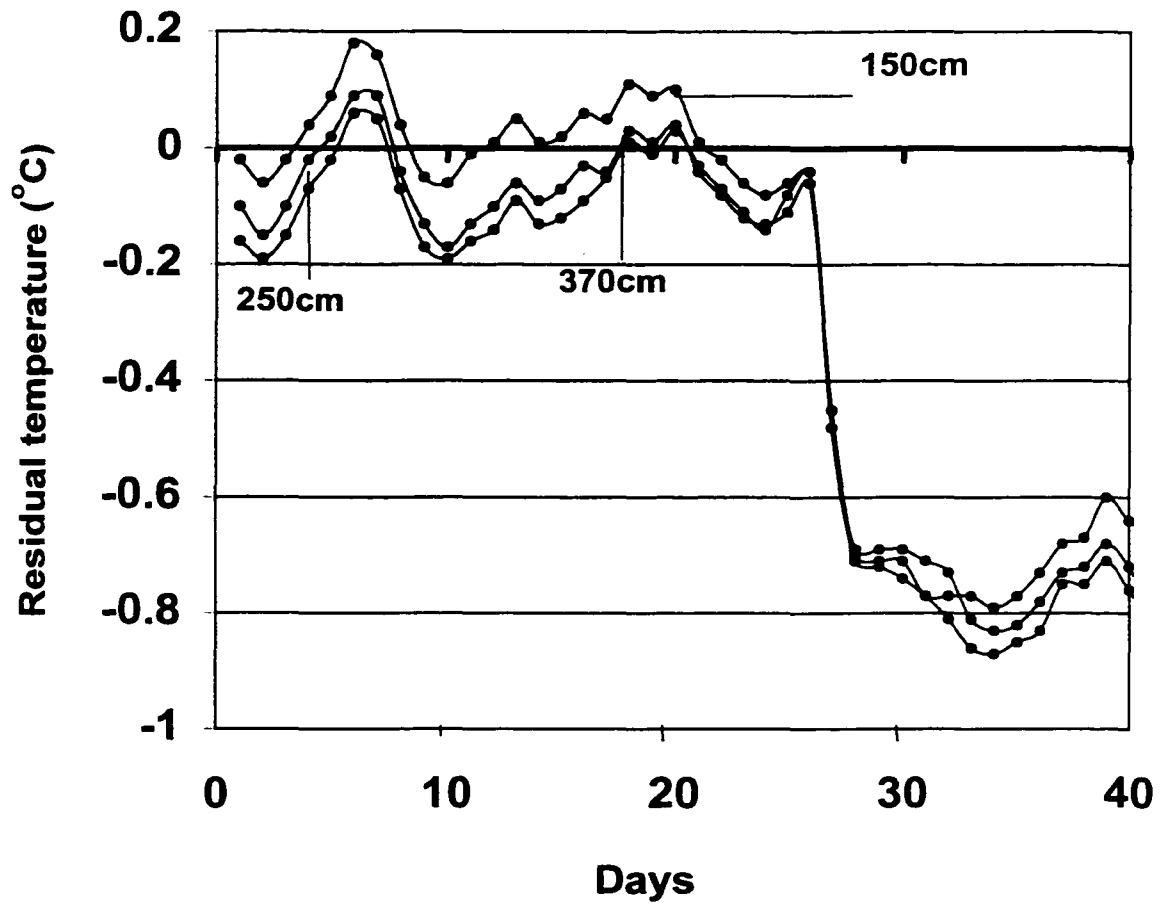


Figure 46. Subsurface warming due to a three-day precipitation event at Fargo, beginning 5/27/1984. Daily residual temperatures ($T_{\text{calc}} - T_{\text{obs}}$) are shown for 150, 250 and 370cm depths.

movement on near-surface ground temperatures limit the accuracy of temperature modeling in this region. Modeling the effects of these nonconductive factors is complicated because of the many variables involved that are difficult to estimate.

CHAPTER 7

LATENT ENERGY AND PRECIPITATION

The possible correlation between total fall precipitation and annual latent energy of freezing values was tested for each site during the 6 and 9-year measurement periods. Because infiltration rates at the ground surface depend largely on antecedent moisture content, the time duration for “totaling” precipitation is relevant in determining soil moisture content at the onset of freezing. The freezing front will take longer to penetrate into soil with high water content because a greater amount of latent heat has to be extracted (Farouki, 1981). The insulating effect of latent energy release is different than snow cover insulation in that it influences varying depths of the ground depending on the position of the freezing front. Energy released at the freezing boundary is conducted upward to cooler areas of the ground. Therefore insulation effects of latent energy are not as pervasive as winter snow cover insulation.

Fargo

Modeled latent energy of freezing values averaged 128 Wm^{-3} and ranged from $70 - 205 \text{ Wm}^{-3}$ for all freezing seasons. These values represent latent heat released per second per cubic meter averaged over the period of a day. Best-fit latent energy values from each freezing season are plotted with precipitation totaled 60 days prior to the onset of ground freezing ($r^2 = .66$, Fig. 47). The correlation between modeled latent energy values and prior precipitation decreases to $r^2 = .36$ if precipitation was totaled for 30

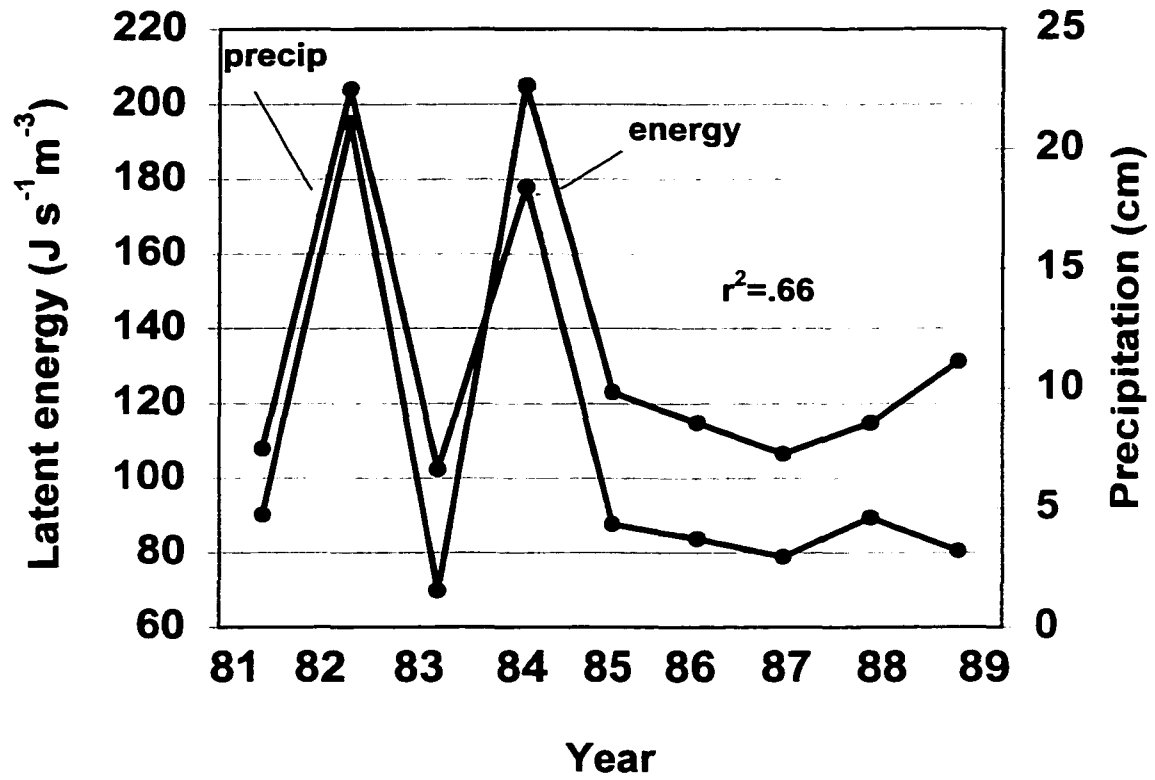


Figure 47. Modeled annual latent energy of fusion (energy) versus precipitation (precip) totaled 60 days prior to the onset of ground freezing from Fargo.

days prior to freezing, and $r^2 = 0.63$ for total fall precipitation (Aug, Sep, Nov). Total fall precipitation at Fargo decreased by 10.32 cm from 1981-1989 despite a long-term trend of increasing fall precipitation in the Northern Plains (Gosnold et al., 1997).

Bottineau, Langdon, Minot, and Streeter

Modeled values of latent energy of ground freezing averaged 89 Wm^{-3} and ranged from $55\text{-}175 \text{ Wm}^{-3}$ at all sites. Best-fit latent energy values are plotted with total fall precipitation (Aug, Sep, Nov) from each site in Figures 48 - 51. Modeled values of latent energy due to freezing vary annually and show a mixed dependence on total fall precipitation among sites (average $r^2 = .51$, Figs. 48 - 51). The variables correlate well at Minot and Langdon sites ($r^2 = .95$ and $r^2 = .69$, respectively). Bottineau and Streeter showed poor correlations ($r^2 = .38$ and $r^2 = .01$, respectively).

Regional differences in correlations

Because latent energy of freezing and total fall precipitation show a varied correlation between sites, the hypothesis that latent energy released during ground freezing is strictly a function of total fall precipitation is rejected. The discrepancy in correlations is probably due to the number of factors that influence total soil moisture, including water table depth, antecedent moisture content, incident radiation, precipitation, permeability, porosity, evapotranspiration, vegetative cover, and infiltration. Depending on the ground-surface forcing temperature, total water content at the onset of freezing is probably the main factor controlling latent energy release. Other possible factors are low

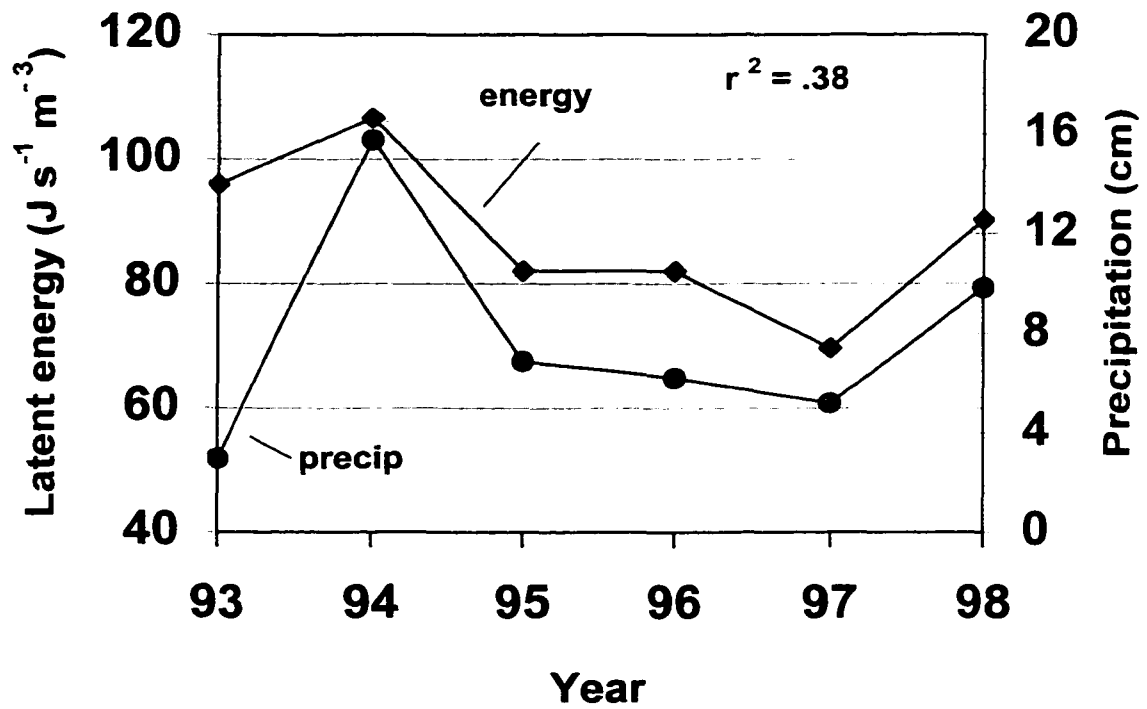


Figure 48. Modeled annual latent energy of fusion (energy) versus total fall precipitation (precip) from Bottineau.

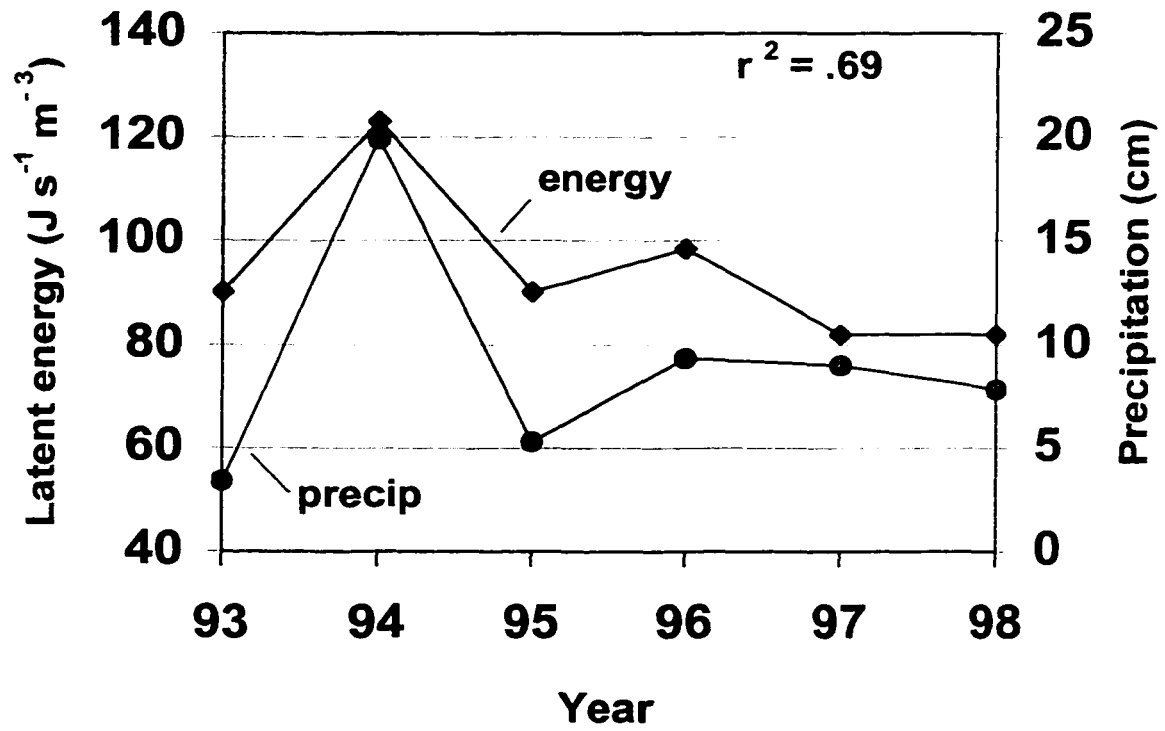


Figure 49. Modeled annual latent energy of fusion (energy) versus total fall precipitation (precip) from Langdon.

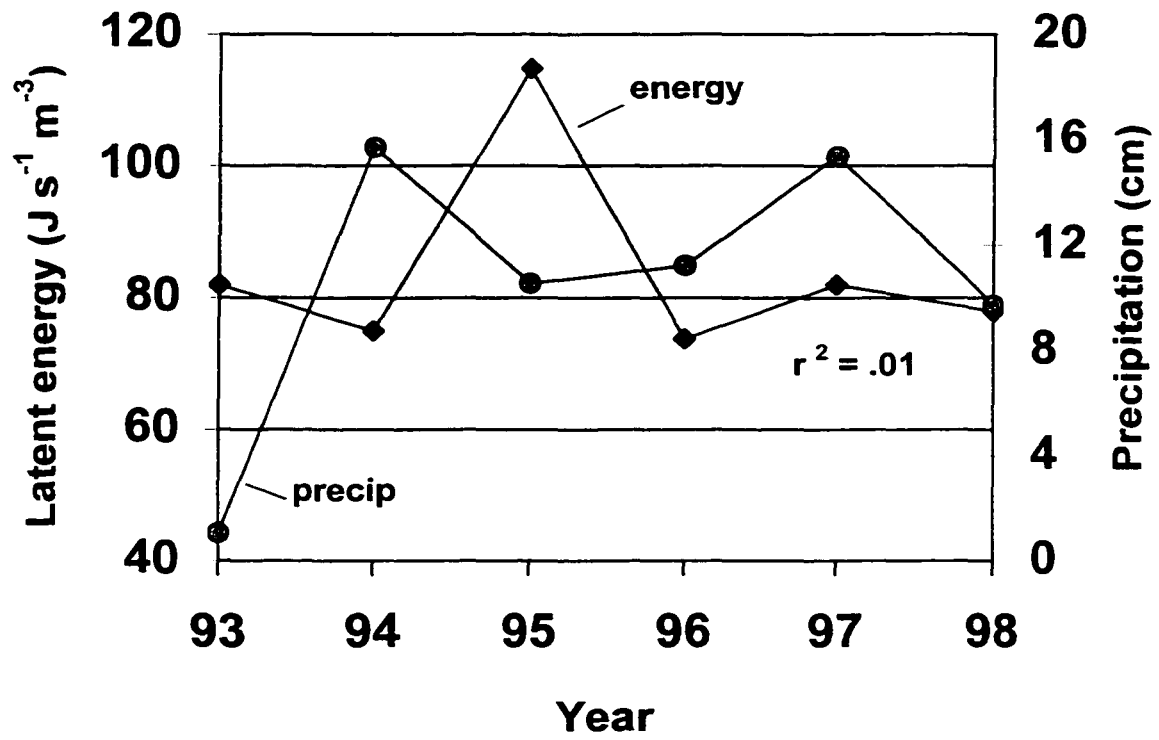


Figure 50. Modeled annual latent energy of fusion (energy) versus total fall precipitation (precip) from Minot.

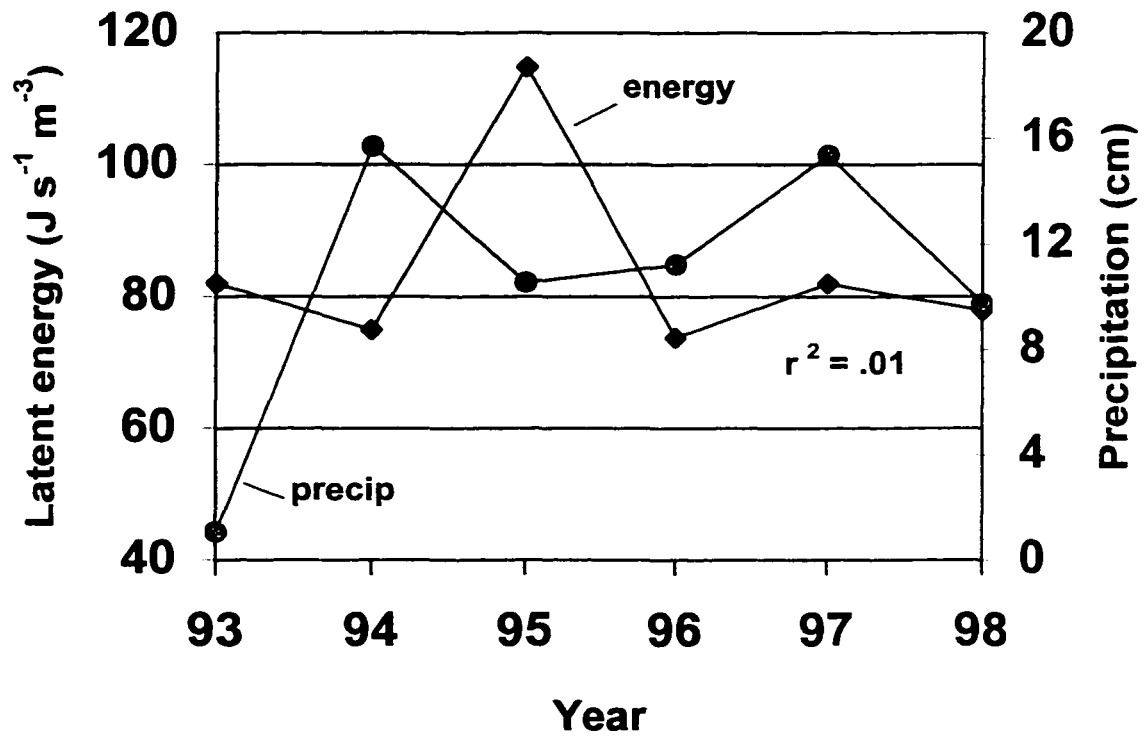


Figure 51. Modeled annual latent energy of fusion (energy) versus total fall precipitation (precip) from Streeter.

model sensitivity to choices in latent energy of freezing and the short nature of this study ($n = 6$ and 9) making correlation coefficients very sensitive to latent energy values.

The occurrence and timing of fall precipitation events can influence soil moisture at the onset of ground freezing, but the extent of these effects is largely a function of baseline antecedent water content. An extremely low antecedent moisture content may have a much higher or lower sensitivity to fall precipitation events. Secular trends in precipitation on the scale of years to decades can also affect water table depth and relative moisture content of the ground (Enz, personal communication). Since soil dries from the surface downward, there is normally an increase in the amount of water present with increasing soil depth (Geiger et al., 1995). The Northern Plains is characterized by large interannual and intra-annual variability of all hydroclimatological parameters, including soil moisture (Todhunter, 1995). Soil moisture content of an area of any size is difficult to measure and is subject to high variation (Geiger et al., 1995).

CHAPTER 8

A FORWARD MODELING ANALYSIS

This chapter describes a forward modeling analysis of recorded air temperatures with direct air-ground coupling. A surface air temperature time series is used as a boundary condition for the ground-surface forcing signal to generate a synthetic transient. The forcing signal is a century long record of monthly mean air temperatures averaged from climate stations in northwestern North Dakota (NCDC, NOAA). A 100-year record of total fall precipitation averaged from climate stations in this region is used as a proxy to model latent energy release during ground freezing.

Regional study of climate change

Differences in warming magnitudes of recorded surface air temperatures and ground-surface temperatures north of 46° latitude in the Northern Plains are attributed to changes in variables including snow cover, latent energy of ground freezing and thawing, and total fall precipitation (Gosnold et al., 1997). Total fall precipitation averaged from climate stations in northwestern North Dakota has undergone significant variability (Fig. 52). The 10-point moving average in Figure 52 indicates that total fall precipitation nearly doubled between the periods 1935 to 1950 and 1970 to 1985. Increased fall precipitation leads to greater soil moisture content at the onset of ground freezing, and therefore increased latent energy released during ground freezing. Although precipitation records for the Northern Plains show that in recent decades winter precipitation has

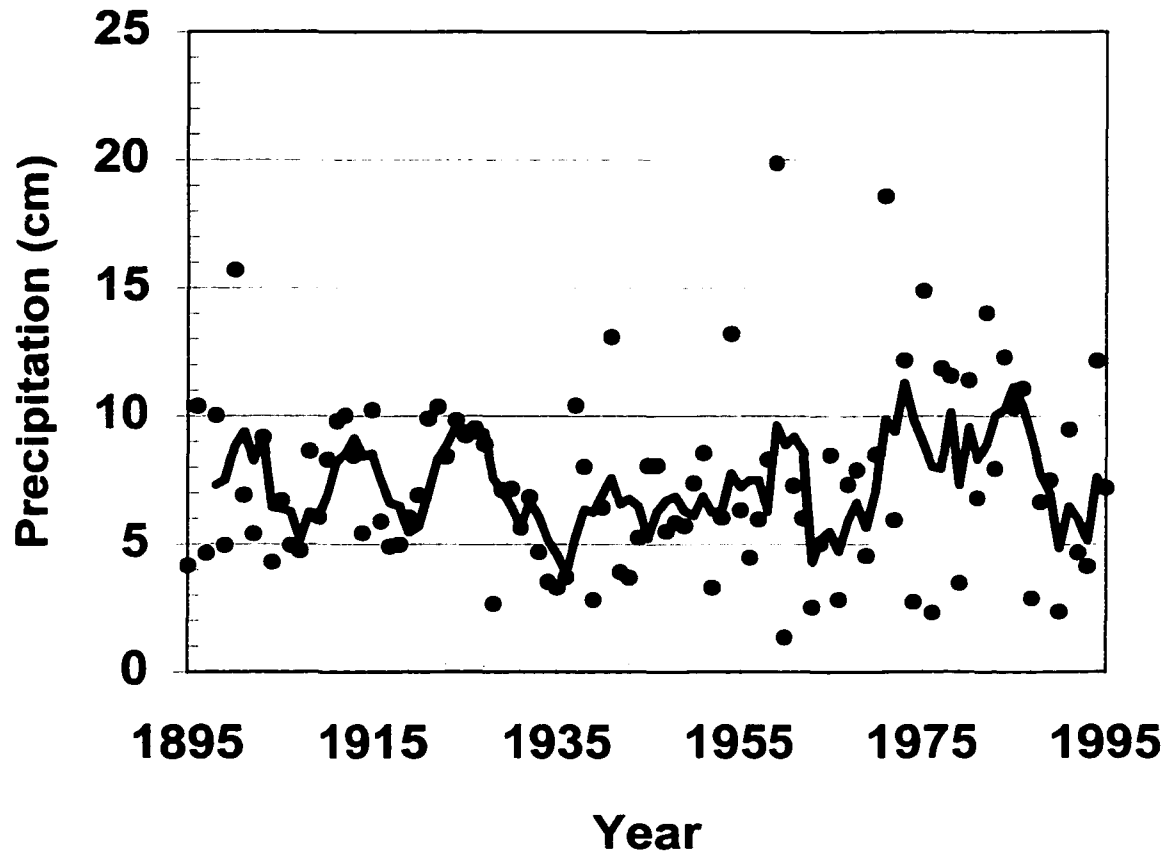


Figure 52. Total fall (Sep, Oct, Nov) precipitation averaged from climate stations in northwestern North Dakota. A 10-point moving average is shown.

decreased (Groisman and Easterling, 1994), the duration of winter snow cover in all regions of the Great Plains has increased from the 1920s to the late 1980s (Hughes and Robinson, 1996, Hughes and Robinson, 1993). Duration of snow cover in the Great Plains region shows significant annual and decadal scale variability as well as significant spatial variability (Hughes and Robinson, 1996, Hughes and Robinson, 1993).

The forcing signal for the modeling analysis is the time series of mean annual air temperatures averaged from climate stations in northwestern North Dakota from 1895 to 1995 (Fig. 53). A least-squares linear regression of these temperatures yields a slope of $+1.57 \pm 0.23^{\circ}\text{C}$ (Fig. 53). Four temperature-depth borehole profiles logged in 1995 are used to determine a regional ground-surface temperature history. Boreholes in the study include Minot N (101.3° , 48.5°), Landa (100.9° , 48.9°), Glenburn (101.2° , 48.5°), and Wawanesa (99.8° , 49.4°). Ground-surface temperature histories are determined with a least-squares functional space inversion algorithm as described by Shen, et al., 1995. Ground-surface temperature histories from individual borehole profiles are shown in Figure 54. The magnitude of warming averaged from the boreholes is 1.8°C per century (Fig. 55). The average ground surface warming (Fig. 55) is shown with error bars that represent ± 1 standard error about the mean.

Forward modeling with direct coupling

The numerical conduction model used in this analysis is described in Chapter 6 and Appendix. Nodal spacing near the ground surface is set at 20cm to closely match freezing conditions and increased to 5m at 15 to 250m depths (Table 6). The bedrock at

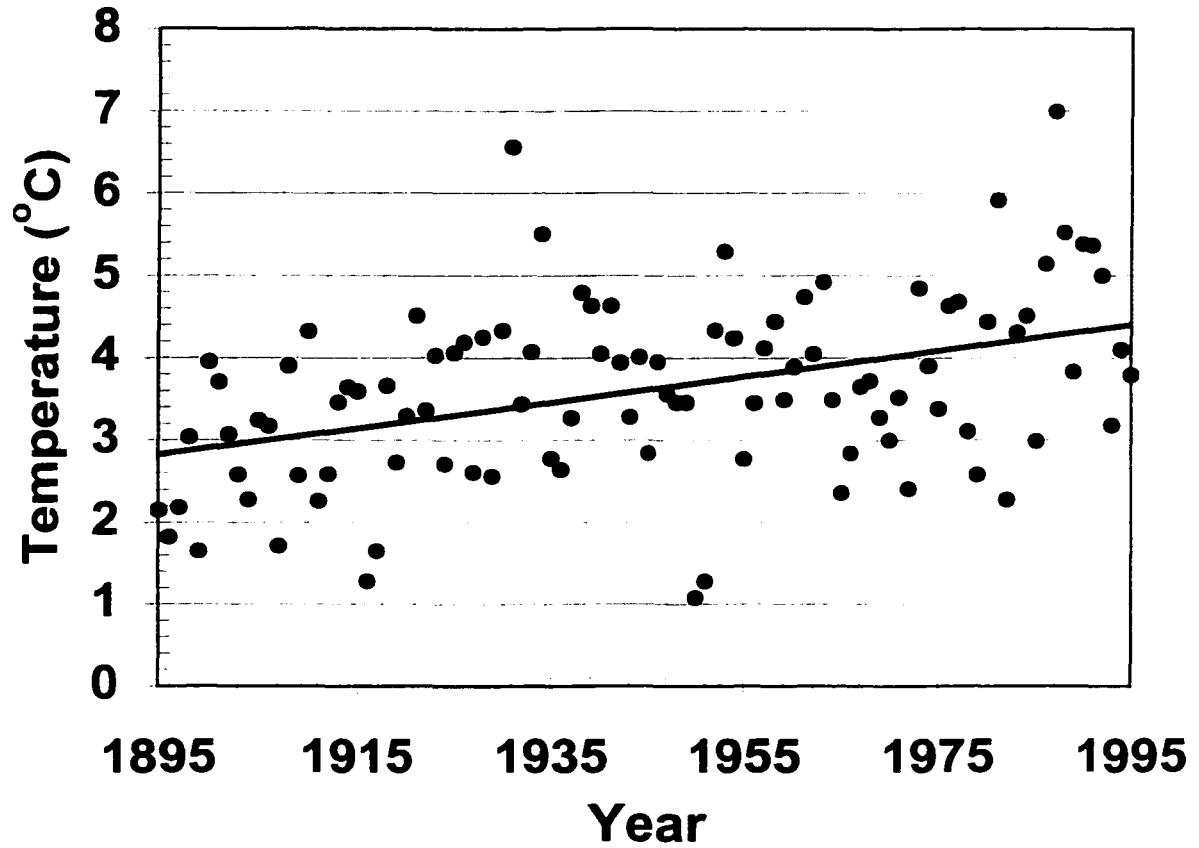


Figure 53. Mean annual surface air temperatures averaged from climate stations in northwestern North Dakota. A least-squares linear regression line indicates a slope of $1.57 \pm 0.23^\circ\text{C}$.

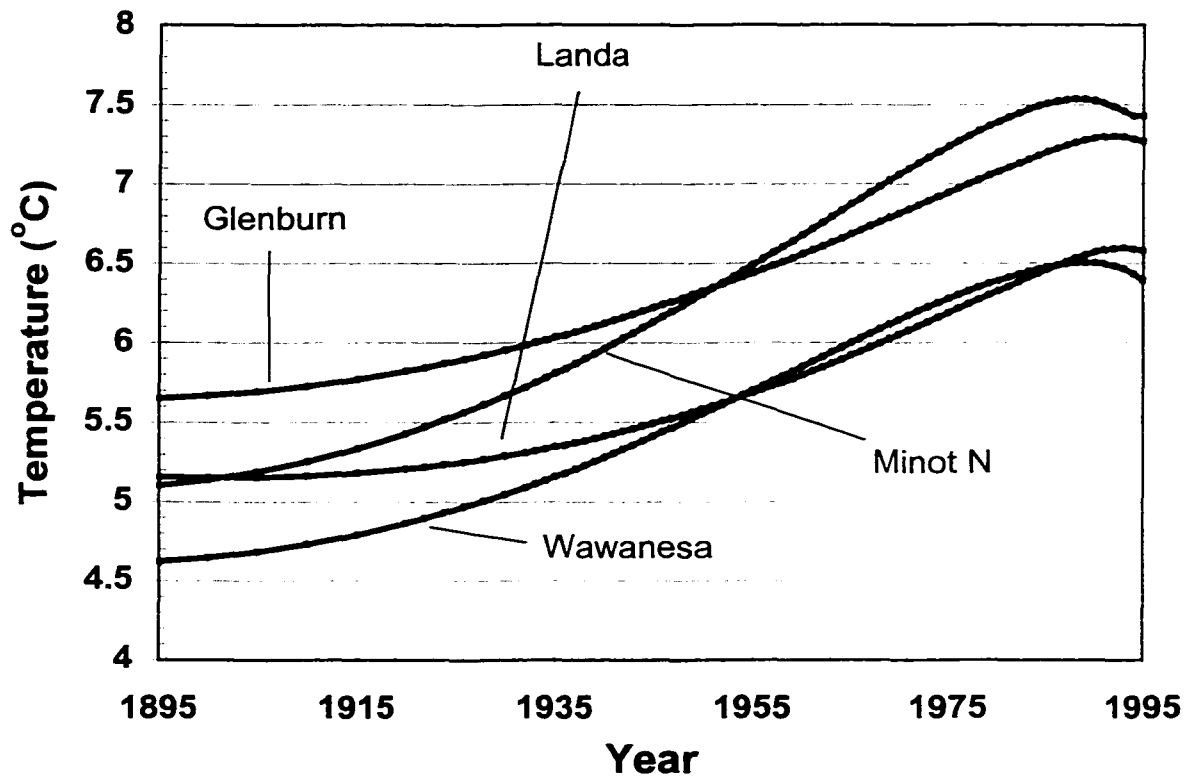


Figure 54. Individual ground surface temperature histories from Minot N, Landa, Glenburn, and Wawanesa boreholes.

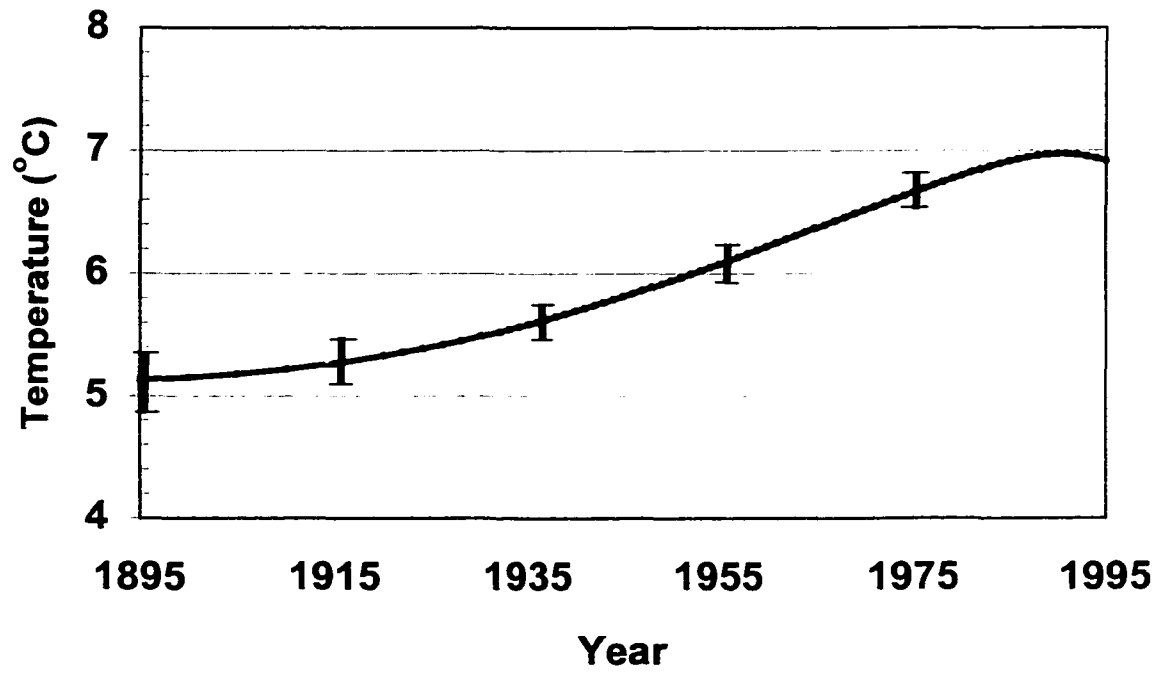


Figure 55. Average ground surface temperature history from the four boreholes showing a warming magnitude per century of 1.8°C . The error bars are the standard deviation of mean warming.

Table 6. Nodal depth and spacing.

Depth (m)	Nodal spacing (m)
0	
0.2	0.2
0.4	0.2
0.6	0.2
0.8	0.2
1	0.2
1.2	0.2
1.4	0.2
1.6	0.2
1.8	0.2
2	0.2
2.2	0.2
2.4	0.2
2.6	0.2
2.8	0.2
3	0.2
3.3	0.3
3.75	0.45
4.4	0.65
5.3	0.9
6.6	1.3
8.5	1.9
11.3	2.8
15	3.7
20	5
25	5
30-270	5

Minot is low thermal conductivity Pierre Shale ($k = 1.2 \pm 0.2 \text{Wm}^{-1}\text{K}^{-1}$; Gosnold et al., 1997). Thermal conductivity is assumed to be uniform at all depths and equal for all boreholes.

Direct coupling explicitly correlates borehole transient temperatures with the air temperature time series. Any variation in the resultant temperature-depth profile from the initial steady-state profile is assumed to be due solely to time-variation in the surface temperature. For an individual site, the synthetic temperature-depth profile generated by direct-coupling will be offset from the actual temperature-depth profile by an amount equal to the time averaged difference between air and ground surface temperatures at the NCDC station and borehole site respectively (Chapman et al., 1992). The only time averaged air and ground temperature data available in this region are from the Minot NDAWN site. For the period 1994 – 1999, the ground temperature at the Minot site averaged from 12 depths ranging from 5 – 175cm was 7.57°C (Fig. 31). The average air temperature during the same period was 4.62°C , giving an offset of 2.95°C . Ground temperatures commonly exceed air temperatures in winter in regions with snow cover, because snow cover maintains ground temperatures near 0°C while air temperatures are much colder. Fall ground temperatures also exceed air temperatures (Fig. 16) because of the higher thermal capacity of soil and the ability of air near the ground to mix and cool by convection. The offset of air and ground temperatures is not relevant for climate change studies provided that ground temperatures track air temperatures through time. However, secular changes in the offset due to boundary layer factors such as snow cover and latent energy of ground freezing must be considered.

Warming or cooling rates of synthetic temperature-depth profiles are sensitive to the choice of initial ground-surface temperature. An initial $z = 0$ temperature significantly different from the time averaged forcing signal will generate spurious warming or cooling. To reduce this effect, mean-annual air temperatures were averaged from the first ten years of record. This average value (2.70°C) was used as the ground surface temperature for the initial steady-state temperature-depth profile.

The ground surface temperature history of the synthetic profile generated by forcing the recorded air temperatures into the ground indicates a warming magnitude per century of 1.7°C (Fig. 56). This warming magnitude is not statistically different from the linear regression of mean annual air temperatures ($+1.57 \pm 0.23^{\circ}\text{C}$).

Latent energy of ground freezing

The hypothesis that modeled latent energy of ground freezing effects as determined by recorded fall precipitation totals are capable of generating a transient subsurface temperature signal is tested. Modeled latent energy of ground freezing values for Minot ground temperatures demonstrated a high correlation ($r^2 = .95$) with total fall precipitation (Fig. 57, see chapter 7). This correlation is assumed to hold for the regional modeling analysis of latent energy of ground freezing effects. The least-squares linear regression line in Figure 57 is used to determine annual latent energy of ground freezing values from the record of total fall precipitation.

In order to closely match the subsurface freezing regime at the Minot site, the observed depth and duration of ground freezing are taken as constraints to model snow cover insulation effects. Snow cover effects were incorporated into the model by

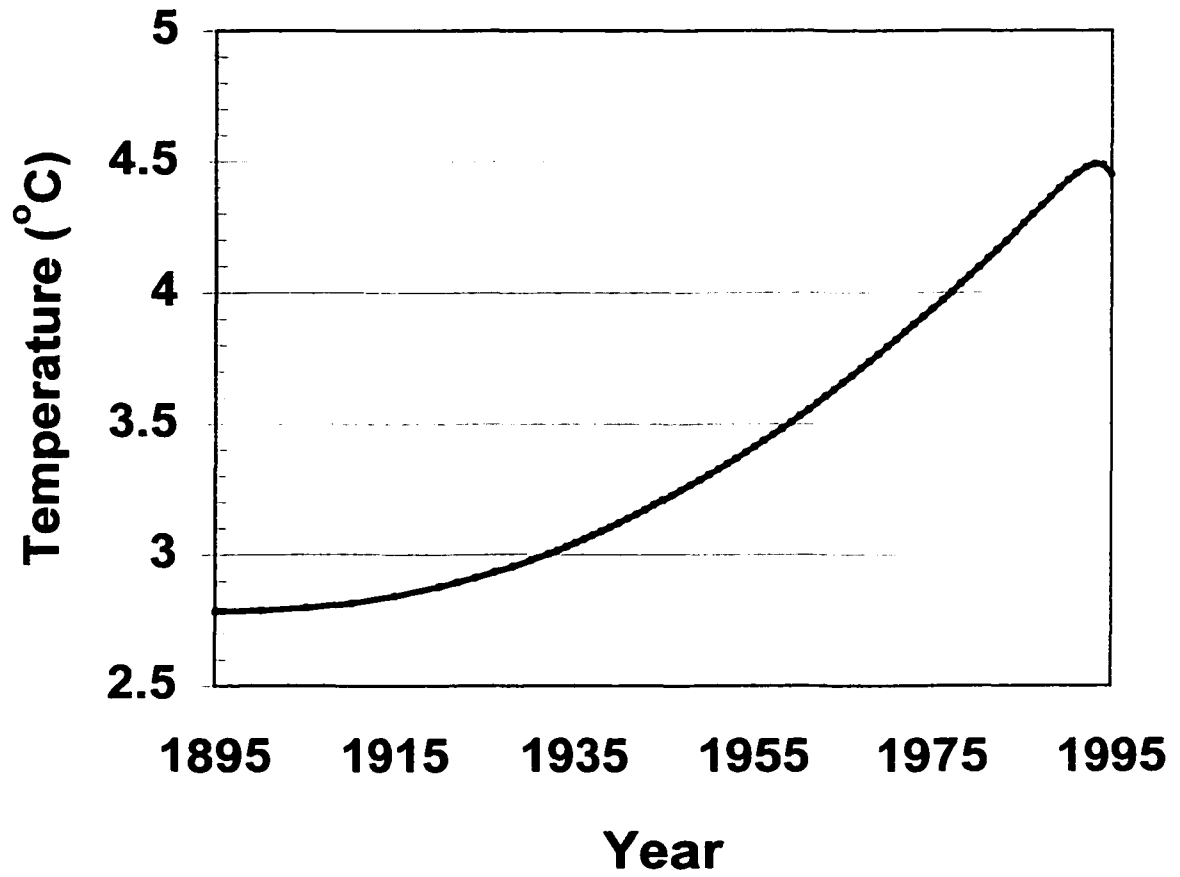


Figure 56. Ground surface temperature history of the transient generated with direct air-ground coupling.

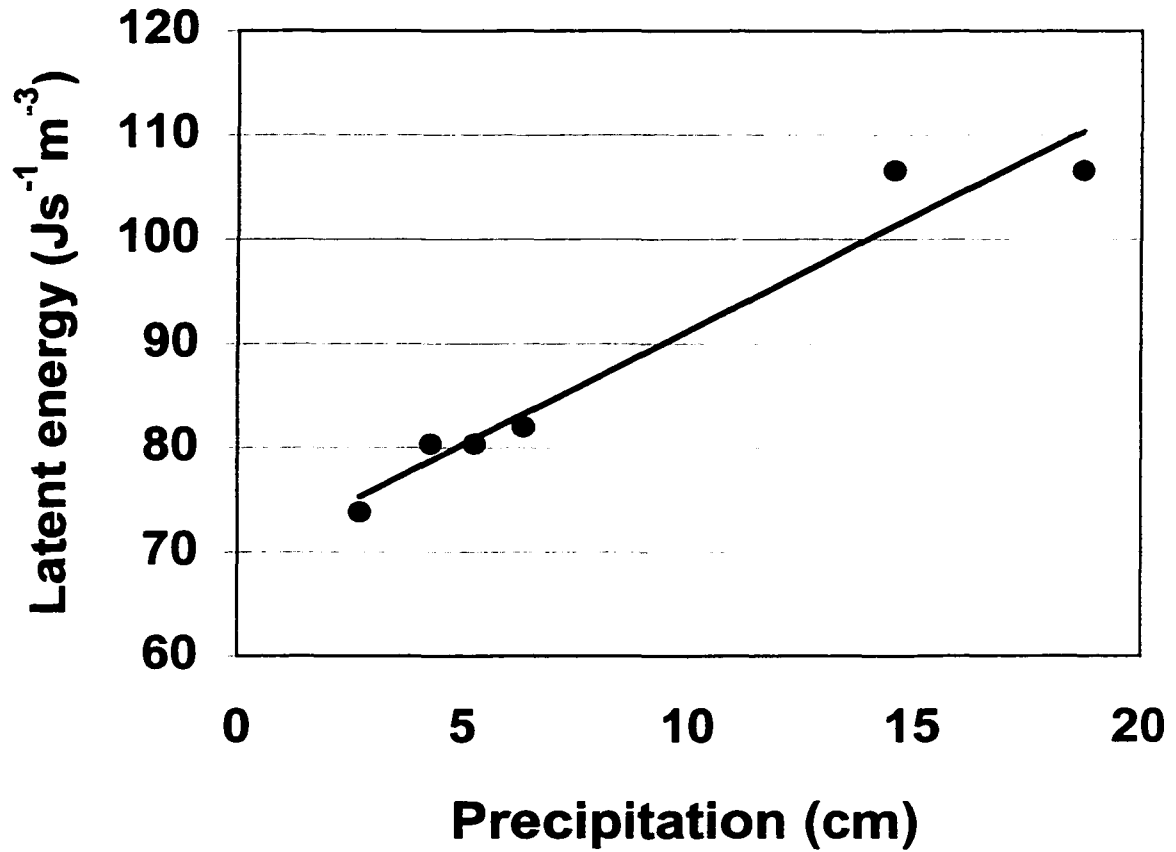


Figure 57. Total fall precipitation and modeled latent energy of ground freezing from the 1994 to 1999 modeling analysis of Minot data. A least-squares linear regression line is shown.

activating a very low thermal conductivity for all below-freezing nodes near the ground surface. This reduction in thermal conductivity has the net effect of reducing the depth and duration of ground freezing and preventing extreme lows from occurring in ground temperatures. The subzero-temperature thermal conductivity that closely reproduced the observed ground freezing regime was $k = 0.033 \text{ Wm}^{-1}\text{K}^{-1}$. Snow cover insulation properties vary significantly depending on factors such as snow density, age, and moisture content (Oke, 1987). Snow cover insulation is only activated in the model when near-surface ground temperatures go below 0°C . This approximation is necessary due to lack of snow cover data.

Latent energy release at the freezing boundary is assumed to occur during the entire duration of ground freezing, including spring thawing periods. This assumption is made because spring thawing periods in observed ground temperatures are very brief compared to freezing periods, and ground temperatures are warmed in the spring by meltwater infiltration (Farouki, 1981). These meltwater effects exceed latent energy effects and cause high residual temperatures during spring modeling periods (see Chapter 6).

To isolate the thermal effects of latent energy of ground freezing, the signal resulting from direct coupling of the surface air temperatures and snow cover insulation was subtracted from the resultant profile. A least-squares functional space inversion of the resultant profile indicates a ground-surface warming signal of 0.4°C per century attributed solely to latent energy release during ground freezing (Fig. 58). The hypothesis that modeled latent energy of ground freezing effects based on observed total fall precipitation are capable of generating a transient subsurface warming signal is

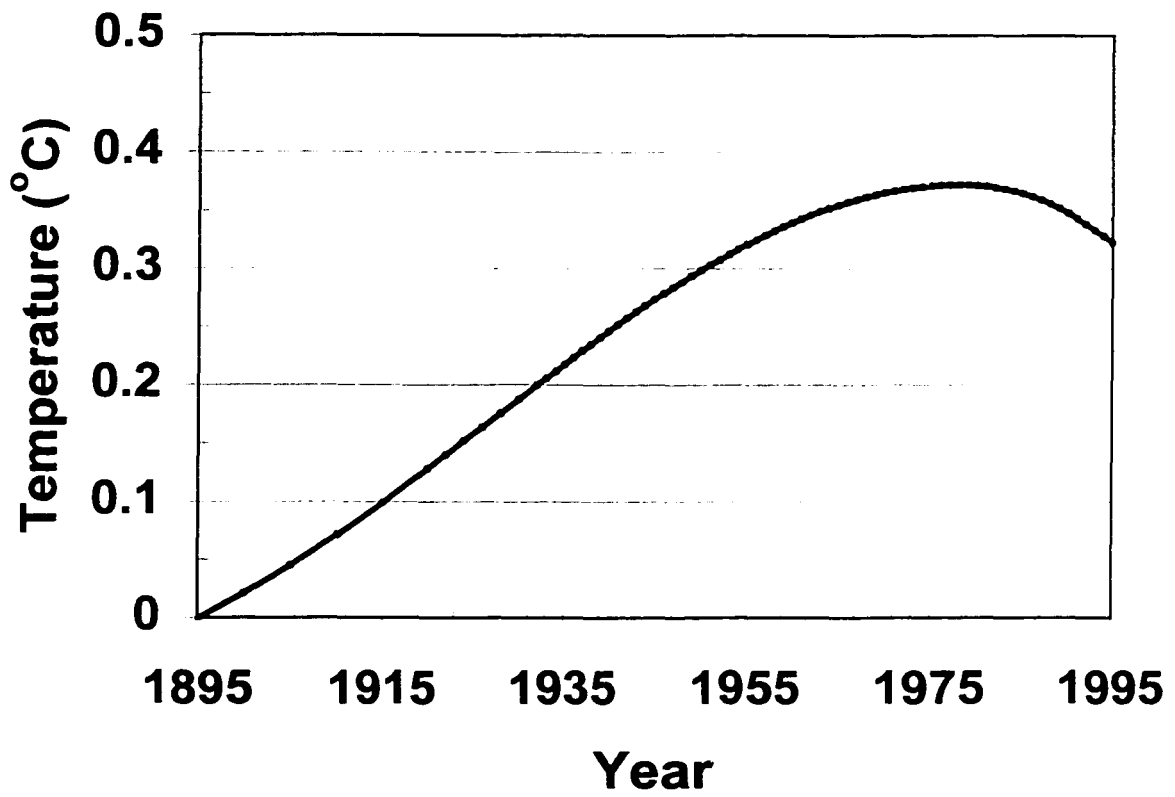


Figure 58. Ground surface temperature history of the transient resulting solely from the effects of latent energy of ground freezing.

therefore not rejected. This 0.4°C warming signal is significant to borehole climate change studies because it links changes in fall precipitation with the generation of a transient temperature signal. The signal represents a component of ground warming attributed to long-term changes in soil moisture at the onset of freezing, and is unrelated to the warming signal generated by direct coupling of recorded air temperatures.

It is possible that the 6-year correlation of modeled latent energy of ground freezing and total fall precipitation from Minot is unique to a particular hydrogeologic or climatic condition. In this case the magnitude of the warming signal due to latent energy of freezing could vary regionally. Unfortunately this is not testable due to the lack of continual temperature and boundary layer data prior to and during the modeling period.

CHAPTER 9

CONCLUSIONS

This dissertation is an investigation of factors that cause separation in air and ground temperatures on a seasonal to multi-annual time scale. Assuming a consistent 1:1 coupling of air and ground temperatures and heat transfer purely by conduction, climate change inferred from ground temperatures is a reliable complement to the instrumental air temperature record. Resolving any boundary layer effects on air-ground temperature exchange is complicated because of the number of variables involved, the interconnectedness of the variables, and limited boundary layer data.

Ground-surface variables examined in this study include daily percentage sunlight, incident radiation, vegetation, daily total precipitation, annual snow cover duration, and latent energy of ground freezing and thawing. The following hypotheses were tested: 1) Ground-surface factors are capable of generating trends in mean annual ground temperatures that do not occur in mean annual air temperatures during 6 and 9-year periods; 2) Annual air-ground temperature differences averaged during winter months are mainly controlled by total duration of winter snow cover; 3) Modeled latent energy of ground freezing is a function of precipitation totaled 2-3 months prior to the onset of ground freezing; 4) The thermal effects of latent energy of ground freezing determined by observed fall precipitation values are capable of generating a transient subsurface temperature signal in a 100-year period.

The data support the following conclusions:

i). Statistical regressions of mean annual ground temperatures from Fargo and Bottineau sites indicated respective warming trends of $0.93 \pm 0.09^\circ\text{C} / 9$ years and $1.17 \pm 0.15^\circ\text{C} / 6$ years. Mean annual air temperatures and modeled ground temperatures generated with direct air-ground coupling do not display any significant-fit trends. Because the modeled ground temperatures do not show any significant trend, the warming of recorded ground temperatures is attributed to nonconductive ground-surface factors.

ii). Annual duration of measurable snow cover was compared with temperature differences ($T_{5\text{cm}} - T_{\text{air}}$) averaged from November 15 to April 1. The correlation coefficients are: **Bottineau**: $r^2 = .84$ (6 year period), **Fargo**: $r^2 = .71$ (9 year period), **Langdon**: $r^2 = .56$ (6 year period), **Minot**: $r^2 = .79$ (6 year period), and **Streeter**: $r^2 = .87$ (6 year period). These correlations demonstrate the influence of winter snow cover duration on air-ground temperature exchange.

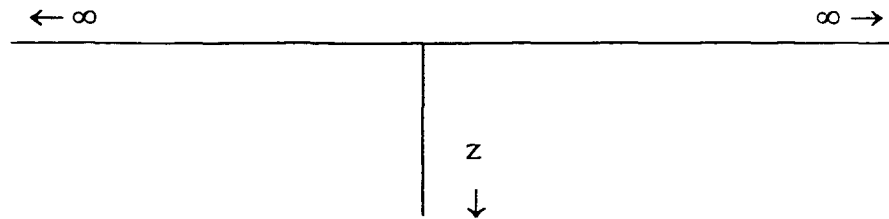
iii). Continually recorded ground temperatures from five sites were modeled with a one-dimensional heat conduction algorithm. Best-fit thermal parameters including thermal conductivity and latent energy of freezing were determined with a trail and error 'tuning' method. Maximum average residual temperatures during the modeling periods are: $\pm 0.2^\circ$ (freezing), $\pm 0.5^\circ$ (summer), and $\pm 0.7^\circ\text{C}$ (thawing). Modeled latent energy of ground freezing values from each winter were compared with total fall precipitation at four sites in North Dakota during 6-year periods. Correlation coefficients from these period are **Bottineau**: $r^2 = .38$, **Langdon**: $r^2 = .69$, **Minot**: $r^2 = .95$, **Streeter**: $r^2 = .01$. Modeled values

of latent energy of ground freezing were compared with precipitation totaled 60 days prior to ground freezing at Fargo during a 9-year modeling period ($r^2 = .66$). The sites show a mixed dependency of modeled latent energy of ground freezing on total precipitation prior to ground freezing. The discrepancy is attributed to low model sensitivity to choices of latent energy, the brevity of the study, and the high dependency of soil moisture on antecedent moisture content and water table depth.

iv). The least-squares linear regression of mean annual air temperatures recorded in northwestern North Dakota from 1895 to 1995 indicates a warming magnitude of $1.57 \pm .23^\circ\text{C}$ per century. A forward modeling analysis of this temperature series with direct air-ground coupling generated a synthetic temperature-depth profile indicating ground-surface temperature warming of 1.7°C per century. Recorded fall precipitation totals were used as proxies for latent energy of ground freezing. The thermal effects of latent energy of ground freezing are modeled for the 100-year period of record. The resultant ground-surface temperature history yielded a 0.4°C warming signal attributed to latent energy effects.

APPENDIX: MODEL DESCRIPTION

Several factors influence three-dimensional heat transfer in the subsurface, including spatial variation in terrain (topography, lateral changes in ground cover and vegetation), temporal changes to the terrain (deforestation, agriculture, post-glacial lakes, urbanization, roads, sedimentation, erosion, distribution and thickness of snow cover, water table depth, ground water movement, and latent energy due to water freezing), and anisotropy of thermophysical parameters (Lewis and Wang, 1992, Roy et al., 1968). In the absence of terrain effects and thermal conductivity anisotropy, the three-dimensional problem is reduced to one-dimensional heat conduction in a semi-infinite half space.

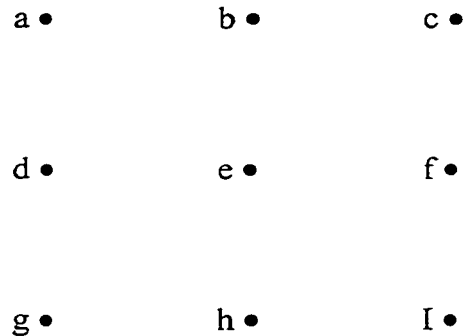


Boreholes used in this study were chosen for having uniform vertical thermal conductivity, negligible topographic and groundwater effects, and no vegetation or ground surface changes in the past century. The assumption of one-dimensional heat flow is therefore appropriate.

For a homogeneous, continuous, source-free half space, the equation governing heat conduction in the z direction is:

$$\rho C_p \frac{\partial T}{\partial t} = \frac{\partial}{\partial z} (k \frac{\partial T}{\partial z}) + A(z) \quad (2)$$

where z = depth, T = temperature, t = time, k = thermal conductivity, ρ = density, C_p = specific heat, and $A(z)$ = heat production due to latent energy release (Carslaw and Jaeger, 1959). The solution to Equation 2 can be analytical or numerical. The model used in this dissertation is a finite-difference numerical algorithm. Partial differential equations in Equation 2 are expressed in finite difference form for spatial variation of temperature. The time steps for temperature calculations within the model are iterated for a specified period. For the given nodal distribution:



the heat flow Q into each node from any adjacent node is calculated as:

$$Q = k A \Delta T/L \quad (3)$$

where A = area per unit depth perpendicular to the direction of heat flow and L = horizontal or vertical spacing between nodes. Heat flow is assumed to be constant within the model. The sum of heat flow into a node from the surrounding four nodes causes the temperature change of the node. The values ρ , C_p and k are held constant for each time step but can be varied within the model. An initial temperature is assigned to all nodes on the grid. The resultant temperature distribution is then used in calculations for the successive step.

The model consists of three nodes at every depth. Horizontal spacing of the nodal columns was set at 10cm. The condition of no horizontal heat flow into the model is applied to the outer two columns of nodes. The condition for a constant heat flow boundary for basal heat flow is $\partial T/\partial z = \text{constant}$.

Latent energy effects are incorporated into the model by assigning a heat production value that accounts for the enthalpy change that occurs during a phase change. The assigned heat production value is converted to a volumetric heat production per given time interval. The model incorporates the positive or negative volumetric heat production into the inter-nodal heat flow calculations at the specific nodes. In the case of freezing or thawing, the effect is applied at the nodes adjacent to the freezing isotherm. Positive heat production values represent the release of latent energy due to freezing or condensation, while negative heat production values represent latent energy adsorption due to thawing or evaporation.

Model comparison

The results of the numerical model are compared to an analytical solution of Equation 4. The vertical discretization was taken as 1m. Temperatures were calculated to 250m depth. The condition of a ‘boxcar’ forcing signal is applied to the half space. The solution to this problem is well-documented (Lachenbruch and Marshall, 1986):

$$T(z,t) = \Delta T_s \operatorname{erfc} z / (4Kt)^{1/2} \quad (4)$$

where z = depth, T_s = temperature at $z = 0$, K = thermal diffusivity, t = time, and erfc = complementary error function. The temperature distribution in the subsurface is the solution to the equation subject to the condition:

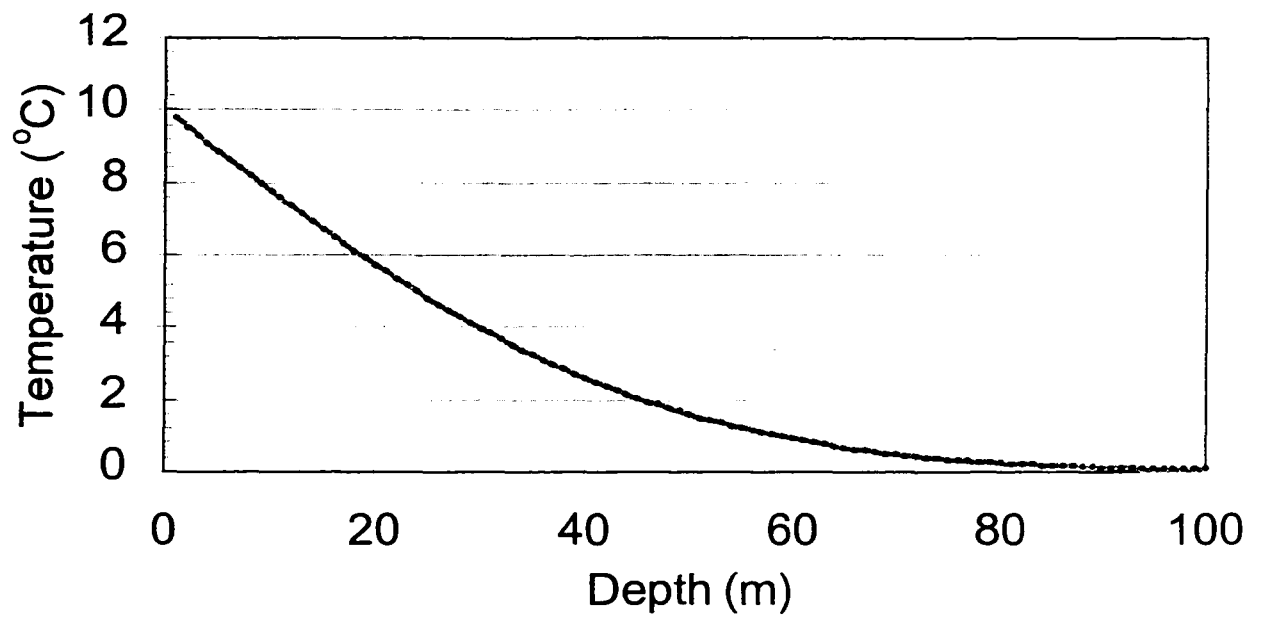
$$T = T_i \text{ at } t = 0, z > 0$$

$$T = T_s \text{ at } z = 0, t > 0$$

$$T \rightarrow T_i \text{ as } z \rightarrow \infty, t > 0$$

For comparison, the following values were used:

$T_i = 0$, $T_s = 10^\circ\text{C}$, $t = 20$ years, $K = 10^{-6}\text{m}^2/\text{s}$, $k = 2.2 \text{ Wm}^{-1}\text{K}^{-1}$, $c = 1000\text{kJ kg}^{-1} \text{K}^{-1}$. The resultant temperature-depth profiles are shown below. The results show excellent agreement between the analytical solution (black dots) and the numerical solution (gray line).



REFERENCES CITED

REFERENCES CITED

- Beltrami, H. and Mareschal, J-C., 1992. Ground temperature changes in eastern Canada: borehole temperature evidence compared with proxy data. *Terra Nova*, 5: 21-28.
- Beltrami, H., and Mareschal, J-C., 1991. Recent warming in eastern Canada inferred from geothermal measurements. *Geophys. Res. Lett.*, 18: 605-608.
- Blackwell, D.D., Steele, J.L., and Brott, C.A., 1980. The Terrain Effect on Terrestrial Heat Flow. *J. Geophys. Res.*, 85: 4757-4772.
- Carslaw, H.S., and Jaeger, J.C., 1959. *Conduction of Heat in Solids*, 510pp., 2nd ed., Oxford Univ. Press, New York.
- Cermak, V., 1971. Underground temperature and inferred climatic temperature of the past millenium. *Paleogeogr. Paleoclimatol. Paleoecol.*, 10: 1-19.
- Chapman, D.S., Chisholm, T.J., and Harris, R.N., 1992. Combining borehole temperature and meteorologic data to constrain past climate change. *Palaeogeogr., Palaeoclimatol., Palaeoecol. (Global Planet. Change Sect.)*, 98: 269-281.
- Clow, G.D., 1992. The extent of temporal smearing in surface-temperature histories derived from borehole temperature measurements. *Palaeogeogr., Palaeoclimatol., Palaeoecol. (Global Planet. Change Sect.)*, 98: 81-86.
- Desrochers, D.T. and Granberg, H.B., 1988. Schefferville snow-ground interface temperatures. *Fifth International Conference on Permafrost, Trondheim, Norway*. 1: 67-72.
- Enz, J.W., 1985. The climatology of solar radiation at Bismarck, ND. *Agricultural Experiment Station, North Dakota State University, Fargo, ND. Bulletin 516.*
- Enz, J.W., 1998. *Contribution of temperature data sets and personal communications.* North Dakota State University Soil Science Department, Fargo, North Dakota.
- Fanning, C., Enz, J, Patterson, D., Echart, S., Black, A., 1981. Available soil moisture – North Dakota. *Cooperative Extension Service, North Dakota State University, Fargo, ND.*
- Farouki, O.T., 1981. *Thermal Properties of Soils.* CRREL Monograph 81-1, US Army Corps of Engineers, Cold Regions Research and Engineering Laboratory, Hanover, New Hampshire.
- Geiger, R., Aron, R.H., Todhunter, P., 1995. *The Climate Near the Ground.* Germany, Friedr. Vieweg & Sohn Verlagsgesellschaft mbH, Braunschweig / Wiesbaden.

- Goodrich, L.E., 1978. Some results of a numerical study of ground thermal regimes. *International Conference on Permafrost, Proceedings 3, Vol. 1*: 29-34.
- Goodrich, L.E., 1982. The influence of snow cover on the ground thermal regime. *Canadian Geotechnical Journal*, 19: 421-432.
- Gosnold, W.D., 1990. Heat flow in the Great Plains of the United States. *J. Geophys. Res.*, 95: 353-374.
- Gosnold, W.D., Todhunter, P.E., Schmidt, W., 1997. The borehole temperature record of climate warming in the mid-continent of North America. *Global Planet. Change*, 15: 33-45.
- Groisman, P.Ya. and Easterling, D.R., 1994. Area-averaged precipitation over the contiguous United States, Alaska, and Canada. In: T.A. Boden, D.P. Kaiser, R.J. Sepanski and F.W. Stoss (Editors), *Trends '93: A Compendium of Data on Global Change. ORNL/CDIAC-65, Oak Ridge Nat. Lab.*, 786-798.
- Hansen, J.A., Lacis, D., Rind, G., Russell, P., Stone, I., Fung, R., Ruedy, Lerner, J., 1984. Analysis of feedback mechanisms, In: *Climate Processes and Climate Sensitivity, Geophysical Monograph Series, 29 (AGU)*, 130-135.
- Harris, R.N., and Chapman, D.S., 1997. Borehole temperatures and a baseline for 20th-century global warming estimates. *Science*, 275: 1618-1621.
- Hinkel, K.M., and Outcalt, S.I., 1994. Identification of heat-transfer processes during soil cooling, freezing, and thaw in Central Alaska. *Permafrost and Periglacial Processes*, 5: 217-235.
- Hughes, M.G., and Robinson, D.A., 1993. Snow cover variability in the Great Plains of the United States: 1910 – 1988. *Proceedings of the 50th Eastern Snow Conference, Quebec City, Quebec.*, 150-163.
- Hughes, M.G., and Robinson, D.A., 1996. Historical snow cover variability in the Great Plains of the USA: 1910 through 1993. *Int. Journ. Climate*, 16: 1005-1018.
- Intergovernmental Panel on Climate Change; A special Report of IPCC Working Group II, 1997. *The Regional Impacts of Climate Change: An Assessment of Vulnerability. Intergovernmental Panel on Climate Change.*
- Lachenbruch, A.H., and Marshall, B.V., 1986. Changing climate: Geothermal evidence from permafrost in the Alaskan Arctic. *Science*, 234: 689-969.
- Lewis, T.J., and Wang, K., 1992. Influence of terrain of bedrock temperatures. *Palaeogeogr., Palaeoclimatol., Palaeoecol. (Global Planet. Change Sect.)*, 98: 87-100

- Majorowicz, J.A., 1993. Climate change inferred from analysis of borehole temperatures: first results from Alberta, western Canada. *Pure Appl. Geophys.*, 140: 87-100.
- Majorowicz, J.A., and Skinner, W.R., 1997. Anomalous ground warming versus surface air temperature warming in the Prairie Provinces of Western Canada. *Climatic Change*, 35: 485-500.
- National Oceanic and Atmospheric Administration, National Climatic Data Center. Asheville, North Carolina.
- Oke, T.R., 1987. *Boundary Layer Climates*. London, Methuen and Company.
- Outcalt, S. I., Nelson, F. E., and Hinkel, K. M., 1990. The zero-curtain effect: Heat and mass transfer across an isothermal region in freezing soil. *Water Resources Res.* 26: 1509-1516.
- Pollack, H.N., Huang, S., Shen, P.Y., 1998. Climate change record in subsurface temperatures: A global perspective. *Science*, 282: 279-281.
- Putnam, S.N., and Chapman, D.S., 1996. A geothermal climate change observatory: First year results from Emigrant Pass in northwest Utah. *J Geophys. Res.*, 101: 21877-21890.
- Roy, R.F., Blackwell, D.D., and Decker, E.R., 1972. *Continental heat flow; The Nature of the Solid Earth*. McGraw-Hill Book Company., New York, NY.
- Scattolini, R., 1978. Heat flow and heat production studies in North Dakota. Dissertation, University of North Dakota.
- Shen, P.Y., Pollack, H.N., Huang, S., Wang, K., 1995. Effects of subsurface heterogeneity on the inference of climate change from borehole temperature data: model studies and field examples from Canada. *J. Geophys. Res.*, 100: 6383-6396.
- Smith, M. W., and Riseborough, D.W., 1996. Permafrost monitoring and detection of climate change. *Permafrost and Periglacial Processes*. 7: 301-309.
- Smith, M.W., 1975. Microclimatic influences of ground temperatures and permafrost distribution, Mackenzie Delta, Northwest Territories. *Can. J. Earth Sci.*, 12: 1421- 1438.
- Todhunter, P., 1995. Hydroclimatic perspectives on waterfowl production in the North Dakota Prairie Pothole Region. *Great Plains Research*. 5: 137-162.
- Touloukian, Y.S., Judd, W.R., and Roy, R.F., 1981. Physical properties of rocks and minerals. McGraw – Hill / CINDA data series on material properties. II – 2: 427 – 502.

Turcotte, D.L., and Schubert, G., 1982. *Geodynamics, Applications of Continuum Physics to Geological Problems*. John Wiley and Sons, New York, NY.

USDA Soil Survey of Cass County, North Dakota. 1990. United States Department of Agriculture. Soil Conservation Service.

Zhang, T., Osterkamp, T.E., and Stamnes, K., 1996. Influence of the depth hoar layer of the seasonal snow cover on the ground thermal regime. *Water Resources Res.*, 32: 2075-2086.